NTNU

Norwegian University of
Science and Technology

Comparison of methods for calculation of immature organic carbon values and initial hydrocarbon potential from mature organic carbon measurements

Laura Bérdi

Petroleum Geosciences
Submission date: July 2016
Supervisor: Maarten Felix, IGB
Co-supervisor: Ute Mann, Statoil

Norwegian University of Science and Technology
Department of Geology and Mineral Resources Engineering

Abstract

In this study, five mass-balance-based (Peters et al., 1996; Jarvie et al., 2007; Jarvie, 2012) and curve-fitting methods (Banerjee et al., 1998; Dahl et al., 2004) are analysed that have been developed to determine the immature geochemical properties of mature organic matter on the basis of measured values. Based on the published workflowof these methods, a MATLAB code was constructed for each method. Four data sets were selected from various locations representing immature to overmature organic matter of kerogen types I−IV, to observe how their results compare and to determine the limitations of the methods. On the basis of the calculated initial values, interpretations of the organic-richness, of the quality of the immature organic matter and of the organic facies and depositional environment were made, to test whether these would change depending on the method used for back calculation.

The mass-balance-based and line-fitting methods calculated comparable original organic carbon values, suggesting the same organic-richness for each data set. The initial hydrocarbon generative potential and original hydrogen index values show large variations and the interpretation of these parameters is dependent on the applied method. The Jarvie et al. (2007) method yielded the highest initial hydrocarbon generative potential values for most of the data sets, while there is no method which computed consistently lower values than the others. The matrix corrected original hydrogen index values calculated by the Dahl et al. (2004) method were larger than the uncorrected values of the same method and the results of the other methods for the majority of the data sets. The uncorrected initial hydrogen index values of the Dahl et al. (2004) method were similar to the results of the other methods in general. Furthermore, due to the variation in the calculated original hydrogen index values of the different methods, the results suggested different depositional environment interpretations in most cases depending on the method used for back calculation. The transformation ratio values computed by the methods indicated the same maturity stage for the organic matter in most of the data sets.

Furthermore, it was observed that the mass balance based methods do not provide realistic results in the absence of proper data about the quality and origin of the immature organic matter. Moreover, this study confirms the conclusions of Dahl et al. (2004), that their method cannot account for frequent changes in the depositional environment

Acknowledgements

This study was carried out at the Department of Geology and Mineral Resources Engineering at the Norwegian University of Science and Technology (NTNU) in collaboration with Statoil, under the supervision of Dr. Ute Mann and Dr. Maarten Felix. I am very grateful to Dr. Maarten Felix for his valuable guidance, inspiring ideas and constructive comments improving this thesis. I owe special thanks to Ute Mann for the help, support and suggestions during my work. I am also thankful to Justin Fadipe from the Department of Geology and Mineral Resources Engineering at NTNU for his valuable guidance and comments in geochemistry. I would like to express my gratitude to Dr. Przemysław Karcz from the Polish Geological Institute for his guidance in the application of the Jarvie et al. (2007) method.

I would like to thank my parents and family for their invaluable guidance, encouragement and support throughout my studies. I am also thankful to my friends who inspired me in every aspect of life during my stay in Norway. I would also like to express my gratitude to my former supervisor, Dr. Katalin Milota for her invaluable guidance throughout my educational and professional career. Furthermore, I would like to thank my former colleagues and friends at MOL Group for encouraging me to pursue studies abroad.

Table of contents

List of figures

List of tables

1. Introduction

Sedimentary organic matter provides indirect indicators, or proxies, that can be used to reconstruct marine and continental palaeoclimatic and palaeoenvironmental conditions (Meyers, 1997). The type and amount of organic carbon reflect environmental and climatic conditions conditions at the time of deposition as well as changes in the carbon cycle (Killops & Killops, 2013). Otherwidely used proxies include biomarkers, isotopic and elemental compositions of bulk organic matter and trace element abundance (Bradley, 2015). Studying these palaeoclimatic indicators enablesgeochemists to obtain information on past ecosystems and sedimentary conditions in which the organic carbon was formed and deposited (Meyers, 1997).

The origin and quantity of organic carbon are generally determined by organic petrography and laboratory methods, such as analysis of bulk properties and especially Rock-Eval pyrolysis data (Meyers, 1977). The changes in the primary source of organic carbon are indicative of fluctuations in sea-level and oceanic surface currents, depending on climatic factors (Bradley, 2015). Furthermore, biological palaeoproductivity can be determined on the basis of mass accumulation rates of organic carbon (Meyers, 1977).

During diagenesis, the deposited organic matter buried within the sediment is subjected to compaction and consolidation (Killops & Killops, 2013). As maturation of the organic matter continues, the temperature and pressure regime increases. The rising temperatureprovides enough thermal energy to break the chemical bonds of the organic matter (Killops & Killops, 2013). Then, in the phase of catagenesis, the chemical composition of the organic matter is altered and degraded (Killops & Killops, 2013). This restricts the determination of palaeoenvironmental conditions directly from sedimentary organic matter (Meyers, 1977). For this reason, several methods have been developed to determine immature properties from measured values of thermally mature organic matter (Jarvie, 2012).

1.1 Theoretical background

The methods constructed to back calculate the immature properties of degraded organic matter use data determined by Rock-Eval pyrolysis and/or visual kerogen assessment (Dahl et al., 2004; Jarvie et al., 2007).

1.1.1 Rock-Eval analysis

Rock-Eval analysis was initially developed to estimate the hydrocarbon generative potential of the organic matter (Espitalié et al., 1977) but it has also been proven useful for palaeoceanographic studies (Meyers, 1977). During Rock-Eval pyrolysis, sediment samples are heated up to temperatures between 200–600 ˚C, where the amounts of released hydrocarbons are recorded (Peters et al., 2005); this is illustrated in Fig. 1. The measured Rock-Eval parameters include total organic carbon (TOC, wt.%), which is the sum of residual and pyrolysed organic carbon content, S1 (mg HC/g Rock) are the thermally vapourised free hydrocarbons, S2 (mg HC/g Rock) represents the amount of hydrocarbons released due to the degradation of organic matter, and S3 (mg CO_2/g Rock) is the carbon dioxide generated (Peters et al., 2005). T_{max} (˚C) corresponds to the temperature where S2 reaches its maximum (Tissot & Welte, 1984). The hydrogen index (HI, mg HC/g TOC) represents the quantity of pyrolysable organic matter from S2 relative to TOC (Peters, 1986). The oxygen index (OI, mg CO_2/g TOC) corresponds to the amount of carbon dioxide generated from S3 relative to TOC, and the production index (PI, S1/[S1+S2]) is the ratio of vapourised hydrocarbons to the total hydrocarbon generative potential (Peters, 1986; Peters et al., 2005).

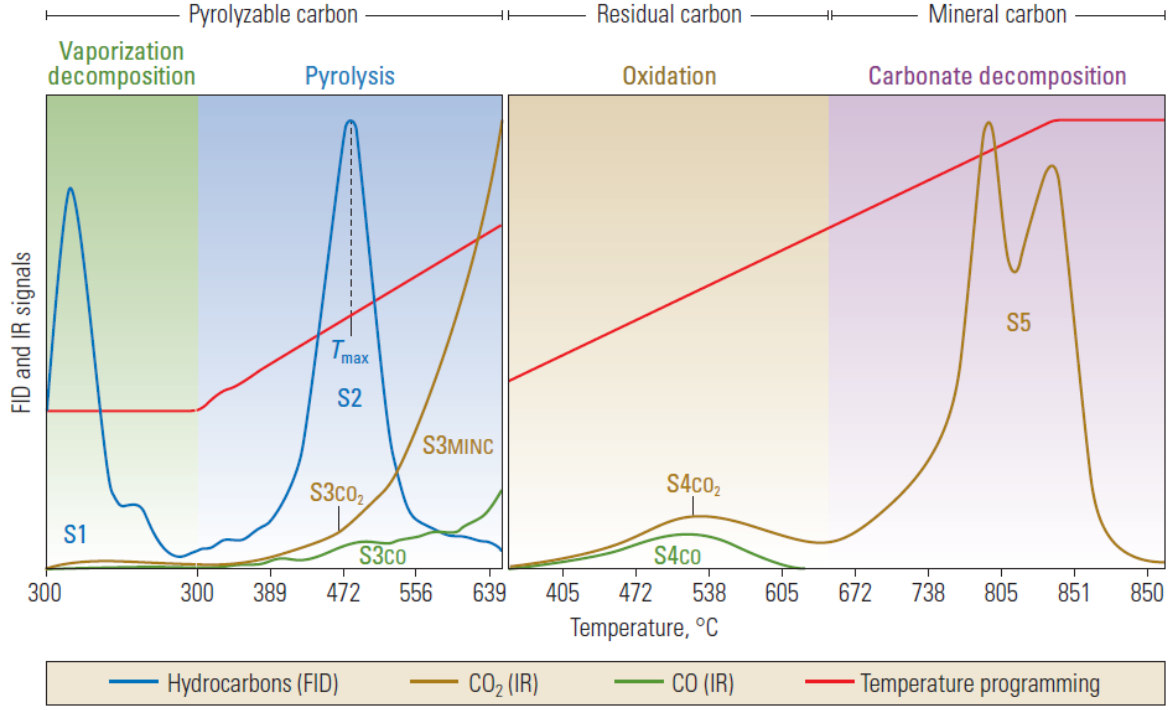

Figure 1. Results of Rock-Eval pyrolysis. The S1 peak represents the amount of free hydrocarbons, the S2 peak provides the amount of residual hydrocarbons. T_{max} represents the temperature when the S2 peak reaches its maximum and the S3 peak is the generated amount of carbon dioxide (from McCarthy et al., 2011).

The hydrogen and oxygen index obtained by pyrolysis reflect the origin of the organic carbon (Tissot & Welte, 1984). The quality of the organic matter can be deduced by plotting the measured oxygen and hydrogen index values on a van Krevelen diagram, where the main kerogen types and their maturation paths are shown (Peters et al., 2005).

1.1.2 Visual kerogen assessment

Organic petrography enables identification of organic matter particles by reflected light microscopy, after a hydrochloric and hydrofluoric treatment of a sample to remove mineral particles (Peters et al., 2005). Microscopic inspection of the organic particles enables the assessment of the quality, quantity and thermal maturity of organic matter as well as the determination of the relative percentages of oil- and gas-prone macerals (Tissot & Welte, 1984). The identified particles are classified as liptinites, vitrinites or inertinites (Tissot & Welte, 1984). Liptinites are oil-prone macerals and represent kerogen type I or II. Particles classified as vitrinite are gas-prone macerals and are indicative of kerogen type III (Peters et al., 2005). Inertinite particles represent kerogen type IV, which does not have any hydrocarbon generative potential (Peters et al., 2005).

1.1.3 Uncertainties in Rock-Eval results

Katz (1983) showed that the predominance of a calcite mineral matrix increases the amount of generated carbon dioxide (CO_2) and as a result, the derived oxygen index. Furthermore, the carbonate dominated mineral matrix also raises the hydrogen index values (Katz, 1983). Moreover, experiments of Katz (1983) indicated that hydrogen index increases and oxygen index decreases with increasing total organic carbon content. These findings limit the applicability of the van Krevelen and modified van Krevelen diagrams for describing the organic matter, as well as the applicability of the hydrogen index values in any methods without corrections in the presence of adsorptive mineral matrix (Katz, 1983; Espitalié et al., 1985).

The study of Espitalié et al. (1985) showed that the average hydrogen index of a sample population can be derived by a regression line from an S2–TOC cross plot. In case the regression line passes through the origin, there is no retained pyrolysable organic matter in the studied samples (Espitalié et al.; 1985). Generally, the trend line crosses the positive TOC-axis and the negative S2-axis (Langford & Blanc-Valleron, 1990). The intersection of the trend line at the negative S2-axis indicates the amount of hydrocarbons retained by mineral matrix (Langford & Blanc-Valleron, 1990). The matrix retention effect can cause erroneous results,

especially for lean samples (S2 = 0−3 mg HC/g Rock), while the error is less for samples containing larger amounts of pyrolysable organic material (S2>3 mg HC/g TOC) (Dahl et al., 2004).

1.1.4 Original hydrogen index

Several methods exist to determine the original hydrogen index of mature organic matter. According to Baskin (1997), the initial hydrogen index can be determined on the basis of the atomic H/C ratio. Baskin (1997) concluded that this method is preferable over Rock-Eval pyrolysis as the latter shows fluctuations even for kerogens with the same H/C ratio. Peters et al. (2005) suggested to either assign a representative value of the dominant organic matter type in the studied samples based on organic petrographic analysis, or to apply the Rock-Eval hydrogen index of an immature facies equivalent of the studied mature organic matter. The initial hydrogen index can also be estimated by the Jarvie et al. (2007) method, using visual kerogen assessment. Then, the original hydrogen index can be calculated by applying representative hydrogen index values for the main kerogen types (Jarvie et al., 2007).

Jarvie (2012) eamphasized that using a representative value for a certain kerogen type is incorrect due to the large variation in the hydrogen index within the same kerogen type. Jarvie (2012) conducted a study on a global collection of immature marine organic carbon to find P10, P50 and P90 value for the sample population, which represent the probability (10%, 50% and 90% respectively) that the initial hydrogen index of a given marine organic matter exceeds a certain value. Then, one of the values corresponding to P10, P50 and P90 can be used as an initial hydrogen index assumption depending on the composition of the studied organic matter (Jarvie, 2012). According to Figure 2, 90% of marine shales yield an initial hydrogen index of more than 340 mg HC/g TOC, 50% yield a value greater than 475 mg HC/g TOC and 10% of the samples exceed 645 mg HC/g TOC (Jarvie, 2012).

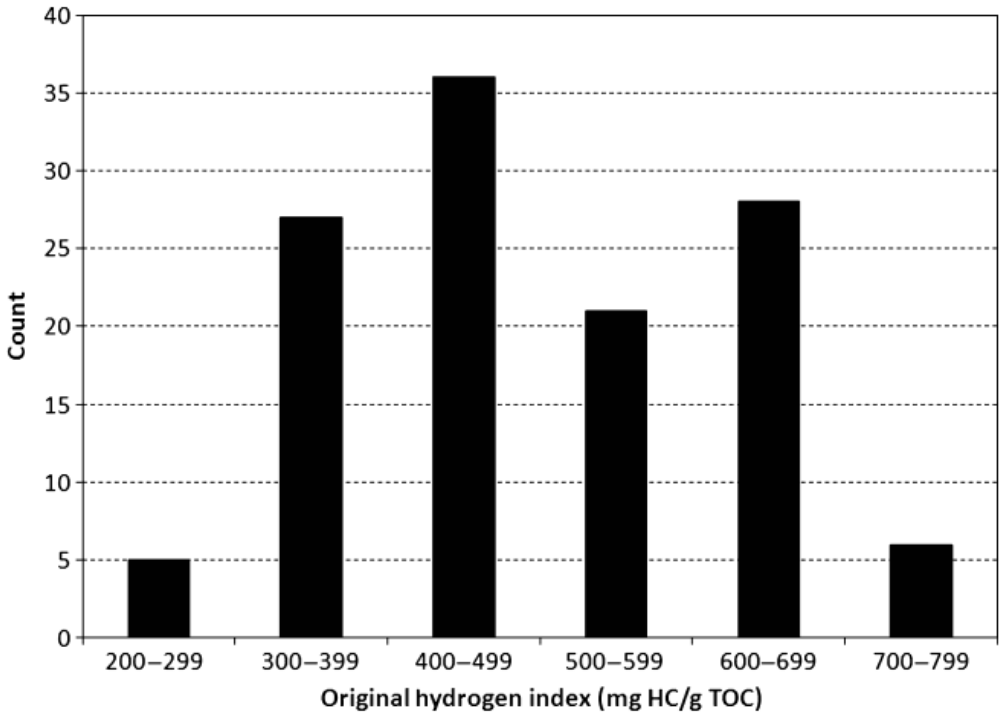

Figure 2. Original hydrogen index (HI_o) distribution in immature marine shales. The distribution from the graph yields a hydrogen index P90 value of 340, a P50 of 475, and a P10 of 645 mg HC/g TOC (from Jarvie, 2012). TOC = total organic carbon.

1.1.5 Types of back calculation methods

Estimates of the organic-richness and quality of non-degraded organic matter as well as the amount of initially deposited total organic carbon can be calculated in different ways (Peters et al., 1996; Jarvie et al., 2007; Chen & Jiang, 2016). These estimates can be obtained by mass balance and line-fitting based methods (Peters et al., 1996; Banerjee et al., 1998). This includes the calculation of the original carbon content (TOC_o, wt.%), which indicates the original organic-richness of the thermally mature organic matter; the initial hydrocarbon generative potential ($S2_o$, mg HC/g Rock) that provides information about the initial quantity of the deposited organic matter capable of generating hydrocarbons and the transformation ratio (TR, %) showing the amount of organic matter already converted to hydrocarbons (Peters & Cassa, 1994; Peters et al., 2005).

The original hydrogen index (HI_o; mg HC/g TOC) is also estimated by the methods and is an indicator of the quality of the organic matter and the initial depositional environment (Jones, 1987; Jarvie et al., 2007). Large variations in the estimation of the latter parameter could lead to different interpretations about the sedimentary conditions under which the organic matter formed (Jones, 1987; Karcz, 2014).

Most of the equations estimating the initial geochemical parameters of thermally mature organic matter are based on mass balance calculations (Peters et al., 1996; Jarvie et al., 2007; Jarvie, 2012). The mass balance equations use the measurements of present-day geochemical parameters decreased upon maturation to restore the original values of the immature organic matter (Jarvie et al., 2007). Several mass balance equations exist in the literature, such as the ones constructed by Espitalié et al. (1987), Peters et al. (1996), Jarvie et al. (2007), Modica & Lapierre (2012), Romero-Sarmiento et al. (2013) and Chen & Jiang (2016).

Line-fitting methods are also used to obtain back calculated geochemical values but are not as frequent in the literature as mass balance based equations (Banerjee et al., 1998; Dahl et al., 2004). Among the best-fit methods, the work of Banerjee et al. (1998) and Chen & Jiang (2015) are solely based on curve fitting, while the method of Dahl et al. (2004) includes both curve-fitting and additional calculations.

Both groups of methods depend on different variables. Mass balance equations generally use an original hydrogen index assumption of the immature organic matter (Peters et al., 1996; Jarvie et al., 2007; Jarvie, 2012). The most widely usedmass balance based methods are the Peters et al. (1996), Jarvie et al. (2007) and Jarvie (2012) methods. Among these, only the Jarvie et al. (2007) method has a formula to obtain the original hydrogen index of the degraded organic matter, the other approaches need to be used either with a calculated original hydrogen index value obtained by the Jarvie et al. (2007) method or with an assumption of this value (Jarvie, 2012). Among the curve-fitting approaches, the Dahl et al. (2004) method requires an assumption about the transformation ratio of the organic matter.

Authors usually apply only a single method to restore the original geochemical parameters of thermally mature organic matter and to interpret the results. For this reason, it is unknown how large the variation is between the results of the different methods, how the results compare to each other and how the limitations of the initial data and data availability affect the results.

1.2 Aims and objectives

In this thesis, five mass balance based (Peters et al., 1996; Jarvie et al., 2007; Jarvie, 2012) and line-fitting (Banerjee et al., 1998; Dahl et al., 2004) methods described in the literature were applied to back calculate geochemical parameters of thermally mature organic carbon to the values before maturation.

First, all methods were coded in MATLAB and were tested on different data sets to compare the back calculated values given by each method (see Appendix A–F). The selected data sets come from either the original publications where the methods were first described or from publications where the methods were applied.

During the testing of the different methods, the variability between the obtained results and the interpretations based on them are compared. Furthermore, the limitations of the different approaches are determined. The methods are also tested and compared in the presence and absence of sufficient data about the original depositional environment and the origin of the organic matter. Moreover, the interpretations of the original geological setting where the organic matter was deposited are compared on the basis of the results of the different methods.

Finally, suggestions for further work on how to improve the existing equations, how to determine which method provides the most realistic results and how to mitigate the absence of proper data are also discussed.

2. Data

The geological and geochemical characteristics of four data sets are discussed within this chapter; these data sets were used for testing the different geochemical back calculation methods. In the text subscripts 'pd' and 'o' refer to present day measured and original values. The notations of TOC and TOC_{pd}; HI and HI_{pd}; PI and PI_{pd} are used interchangeably.

2.1 Passhatten Member (Bravaisberget Formation), Spitsbergen

2.1.1 Geological setting

The Middle Triassic Passhatten Member (Anisian–Ladinian age) is located at the western Spitsbergen margin (Fig. 3) and is the oldest member of the Bravaisberget Formation in the area (Birkenmajer, 1977; Mørk et al., 1982; Karcz, 2014).

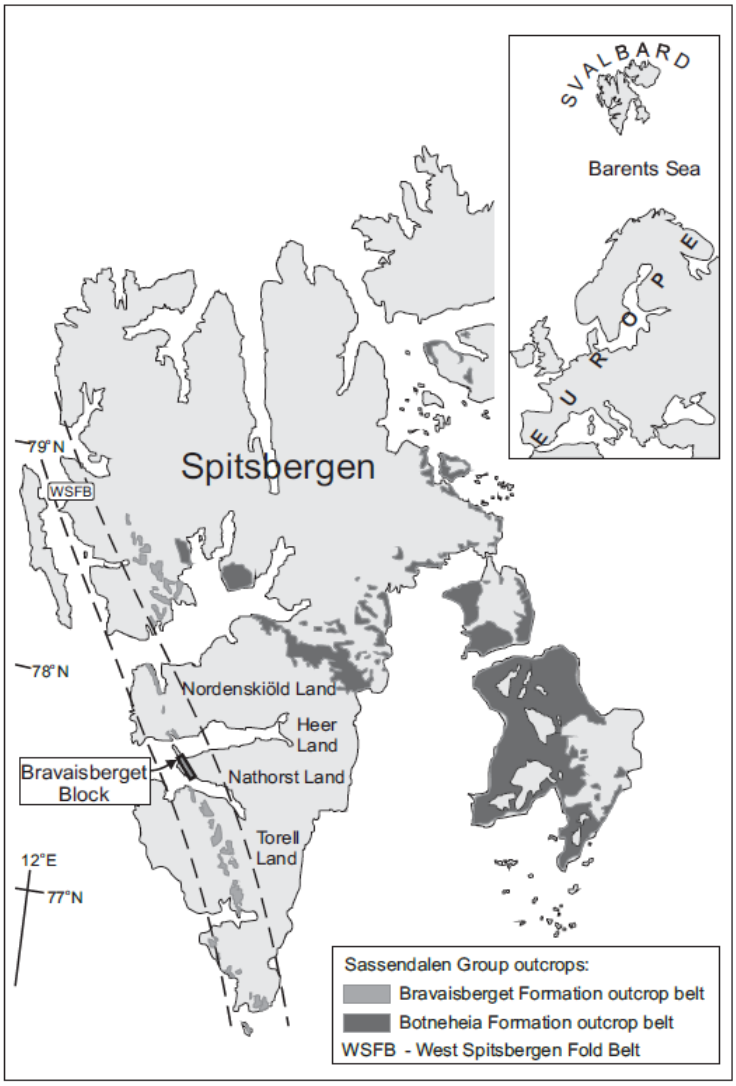

Figure 3. Map of Spitsbergen showing the Triassic outcrops of the Bravaisberget Formation with the location of the Bravaisberget Block (from Karcz, 2014).

The Passhatten Member comprises the lower and middle parts of the Bravaisberget Formation (Sassendalen Group) in the West Spitsbergen Fold-and-Thrust Belt, and is the thickest member of the formation (Krajewski & Weitschat, 2015).

2.1.2 Geochemical characteristics

Fifty-seven black shale outcrop samples were collected from the Bravaisberget Block (Fig. 3), the stratotype section of the Bravaisberget Formation in the western Nathorst Land. Rock-Eval pyrolysis was carried out on all samples. Visual kerogen assessment was applied on twenty-one samples representing both the lower and upper part of the section (Karcz, 2014).

The lower part of the Passhatten Member contains less organic matter than the upper section as shown in Table 1. Furthermore, TOC_{pd} shows a wide fluctuation in the section (Fig. 4; Karcz, 2014). The lower part of the section is characterised by wide variation of the isotopic composition of pyritic sulphur ($\delta^{34}S$; Fig. 5) and high rate of dissimilatory sulphate reduction (Karcz, 2010). In the upper part of the section, the isotopic composition of pyritic sulphur shows narrow variation (Fig. 5) and the dissimilatory sulphate reduction rate is low (Karcz, 2010).

Table 1. Rock-Eval pyrolysis data of the Passhatten Member (from Karcz, 2014).

Samples	Location	TOC_{pd} (wt.%)	T_{max} (˚C)	$S1_{pd}$ (mgHC/g Rock)	$S2_{pd}$ (mgHC/g Rock)	HI_{pd} (mgHC /gTOC)	OI_{pd} ($mgCO_2$/ gTOC)	PI_{pd} (mgHC/ gRock)
B1- 146	Upper section	2.44	457	0.53	2.77	114	12	0.16
B1- 144 D	Upper section	1.85	459	0.42	1.84	99	17	0.19
B1- 144 C	Upper section	3.09	461	0.76	3.27	106	10	0.19
B1- 144 B	Upper section	2.16	453	0.56	2.20	102	13	0.20
B1- 142	Upper section	1.88	457	0.39	1.69	90	12	0.19
B1- 140	Upper section	2.22	458	0.45	2.23	100	23	0.17
B1- 133	Upper section	2.03	459	0.38	2.18	107	17	0.15
B1- 130	Upper section	2.08	459	0.44	2.22	107	25	0,17
B1- 128	Upper section	2.21	454	0.34	2.16	98	15	0.14
B1- 126	Upper section	1.76	449	0.27	1.25	71	36	0.18
B1- 124	Upper section	2.06	457	0.49	2.06	100	16	0.19
B1- 123	Upper section	2.37	455	0.66	2.21	93	19	0.23
B1- 121	Upper section	2.24	456	0.65	2.24	100	12	0.22
B1- 119	Upper section	3.28	457	0.91	3.44	105	11	0.21
B1- 117	Upper section	2.29	456	0.42	2.33	102	25	0.15
B1- 115 C	Upper section	3.31	458	0.37	3.70	112	11	0.09
B1- 115 B	Upper section	3.99	462	0.53	4.36	109	13	0.11
B1- 115 A	Upper section	3.74	462	0.67	4.22	113	12	0.14
B1- 112	Upper section	4.92	460	0.92	5.38	109	7	0.15
B1- 110	Upper section	3.79	460	0.64	3.98	105	16	0.14
B1- 109	Upper section	1.12	457	0.28	1.05	94	28	0.21
B1- 108	Upper section	2.93	459	0.51	3.23	110	22	0.14
B1- 106	Upper section	2.93	459	0.51	3.23	110	22	0.14
B1- 104	Lower section	1.20	461	0.38	1.36	113	26	0.22
B1- 100	Lower section	2.46	462	0.34	2.20	89	20	0.13
B1- 98	Lower section	1.97	459	0.21	1.94	98	17	0.10
B1- 96	Lower section	2.07	459	0.36	2.02	98	15	0.15
B1- 94	Lower section	2.67	461	0.55	2.51	94	24	0.18
B1- 91	Lower section	1.67	462	0.33	1.48	89	26	0.18
B1- 79	Lower section	1.28	462	0.59	1.56	122	26	0.27
B1- 77	Lower section	1.73	460	0.48	1.64	95	17	0.23
B1- 75 E	Lower section	2.16	463	0.43	2.17	100	15	0.17
B1- 75 D	Lower section	1.83	457	0.18	1.59	87	21	0.10
B1- 75 C	Lower section	3.15	463	0.73	3.55	113	9	0.17
B1- 75 B	Lower section	2.08	461	0.44	1.93	93	15	0.19
B1- 75 A	Lower section	1.90	459	0.28	1.86	98	21	0.13
B1- 71	Lower section	3.17	464	0.65	3.37	106	9	0.16
B1- 69	Lower section	3.00	465	0.47	2.59	86	13	0.15
B1- 67	Lower section	2.29	463	0.64	2.42	106	17	0.21
B1- 65	Lower section	2.76	460	0.72	3.32	120	8	0.18
B1- 63	Lower section	2.27	460	0.67	2.35	104	15	0.22
B1- 48	Lower section	1.67	467	0.25	1.31	78	21	0.16
B1- 46	Lower section	1.79	462	0.26	0.99	55	26	0.21
B1- 45	Lower section	1.66	458	0.16	1.28	77	24	0.11
B1- 44 B	Lower section	2.81	461	0.30	2.18	78	18	0.12
B1- 42	Lower section	3.10	462	0.27	2.53	82	18	0.10
B1- 40	Lower section	2.47	459	0.17	1.84	74	26	0.08
B1- 36	Lower section	2.41	460	0.21	2.09	87	16	0.09
B1- 34	Lower section	1.21	461	0.20	1.00	83	33	0.17
B1- 32	Lower section	1.59	462	0.36	1.58	99	17	0.19
B1- 30	Lower section	1.16	462	0.29	0.96	83	27	0.23
B1- 28	Lower section	0.87	456	0.21	0.55	63	23	0.28
B1- 24	Lower section	1.57	464	0.33	1.29	82	20	0.20
B1- 22	Lower section	0.84	461	0.29	0.73	87	48	0.28
B1- 20	Lower section	0.74	462	0.14	0.55	74	28	0.20
B1- 16	Lower section	0.82	458	0.15	0.6	73	43	0.20
B1- 12	Lower section	0.65	456	0.15	0.62	95	72	0.19

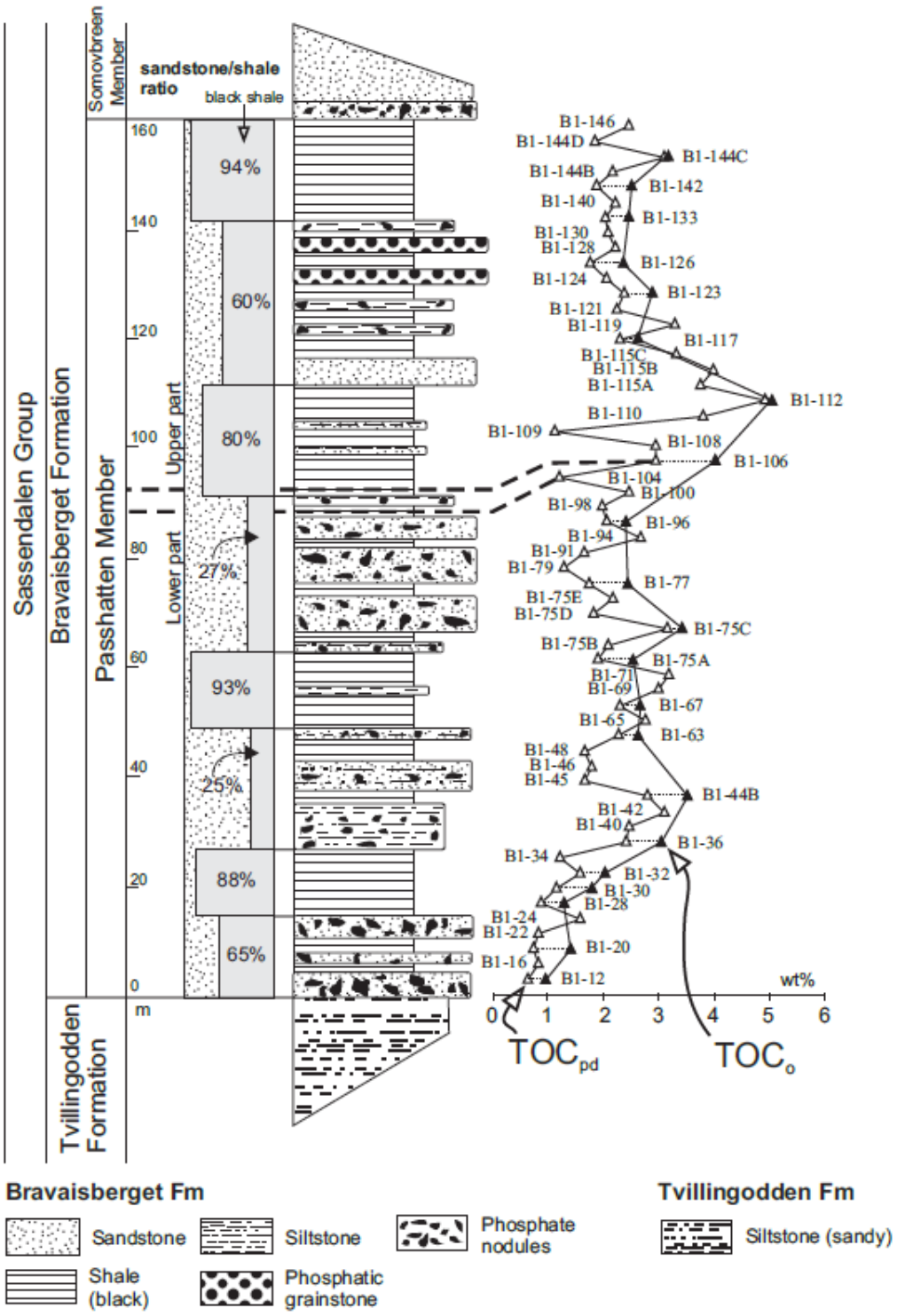

Figure 4. Lithological column of the Passhatten Member showing the interbedded black shale, siltstone and phosphorite-bearing sandstone layers of the section, the sandstone/shale ratio and the TOC_{pd} and TOC_o trends in the member (from Karcz, 2014). The TOC_o values for the samples were calculated by Karcz (2014) on the basis of the Jarvie et al. (2007) method.

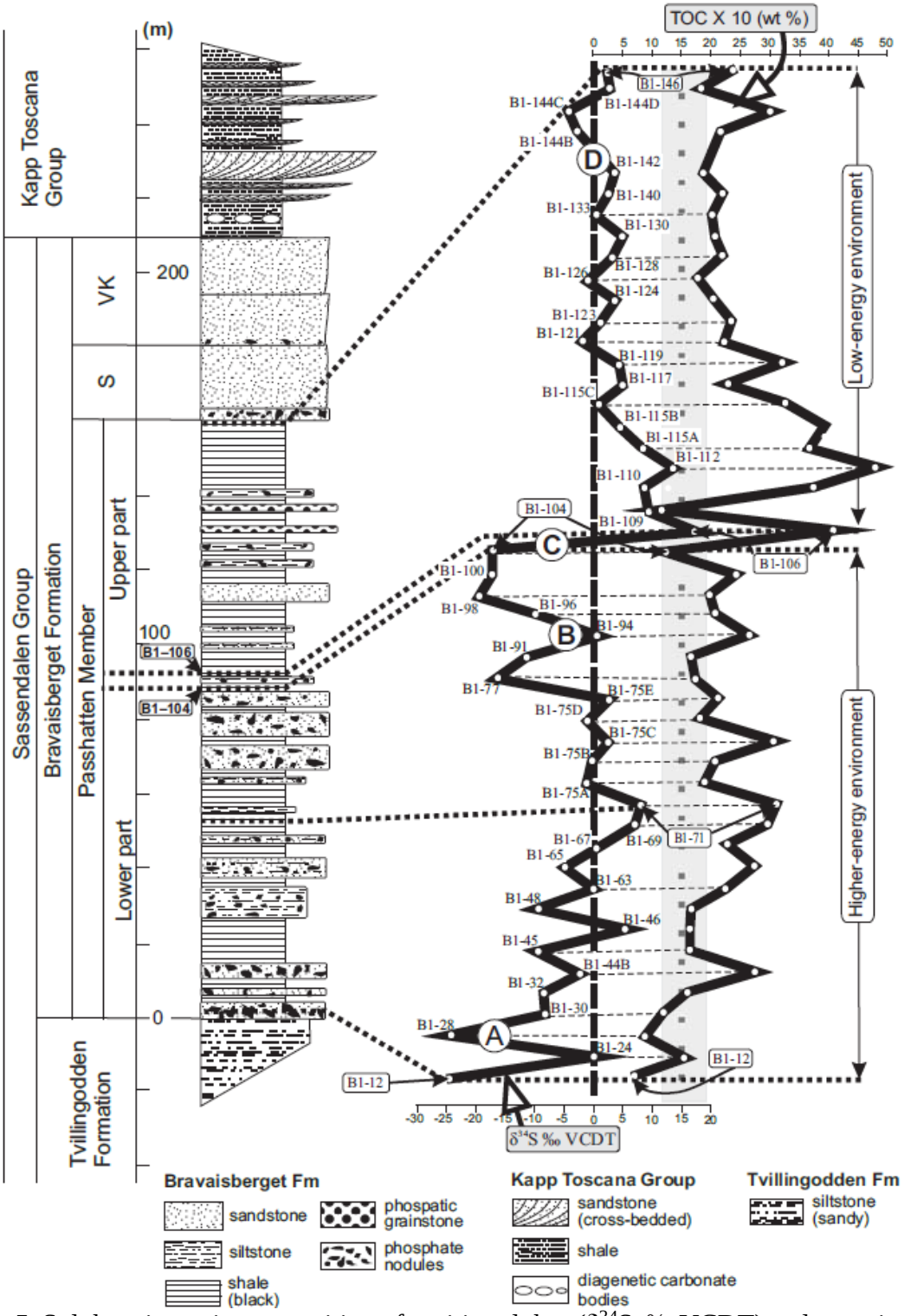

Figure 5. Sulphate isotopic composition of pyritic sulphur ($\delta^{34}S$, ‰ VCDT) and organic carbon content (TOC, wt.%) in the Passhatten Member. A, B, C, D represent different trends of the isotopic curve (described in Karcz, 2010) and the vertical dotted line with the grey field represents the mean $\delta^{34}S$ values of Triassic seawater sulphate. S – Somovbreen Member, VK – Van Keulenfjorden Member (from Karcz, 2010).

2.1.3 Organic matter type and maturity

The hydrogen index range of the section (Fig. 6) suggests the presence of type II kerogen in the organic matter of the Passhatten Member (Karcz, 2014). This is supported by the H-O characteristics of the samples (Fig. 6), indicating oxygen-enriched and hydrogen depleted type II kerogen in the member (Karcz, 2014).

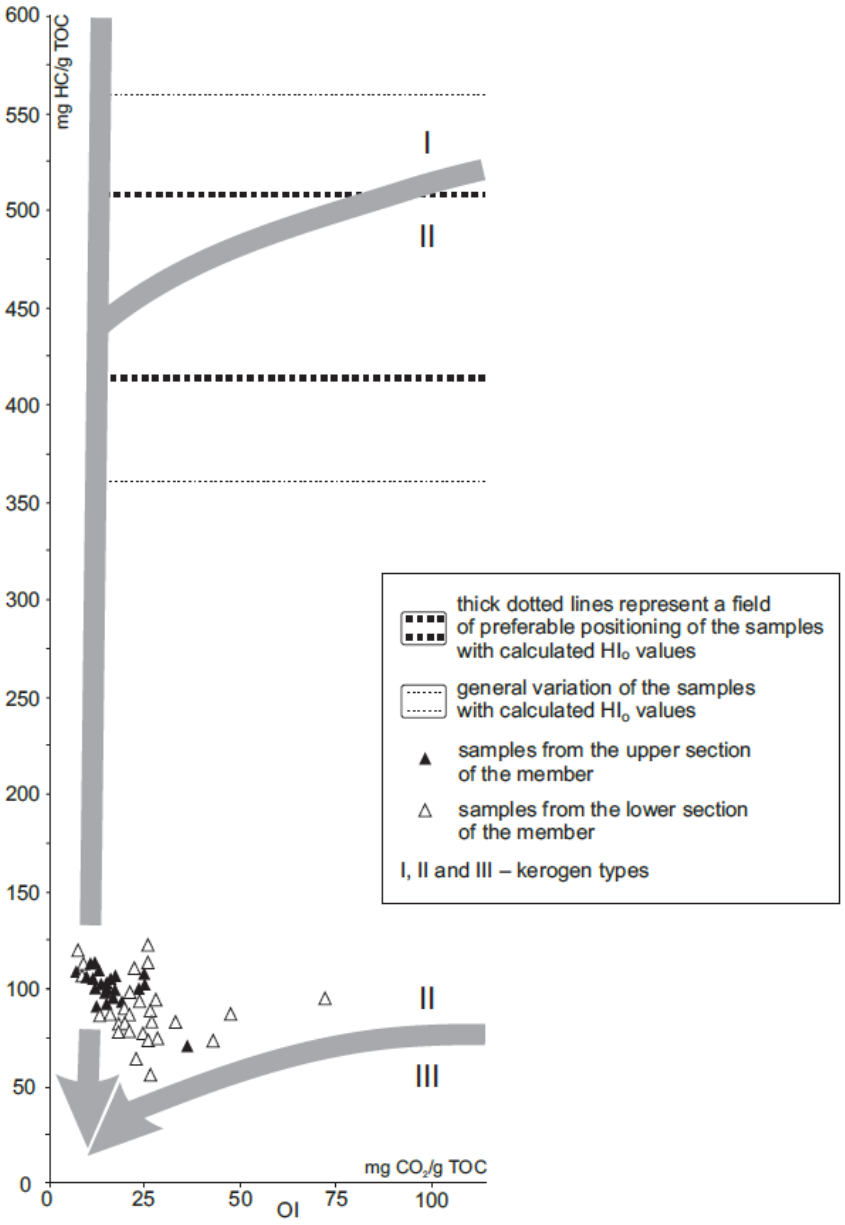

Figure 6. Hydrogen index versus oxygen index diagram showing the difference between the present day hydrogen index (HI_{pd}) and the back calculated (original) hydrogen index (HI_o) of the samples (from Karcz, 2014).

Karcz (2014) calculated the original hydrogen index (HI_o) values of the Passhatten Member samples on the basis of the Jarvie et al. (2007) method. Karcz (2014) observed that the present day hydrogen index (HI_{pd}) increases towards the upper part of the section, while HI_o decreases towards the top of the member as shown in Fig. 7.

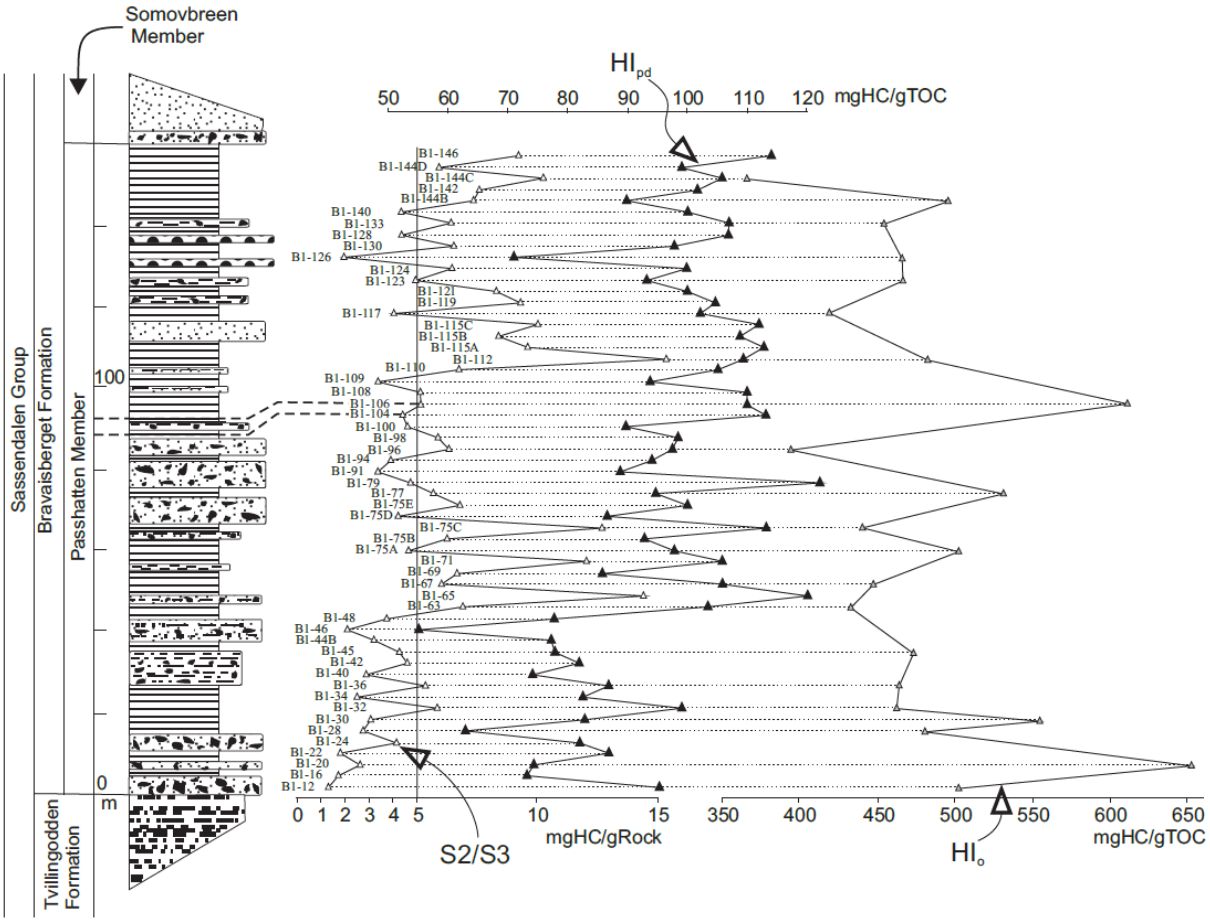

Figure 7. The discrepancy between the present day (HI_{pd}) and original hydrogen index (HI_o) is larger in the lower and smaller in the upper part of the Passhatten Member. The S2/S3 ratio trend is also shown. For the legend of the lithology column and sample locations, refer to Fig. 4 (from Karcz, 2014).

The production index and vitrinite reflectance values ((Fig. 8) indicate early mature to mature organic matter in the Passhatten Member (Karcz, 2014). These values are inconsistent with the general T_{max} values over 455 ˚C (Fig. 8), which suggest the organic matter in the member is overmature (Karcz, 2014).

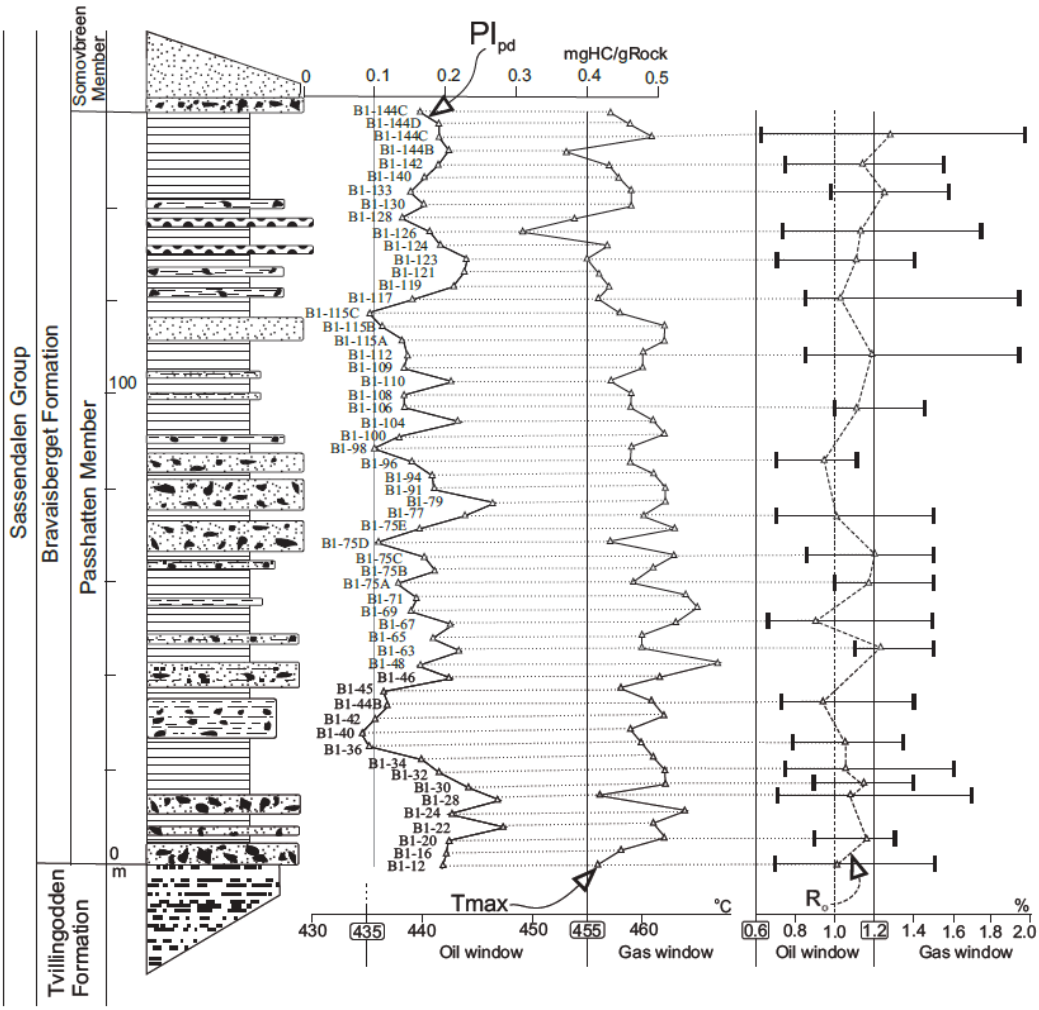

Figure 8. The vitrinite reflectance, T_{max} and production index trend in the Passhatten Member. For the legend of the lithology column and sample locations, refer to Fig. 4 (from Karcz, 2014).

The inconsistency between the vitrinite reflectance values, the T_{max} trend and the back caluclated transformation ratio range in the member might be explained by the presence of bitumen (Karcz, 2014), which is capable of impregnating the vitrinite particles resulting in lower measured vitrinite values (Robert, 1988).

The interpretation based on the T_{max} values is supported by the back calculated transformation ratio values shown in Table 2, indicating the organic matter in the section has reached the upper part of the gas window (Karcz, 2014).

The maceral composition of the samples, presented in Table 2, shows a vitrinite volume percentage of 6% to 40%, decreasing towards the top of the member. The inertinite content of the section increases towards the top of the Passhatten Member. The liptinite volume percentage in the sequence follows the vitrinite trend and decreases towards the top (Karcz, 2014).

Table 2. The table shows the results of visual kerogen assessment and vitrinite reflectance measurements as well as the back calculated transformation ratio (TR), initial organic carbon (TOC_o) and original hydrogen index values (HI_o) (from Karcz, 2014).

Samples	Location	Vitri-nite	Inerti-nite	Lipti-nite	Ro Min	Ro AVG	Ro Max	TR	TOC_o	HI_o
		(%)	(%)	(%)	(%)	(%)	(%)	(%)	(wt.%)	(mgHC/ gTOC)
B1- 144 C	Upper section	26	74	0	0.62	1.28	1.97	77	3.14	366
B1- 142	Upper section	21	41	38	0.75	1.14	1.54	88	2.51	496
B1- 133	Upper section	9	80	11	0.98	1.25	1.57	83	2.47	454
B1- 126	Upper section	10	74	16	0.72	1.13	1.73	89	2.34	466
B1- 123	Upper section	10	74	16	0.69	1.11	1.44	86	2.88	466
B1- 117	Upper section	28	52	20	0.70	1.03	1.40	82	2.63	419
B1- 112	Upper section	29	29	42	0.86	1.19	1.94	84	5.02	482
B1- 106	Upper section	6	34	60	1.01	1.11	1.43	89	4.03	611
B1- 96	Lower section	33	50	17	0.71	0.95	1.16	81	2.4	394
B1- 77	Lower section	13	43	43	0.70	1.01	1.53	89	2.42	532
B1- 75 C	Lower section	40	20	40	0.83	1.02	1.52	81	3.41	440
B1- 75 A	Lower section	17	47	36	1.00	1.17	1.52	86	2.53	503
B1- 67	Lower section	29	43	29	0.64	0.90	1.48	83	2.67	447
B1- 63	Lower section	28	45	26	1.10	1.23	1.50	83	2.62	433
B1- 44 B	Lower section	22	44	33	0.72	0.94	1.40	88	3.54	473
B1- 36	Lower section	30	33	37	0.78	1.06	1.34	86	3.04	464
B1- 32	Lower section	32	32	37	0.74	1.05	1.60	85	2.04	462
B1- 30	Lower section	13	38	49	0.88	1.15	1.39	91	1.79	555
B1- 28	Lower section	25	38	38	0.70	1.08	1.70	91	1.29	481
B1- 20	Lower section	6	20	74	0.89	1.16	1.31	94	1.42	653
B1- 12	Lower section	30	20	50	0.70	1.01	1.45	87	0.96	503

2.1.4 Depositional environment

The lower part of the Passhatten Member was deposited under a high biological productivity zone and therefore the organic matter in this part of the section was more fresh and reactive than in the upper prt of the section (Karcz, 2010 and 2014). This is indicated by the lithological changes, the wide variation in the present day TOC values, the original TOC trend, the present day and initial hydrogen index trends and by wide variation in the isotopic sulphur composition (Karcz, 2010 and 2014). The enhanced biological productivity in the surficial waters and the high inorganic sedimentation rate resulted in the enhanced microbial decomposition of the organic matter (Karcz, 2010 and 2014). The high supply of reactive organic matter is also shown by the high rate of dissimilatory sulphate reduction (Karcz, 2010). The preservation of organic matter was occasionally disturbed by the fluctuation of oxygen levels on the shelf

bottom from anoxic to dysoxic conditions (Krajewski et al., 2007; Karcz, 2010 and 2014). (Karcz, 2010 and 2014).

The upper part of the Passhatten Member was deposited after the Late Anisian transgression, which resulted in the increase of biological productivity at the top of the water column and also increased the water column height (Krajewski et al., 2007; Karcz, 2010 and 2014). Based on the present day and original TOC trends, the measured and back calculated hydrogen index values, lithological changes, maceral group compisition and the narrow variation in the isotopic sulphur composition, this transgressive pulse enhanced the formation of a reductive, low-energy environment creating more favourable conditions for organic matter preservation (Karcz, 2010 and 2014). The narrow variation of the $\delta^{34}S$ values and the low sulphate dissimilatory sulphate reduction rate indicate that the amount of primary production decreased and the distance between the biological productivity zone and the depositional site increased (Karcz, 2010). This is also supported by the decrease in the liptinite and vitrinite macerals towards the top of the member and by the TOC_{pd}, HI_{pd} and HI_o trends (Karcz, 2014). Moreover this caused a decreased supply of organic matter as well as decreased bottom current and burrower activity (Karcz, 2010 and 2014).

The original hydrogen index (HI_o; 481 mg HC/g TOC) calculated by Karcz (2014) based on the Jarvie et al. (2007) method, is indicative of organic facies B (Jones, 1987). Organic matter classified as organic facies B is deposited in a marine or lacustrine environment under an anoxic water column (Jones, 1987) which is in agreement with the depositional environment interpretation of Karcz (2010; 2014).

2.2 Volg-2 sequence of the Jeppe-1 well, Danish Central Graben

2.2.1 Geological setting

The Volg-2 sequence of the Jeppe-1 well located in the Danish Central Graben (Fig. 9) is of Late Jurassic–Early Volgian age and forms part of the Farsund Formation. (Vollset & Doré, 1984; Andsbjerg & Dybkjær, 2003; Ineson et al., 2003).

The studied part of the Volg-2 sequence is within the Farsund Formation (Fig. 10), and is located between 4865 and 4910 metres (Dahl et al., 2004).

The rift basin of the Danish Central Graben was uplifted during the Early–Middle Jurassic and the Early Jurassic sediments were eroded (Jensen et al., 1986). In the middle and northeastern parts of the Danish Central Graben, deposition of sandstone and mudstone beds occurred (Andsbjerg & Dybkjær, 2003). The combination of the collapse of the rift dome and eustatic sea-level rise during the Callovian–Oxfordian induced a transgressive pulse (Ziegler, 1990). The Oxfordian–Kimmeridgian was characterized by deep-water conditions (Andsbjerg & Dybkjær, 2003). During this period, deep marine shales such as the Farsund Formation were deposited in the basins accompanied by shallow marine sandstone deposition on the platforms (Jensen et al., 1986; Ziegler, 1990).

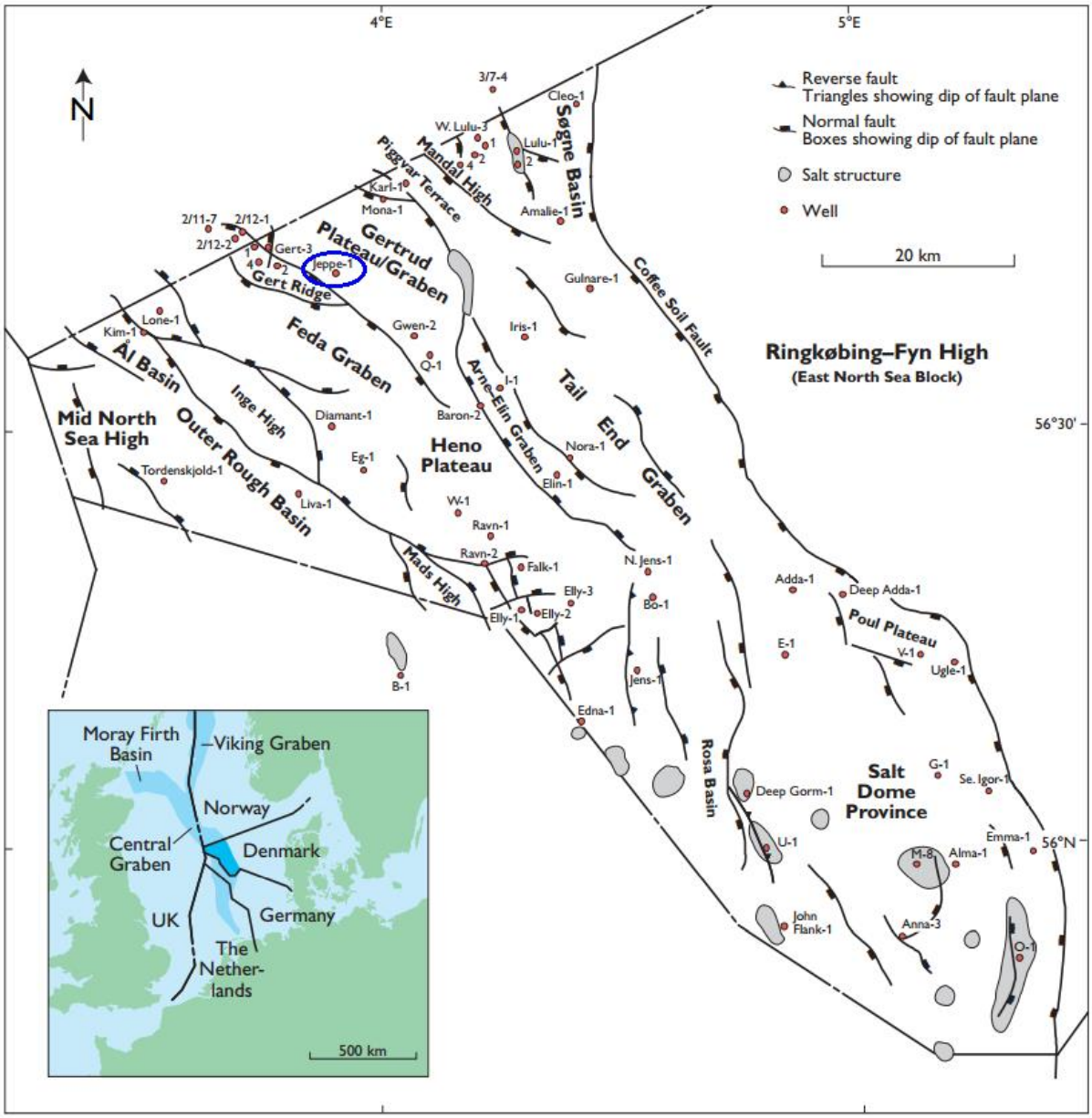

Figure 9. Structural map of the Danish Central Graben. The location of the main figure is marked by dark blue on the regional map. The blue circle marks the location of the Jeppe-1 well (from Andsbjerg & Dybkjær, 2003).

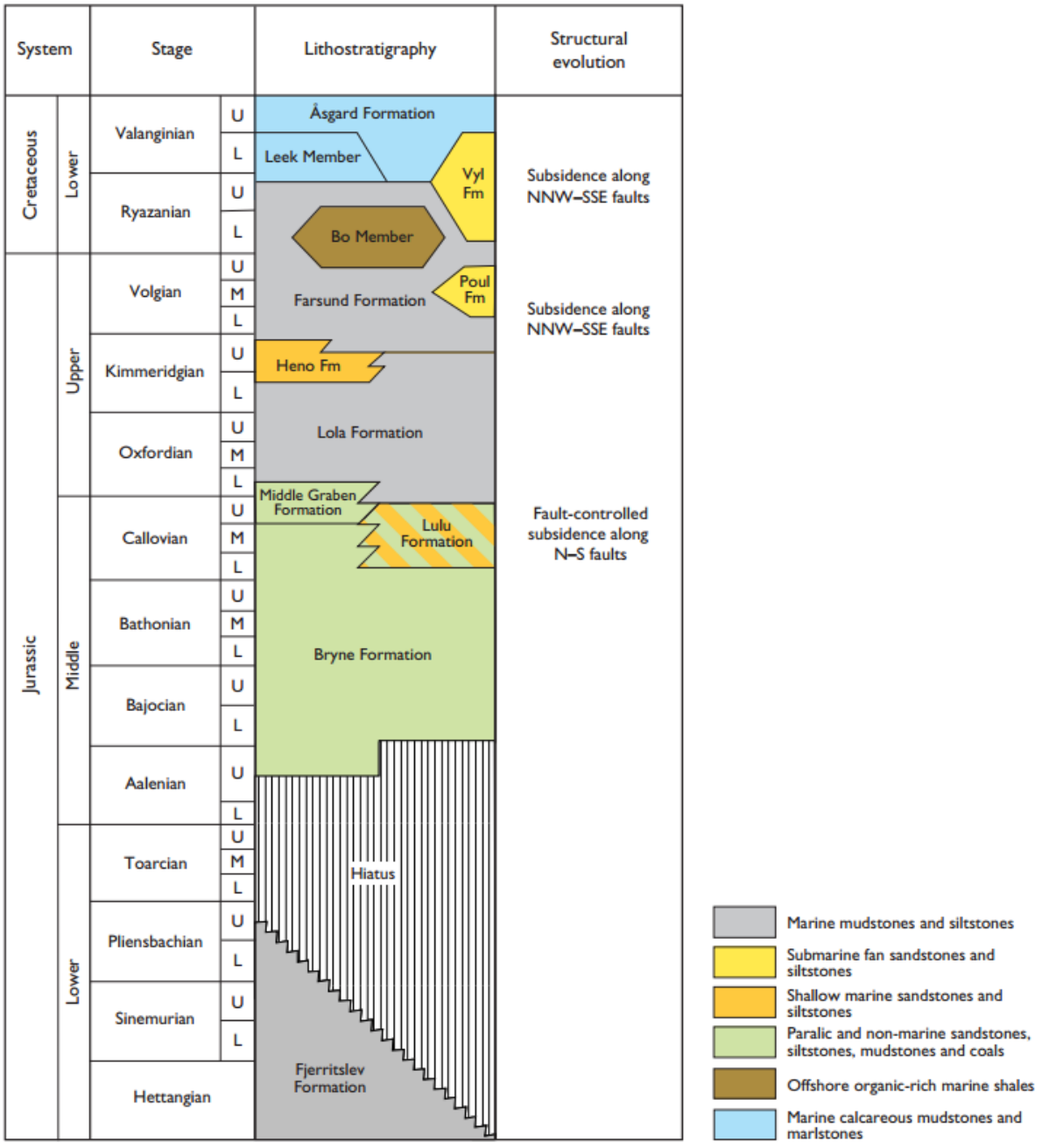

Figure 10. Jurassic lithostratigraphy of the Danish Central Graben showing the stratigraphic position and age of the Farsund Formation (from Andsbjerg & Dybkjær, 2003).

As a response to subsidence and flooding of the area during the Volgian, basinal mudstone deposition prevailed (Andsbjerg & Dybkjær, 2003). Apart from the deposition of mudstones, sandstone beds also developed in some wells along the basin axis of the Tail End Graben and Gertrud Graben (Fig. 11), including the Jeppe-1 well (Andsbjerg & Dybkjær, 2003).

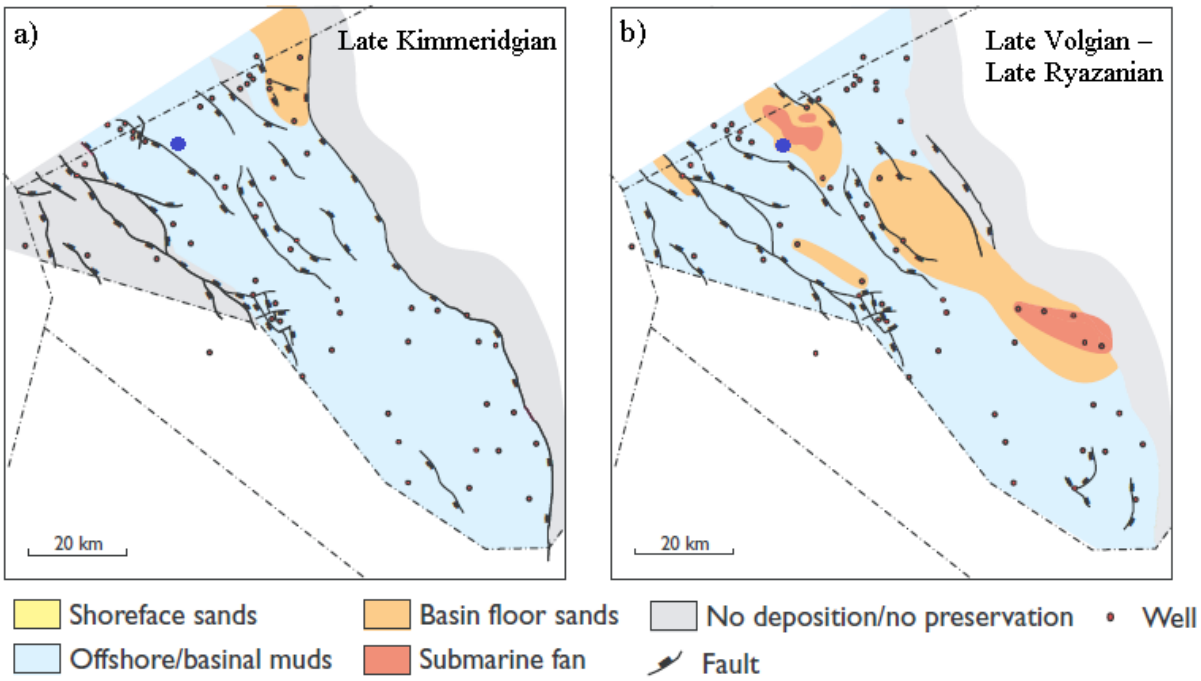

Figure 11. Palaeogeographic maps showing the changes with respect to the depositional environment from the Late Kimmeridgian to the Late Ryazanian. The changes in the sedimentary conditions are reflected in the lithology of the Jeppe-1 well (blue circle) (after Andsbjerg & Dybkjær, 2003).

2.2.2 Geochemical characteristics

Nineteen core samples have been subjected to Rock-Eval pyrolysis from the Farsund Formation of the Jeppe-1 well; the results are shown in Table 3. The geochemical evaluation for the section is based on the data of Dahl et al. (2004) and was carried out in this study.

The tendency of the majority of the geochemical parametres (S1, S2, HI, TOC) to increase towards the upper part of the section is indicative of greater organic-richness in the shallower parts of the Farsund Formation, at 4880 metres and above. The measured values of these parametres are shown in Table 3, while their trends are presented in Fig. 12. The greater organic-richness of the sequence in its upper part is shown by the range of the present day TOC values (Fig. 13). The S1 and S2 values of the sequence show wide variation, suggesting poor to excellent (S1 range) and poor to very good (S2 range) organic matter quantity (Fig. 12) from the base to the top of the sequence (after Peters & Cassa, 1994).

Table 3. Rock-Eval parameters (from Dahl et al., 2004) and calculated vitrinite reflectance (R_o) of the Farsund Formation in the Jeppe-1 well. $R_o = 0.0180 \times Tmax - 7.16$ (equation of Jarvie et al., 2001).

Depth	**S1**	**S2**	**HI**	**TOC**	**PI**	**T_{max}**	**Calculated R_o**
(m)	(mgHC/gRock)		(mgHC/gTOC)	(wt.%)		(˚C)	(%)
4865	5.5	7.5	109	6.85	0.42	439	0.74
4867	3.1	4.2	75	5.59	0.42	435	0.67
4870	5.3	8.3	110	7.56	0.39	440	0.76
4872	9.4	17.1	159	10.7	0.35	439	0.74
4875	6.8	10.1	116	8.73	0.40	437	0.71
4877	8	12.7	133	9.55	0.39	437	0.71
4880	6.9	10.6	127	8.39	0.39	438	0.72
4882	3.1	4.5	81	5.57	0.41	438	0.72
4885	3	4.8	94	5.13	0.38	438	0.72
4887	3	4.6	86	5.33	0.40	439	0.74
4890	2.9	3.9	66	5.91	0.43	438	0.72
4892	3.2	4.6	80	5.79	0.41	438	0.72
4895	0.4	0.3	9	2.74	0.63	439	0.74
4897	0.4	0.3	11	2.66	0.57	438	0.72
4900	1.7	2.4	48	4.98	0.41	439	0.74
4902	0.5	0.5	16	2.89	0.54	439	0.74
4905	0.3	0.1	5	1.82	0.75	431	0.60
4907	0.7	0.6	19	3.32	0.54	441	0.78
4910	0.8	1	27	3.88	0.45	441	0.78

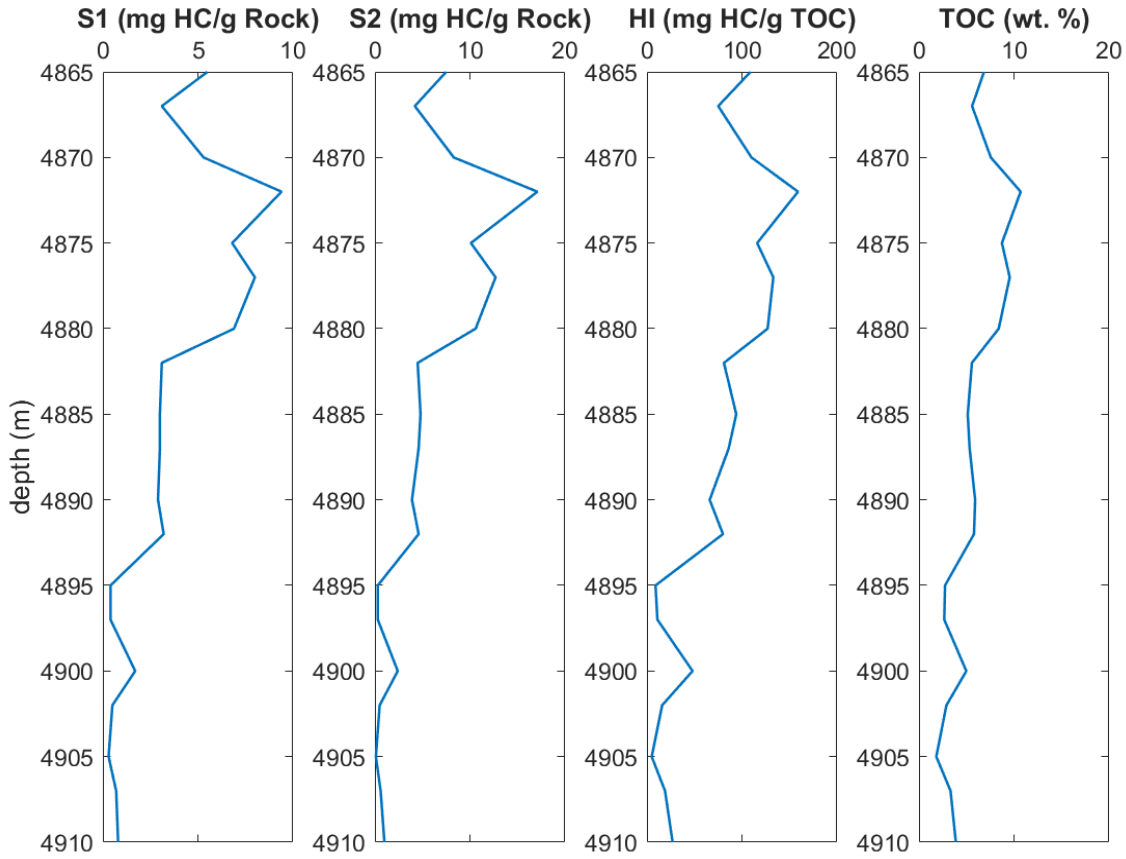

Figure 12. Variation with depth of the Volg-2 sequence showing an increase in the geochemical variables towards the top of the section (after Dahl et al., 2004).

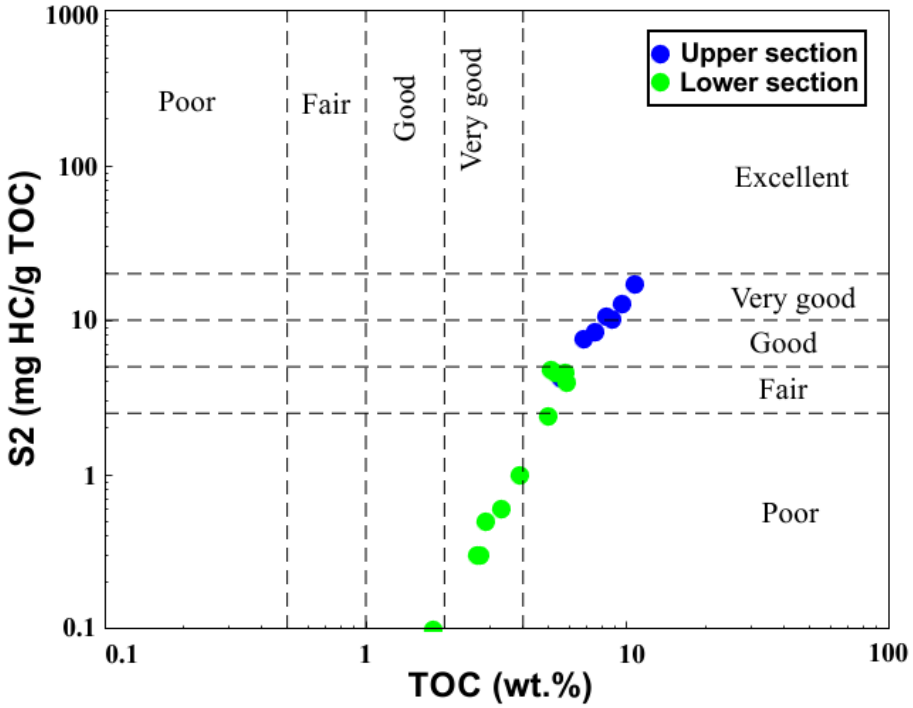

Figure 13. S2 versus TOC cross plot, indicating the organic-richness of the Volg-2 sequence (after Peters & Cassa, 1994 and Dahl et al., 2004).

2.2.3 Interpretation

The geochemical trends described in the previous paragraph might be related to the grading of the Farsund Formation upwards into the organic-rich Bo Member above 4419 metres in the well and to a change in the depositional environment to more favorable conditions for organic matter generation and preservation. Fig. 14 suggests that the organic matter in the section is allochthonous in origin (after Hunt, 1996). Subsequently, the differences in organic matter quality within the Farsund Formation can be related to the presence of a maximum flooding surface around the base of the more organic-rich part of the section as a result of relative sea-level rise not to the degradation of organic carbon due to transportation from the depositional site (Andsbjerg & Dybkjær, 2003). This implies that the organic matter in the upper part of the section was deposited under more favorable conditions than the organic material of the lower part of the section. The reason for this is that the greater water column height might have led to increased biological productivity close to the water surface as well as to decreased bottom stagnation (Killops & Killops, 2013).

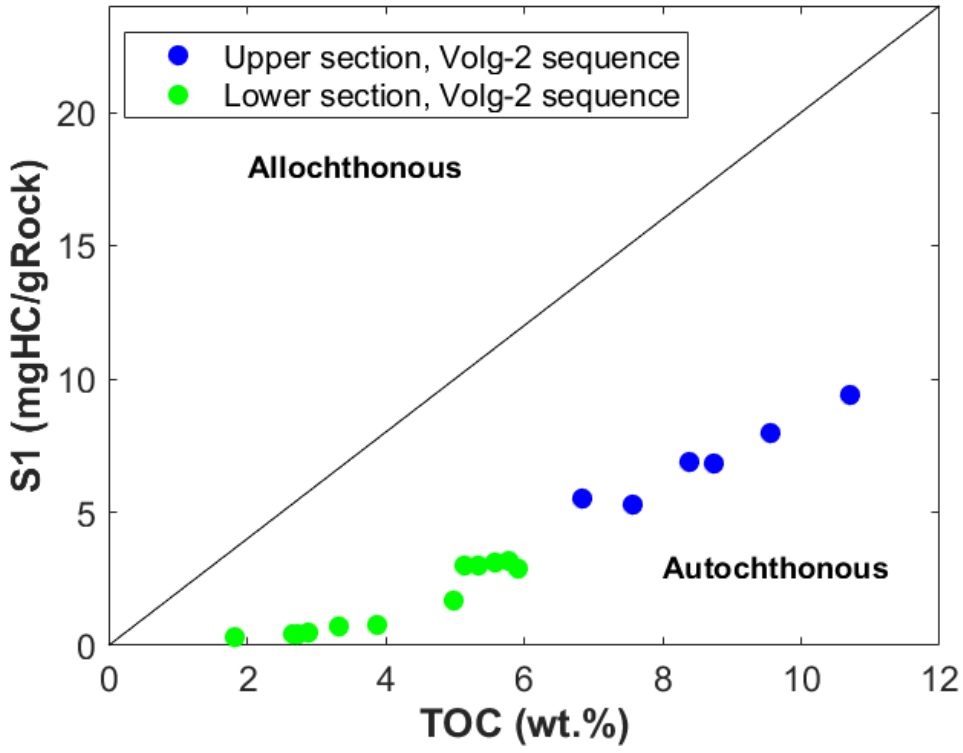

Figure 14. S1–TOC plot of the organic matter in the Volg-2 sequence (Farsund Formation), indicating allochthonous origin (after Hunt, 1996 and Dahl et al., 2004).

2.2.4 Organic matter type and maturity

Information about the non-degraded organic matter of the Volg–2 sequence was not available during this study. The interpretations in this subchapter are based on mature organic matter. Due to the absence of data about the immature organic matter of the sequence, both the kerogen composition of the organic matter based on the degraded material and the assumed kerogen composition of the non-degraded material are tested.

The hydrogen index versus T_{max} (Fig. 15) and S2 versus TOC (Fig. 16) cross plots suggest that the degraded organic matter in the Volg–2 sequence is a mixture of type III (63% of the samples) and type IV (37% of the samples), gas-prone kerogen (after Isaksen & Ledje, 2001 and Langford & Blanc-Valleron, 1990).

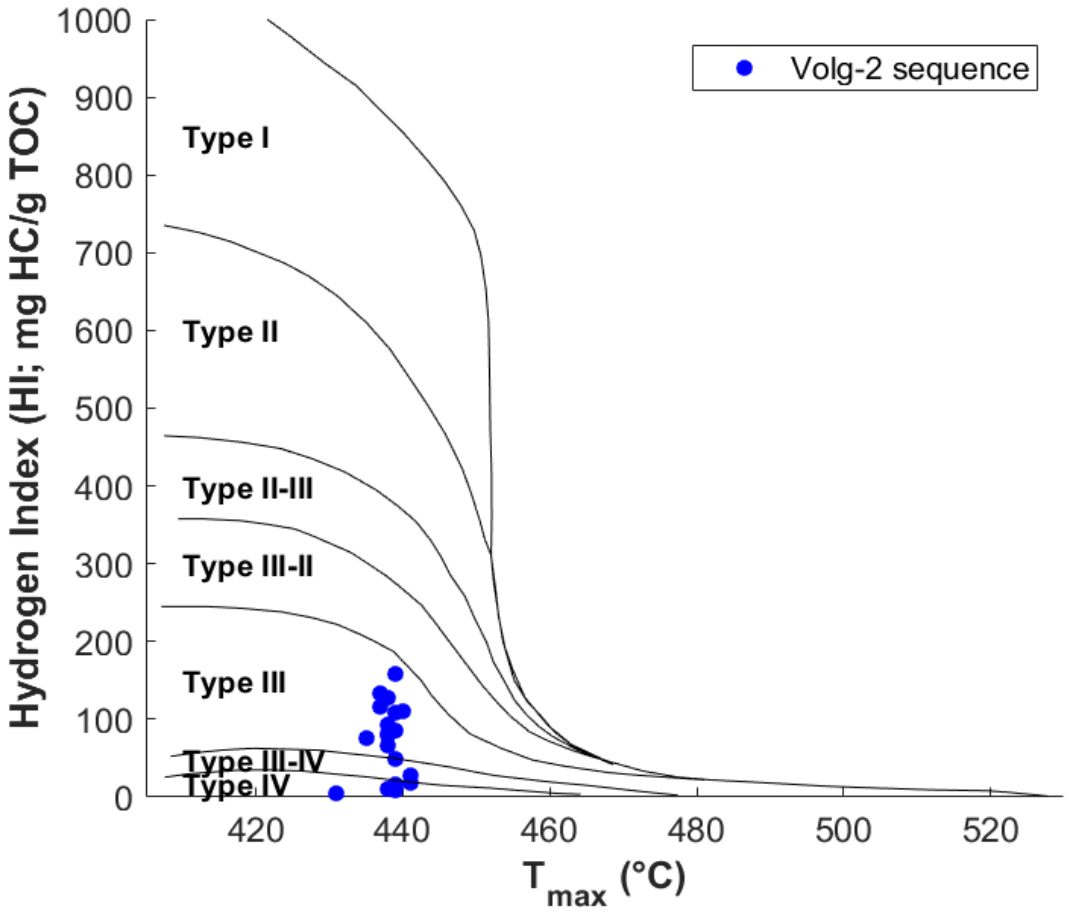

Figure 15. Hydrogen index versus T_{max} cross plot of the Volg-2 sequence in the Jeppe-1 well, indicating a mixture of type III and type IV kerogen of the organic matter (after Isaksen & Ledje, 2001 and Dahl et al., 2004).

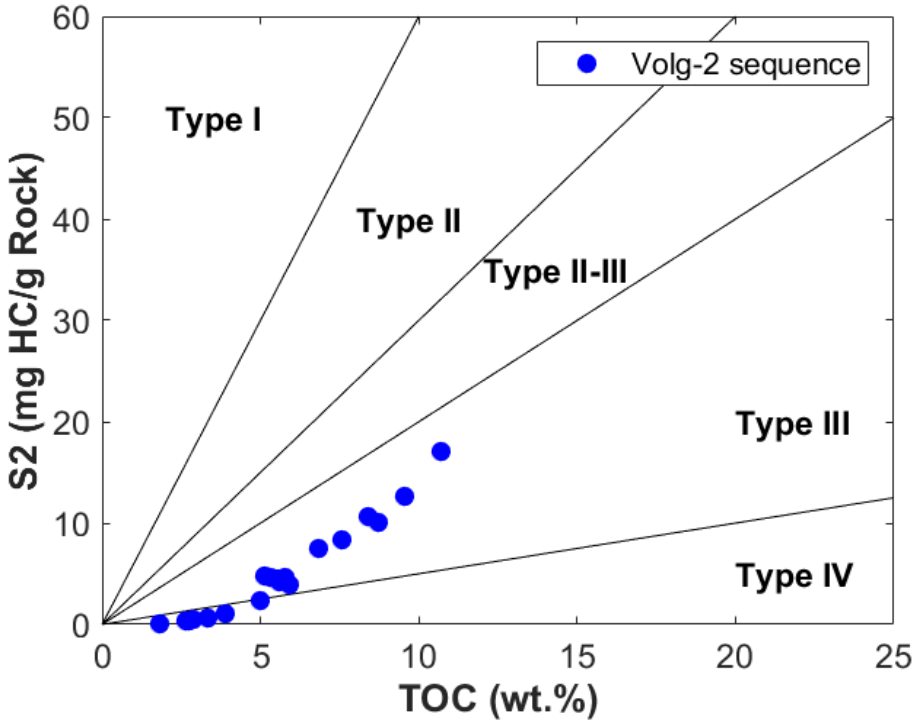

Figure 16. Pyrolysis S2 versus total organic carbon cross plot of the Volg-2 sequence, suggesting the organic matter in the section to be a mixture of type III and type IV kerogen (after Langford & Blanc-Valleron, 1990 and Dahl et al., 2004).

The vitrinite reflectance and T_{max} values in the section (Fig. 17) indicate early to peak oil window maturity for the samples (Peters & Cassa, 1994). The production index indicates 39% of organic matter transformation in the upper and 49% in the lower part of the Farsund Formation (Fig. 17). The overall range of the production index values (0.35–0.75) suggests the presence of peak to late mature organic matter (after Peters & Cassa, 1994).

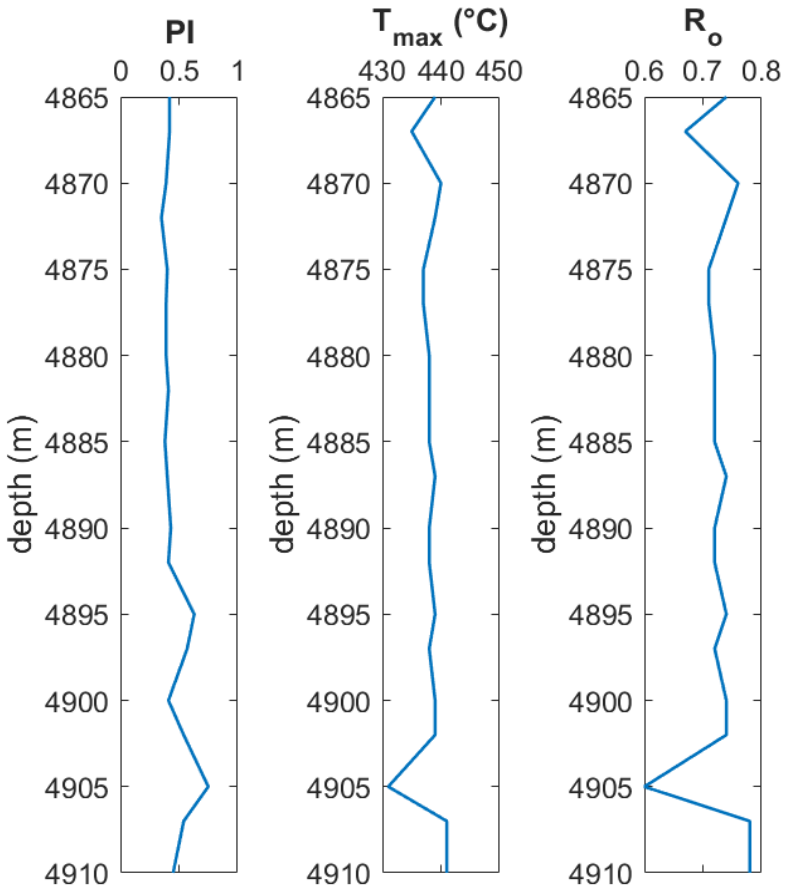

Figure 17. Maturity indicators in the Volg–2 sequence (after Dahl et al., 2004).

2.3 Marine-continental transitional black shales in the Southern North China Basin, central China

2.3.1 Geological setting

The Southern North China Basin (SNCB) is located in the central region of China (Fig. 18) and is a coal-bearing, 15×10^4 km^2 sized basin (Dang et al., 2016). The basin contains organic-rich, marine–continental transitional shales such as the Lower Permian Shanxi and Taiyuan formations (Dang et al., 2016).

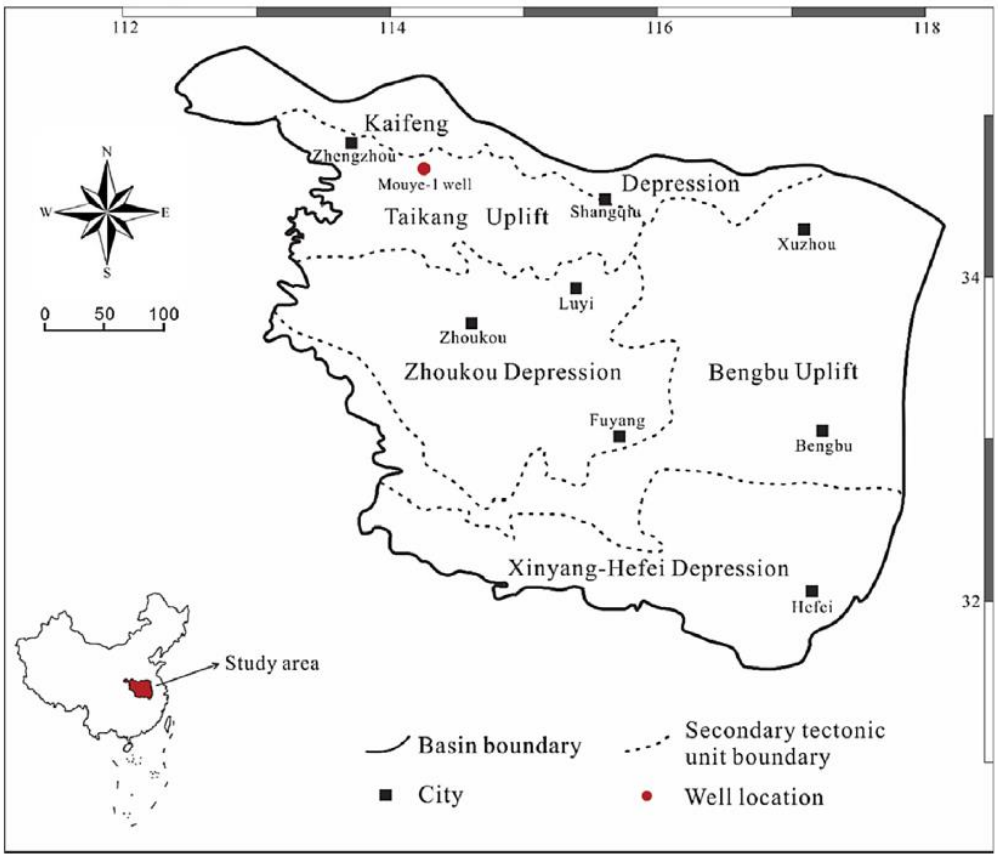

Figure 18. Structural map of the Southern North China Basin showing the location of the Mouye−1 well (from Dang et al., 2016).

The geochemical and geological characterization of these formations were based on outcrop samples and were first studied at the Mouye-1 well (Fig. 18), drilled in the Southern North China Basin in 2014 (Dang et al., 2016).

The Southern North China Basin is filled with Mesozoic–Cenozoic strata lying on the North China Craton (North China Platform) (Dang et al., 2016). The basin incorporates five major structural units: the Kaifeng Depression, the Taikang Uplift, the Zhoukou Depression, the Bengbu Uplift and the Xinyang–Hefei Depression (Yu et al., 2005). The Mouye-1 well is located in the northern part of the Taikang Uplift (Dang et al., 2016).

2.3.2 Geochemical characteristics

Twenty core samples of shale were collected from the Shanxi Formation and thirteen from the Taiyuan Formation in the Mouye-1 well (Dang et al., 2016). The samples were analysed by Rock-Eval pyrolysis, visual kerogen assessment and organic geochemical studies by Dang et al. (2016). The original organic carbon content (TOC_o), initial hydrogen index (HI_o), the

transformation ratio of the organic matter (TR) and the original hydrocarbon generative potential ($S2_o$) were calculated by Dang et al. (2016) according to the Jarvie et al. (2007) method.

According to the total organic carbon values shown in Table 4, the Taiyuan Formation has greater organic richness than the Shanxi Formation in the basin (Dang et al., 2016).

Table 4. Rock-Eval parameters of the studied samples from the Shanxi (Sh.) and Taiyuan (Ta.) formations (from Dang et al., 2016).

Sample	Depth	Formation	TOC_{pd}	S1	S2	T_{max}	PI	HI	Calculated R_o	Measured R_o
	(m)		(wt.%)	(mg HC/g Rock)		(˚C)		(mg HC/ g TOC)	(%)	(%)
JX2	2804.81	Sh.	4.19	0.07	0.40	597	0.15	9.55	3.59	3.44
JX3	2807.74	Sh.	1.00	0.03	0.02	565	0.60	2.00	3.01	3.02
JX4	2810.32	Sh.	0.76	0.06	0.14	576	0.30	18.42	3.20	3.20
JX6	2815.30	Sh.	0.55	0.02	0.14	586	0.13	25.45	3.39	
JX7	2819.27	Sh.	0.53	0.01	0.56	597	0.02	105.66	3.59	
JX8	2821.74	Sh.	1.23	0.03	0.11	562	0.21	8.94	2.96	
JX10	2827.13	Sh.	1.09	0.02	0.09	584	0.18	8.26	3.35	3.35
JX11	2830.72	Sh.	0.52	0.05	0.77	590	0.06	148.08	3.46	
JX12	2831.66	Sh.	0.44	0.03	0.16	581	0.16	36.36	3.30	
JX14	2838.32	Sh.	0.89	0.03	0.08	571	0.27	8.99	3.12	
JX15	2840.23	Sh.	0.48	0.02	0.22	589	0.08	45.83	3.44	
JX16	2841.88	Sh.	2.37	0.09	0.47	598	0.16	19.83	3.60	3.47
JX18	2847.16	Sh.	0.62	0.03	0.09	550	0.25	14.52	2.74	
JX19	2848.82	Sh.	1.98	0.02	0.10	578	0.17	5.05	3.24	3.25
JX22	2852.36	Sh.	2.21	0.05	0.25	579	0.17	11.31	3.26	3.57
JX24	2857.02	Sh.	4.24	0.03	0.34	596	0.08	8.02	3.57	3.55
JX31	2884.30	Sh.	5.10	0.06	0.18	590	0.25	3.53	3.46	3.58
JX32	2886.27	Sh.	1.97	0.01	0.03	579	0.25	1.52	3.26	3.46
JX33	2889.34	Sh.	2.56	0.03	0.10	597	0.23	3.91	3.59	3.55
JX34	2894.31	Sh.	1.78	0.13	0.23	580	0.36	12.92	3.28	
JX36	2913.20	Ta.	3.74	0.05	0.24	586	0.17	6.42	3.39	
JX37	2917.42	Ta	0.92	0.04	0.16	460	0.20	17.39	1.12	
JX40	2925.92	Ta.	1.93	0.03	0.21	588	0.13	10.88	3.42	3.58
JX42	2931.50	Ta.	1.75	0.02	0.10	597	0.17	5.71	3.59	3.59
JX43	2933.86	Ta.	4.14	0.02	0.21	599	0.09	5.07	3.62	
JX45	2939.27	Ta.	1.69	0.07	0.21	577	0.25	12.43	3.23	3.56
JX46	2941.28	Ta.	2.25	0.03	0.18	600	0.14	8.00	3.64	3.50
JX49	2948.32	Ta.	1.87	0.04	0.09	591	0.31	4.81	3.48	3.51
JX50	2950.09	Ta.	1.80	0.03	0.14	594	0.18	2.77	3.53	3.52
JX51	2953.09	Ta.	1.67	0.03	0.18	596	0.14	10.78	3.57	3.46
JX52	2955.71	Ta.	1.88	0.03	0.10	456	0.23	5.32	1.05	
JX53	2958.16	Ta.	2.55	0.02	0.06	590	0.25	2.35	3.46	3.48
JX54	2960.13	Ta.	1.89	0.03	0.03	589	0.50	1.59	3.44	3.34

The TOC_{pd} values measured in the formations (Fig. 19) indicate fair to excellent organic-richness for the entire section with an exception of two samples from the Shanxi Formation showing lower TOC_{pd} values than 0.5 wt.% (Dang et al., 2016). The S1 and S2 trends (Fig. 19) suggest poor organic-richness in the formations (Dang et al., 2016).

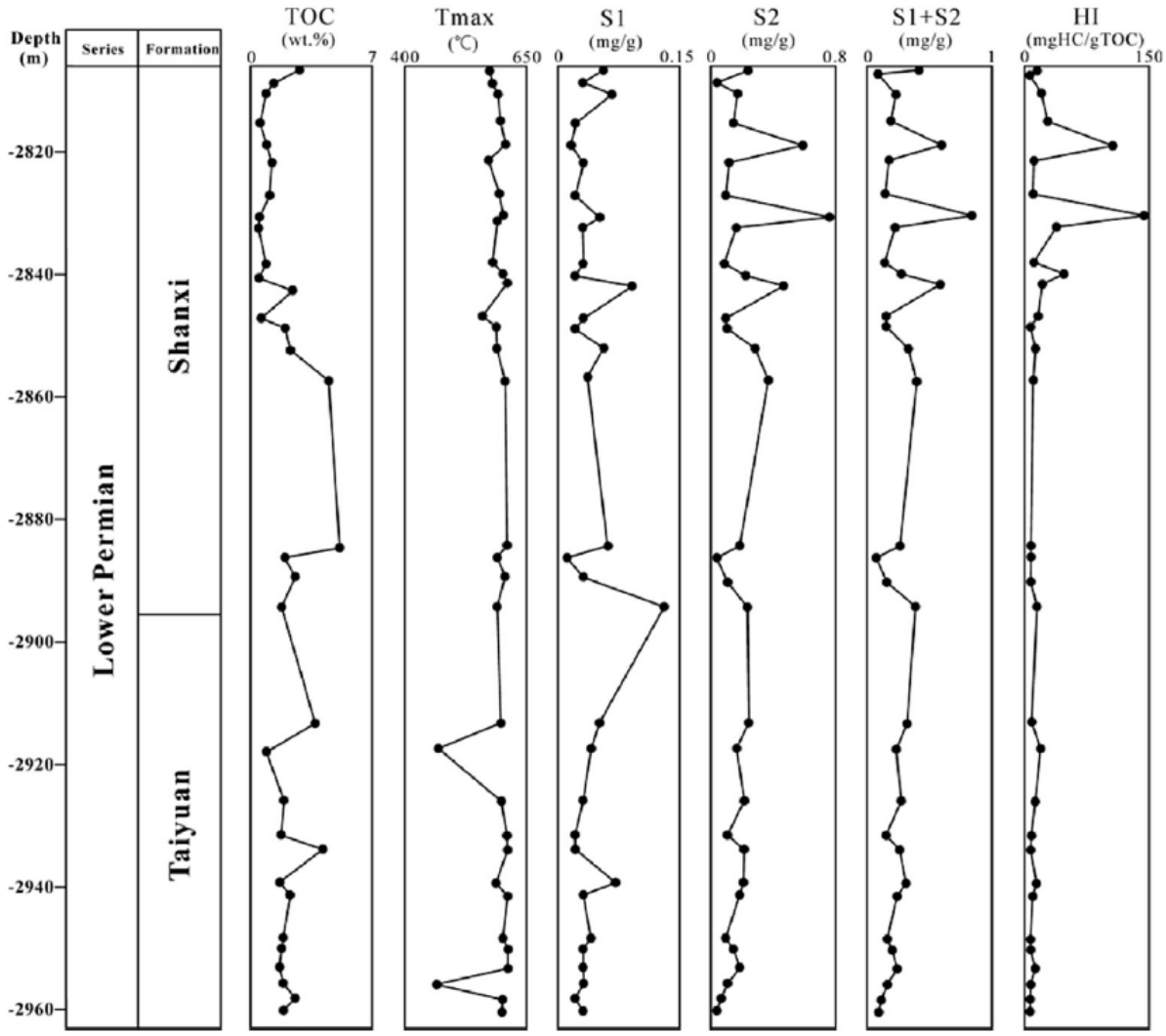

Figure 19. Geochemical log of the Mouye-1 well (from Dang et al., 2016).

2.3.3 Organic matter type and maturity

The organic matter characterization in the well was carried out on the basis of kerogen stable carbon isotope measurements ($\delta^{13}C_{PDB}$) and visual kerogen assessment by Dang et al. (2016) due to the unreliable T_{max} and low hydrogen index values. The kerogen stable carbon isotope values in the formations are between –23.8‰ and –25.0‰ (Table 5), showing the dominance of type III organic matter with the exception of the sample JX19 (Dang et al., 2016). This sample has a kerogen stable carbon isotope value of –25.4‰, indicative of type II kerogen as shown in Table 5 (Hou & Feng, 2011; Dang et al., 2016). This is supported by the calculated

type index values, also shown in Table 5. The type index values are mainly lower than 0 (typical of type III kerogen) with the exception of sample JX19 which yielded a value of 28, indicating type II kerogen (Cao, 1985; Dang et al., 2016).

Table 5. Maceral composition, type index, kerogen stable carbon isotope and organic matter type of the Shanxi (Sh.) and Taiyuan (Ta.) formations (from Dang et al., 2016). TI = type index, calculated by the following formula: $TI = 100 \times a + 50 \times b + (-75) \times c + (-100) \times d$, where a = sapropelinite (%); b = liptinite (%); c = vitrinite (%) and d = inertinite (%) (Dang et al., 2016). The TI classification is as follows: TI ≥80, <80–40, <40–0 and <0 indicate type I, type II_1 (oil-prone organic matter), type II_2 (gas-prone organic matter), type III kerogen respectively (Dang et al., 2016).

Sample	Depth (m)	Formation	Liptinite (%)	Vitrinite (%)	Inertinite (%)	TI	$\delta^{13}C_{PDB}$ (‰)	Organic matter type
JX2	2804.81	Sh.	0	22.4	77.6	–94	–23.9	III
JX3	2807.74	Sh.	0	77	23	–81		III
JX4	2810.32	Sh.	0	94.4	5.6	–76		III
JX6	2815.3	Sh.					–24.7	III
JX10	2827.13	Sh.	64	6	30	–3	–25.0	III
JX12	2831.66	Sh.					–24.5	III
JX16	2841.88	Sh.	0	13.8	86.2	–97	–24.1	III
JX19	2848.82	Sh.	83.5	10.3	6.2	28	–25.4	II2
JX22	2852.36	Sh.	5.6	11.1	83.3	–89	–24.8	III
JX24	2857.02	Sh.	0	14.3	85.7	–96		III
JX31	2884.3	Sh.	11.1	5.6	83.3	–82		III
JX32	2886.27	Sh.	36.9	10.5	52.6	–42		III
JX33	2889.34	Sh.	6.5	7	86.6	–89		III
JX34	2894.31	Sh.					–24.3	III
JX37	2917.42	Ta.					–24.4	III
JX40	2925.92	Ta.	0	7.5	92.5	–98	–24.1	III
JX42	2931.5	Ta.	5.9	11.7	82.4	–88	–24.0	III
JX45	2939.27	Ta.	0	16.1	83.9	–96		III
JX46	2941.28	Ta.	34.3	6.9	58.8	–47		III
JX49	2948.32	Ta.	0	66.7	33.3	–83	–24.4	III
JX50	2950.09	Ta.	0	57.1	42.9	–86	–23.8	III
JX51	2953.09	Ta.	0	15.3	84.7	–96		III
JX52	2955.71	Ta.					–24.0	III
JX53	2958.16	Ta.	0	17.5	82.5	–96		III
JX54	2960.13	Ta.	0	36.8	63.2	–91	–24.4	III

The volume percentages of maceral groups vary throughout the section, indicating frequent changes in the depositional environment (Tissot & Welte, 1984; Dang et al., 2016). According to Table 5, the organic matter in the well is dominated by inertinite (average value of 62.2%; Dang et al., 2016). The liptinite content of the organic material in the Shanxi and Taiyuan formations has an average value of 12.4%, while the second most frequent maceral group in the section is vitrinite with an average value of 25.4% (Dang et al., 2016). The predominance of inertinite in the formations can result from the location of the depositional site being in proximity of a plant matter source as well as from the reworking and oxidization of organic matter (Tissot & Welte, 1984; Killops & Killops, 2013; Dang et al., 2016).

The average vitrinite reflectance values shown in Table 5, 3.35% for the Shanxi and 3.54% for the Taiyuan formations, indicate extremely high thermal maturity as well as that the formation entered the dry gas window (metagenetic stage) and are overmature (Tissot & Welte, 1984; Dang et al., 2016). The explanation of the extremely high thermal maturity of the section lies in the complex thermal evolution history of the Upper Paleozoic succession (Connan, 1974; Zhao et al., 2011; Dang et al., 2016).

2.3.4 Reconstruction of main geochemical parametres

The remaining hydrocarbon generative potential (S2) of the Shanxi and Taiyuan shales, shown in Table 4 is low with average values of 0.22 and 0.14 mg HC/g Rock respectively (Dang et al., 2016). These values indicate that the succession has almost no remaining hydrocarbon generative ability (Dang et al., 2016).

The reconstructed TOC_o values (Table 6) suggest fair to excellent organic-richness for the formations (Fig. 20), while the $S2_o$ values (Fig. 20) indicate poor to very good organic matter quantity (Dang et al., 2016).

Table 6. Back calculated original hydrogen index (HI_o), transformation ratio (TR), initial organic carbon (TOC_o) and original hydrocarbon generative potential ($S2_o$) based on the Jarvie et al. (2007) method for the Shanxi (Sh.) and Taiyuan (Ta.) formations (from Dang et al., 2016).

Sample	Depth (m)	Formation	HI_o (mg HC/g TOC)	TR (%)	TOC_o (wt.%)	$S2_o$ (mg HC/g Rock)
JX2	2804.81	Sh.	66.83	86	4.91	3.28
JX3	2807.74	Sh.	107.75	98	1.12	1.21
JX4	2810.32	Sh.	120.83	86	0.85	1.03
JX10	2827.13	Sh.	310.50	98	1.50	4.65
JX16	2841.88	Sh.	60.34	68	2.61	1.57
JX19	2848.82	Sh.	391.75	99	3.08	12.07
JX22	2852.36	Sh.	80.56	87	2.48	2.00
JX24	2857.02	Sh.	60.73	87	4.95	3.01
JX31	2884.3	Sh.	98.61	97	6.34	6.26
JX32	2886.27	Sh.	205.40	99	2.49	5.12
JX33	2889.34	Sh.	81.05	95	2.92	2.37
JX40	2925.92	Ta.	55.60	81	2.11	1.17
JX42	2931.5	Ta.	82.30	93	1.95	1.61
JX45	2939.27	Ta.	62.10	81	1.84	1.14
JX46	2941.28	Ta.	192.21	96	2.82	5.42
JX49	2948.32	Ta.	100	96	2.13	2.13
JX50	2950.09	Ta.	92.86	97	2.21	2.05
JX51	2953.09	Ta.	61.44	83	1.82	1.12
JX53	2958.16	Ta.	63.10	96	2.86	1.81
JX54	2960.13	Ta.	77.63	98	2.12	1.64

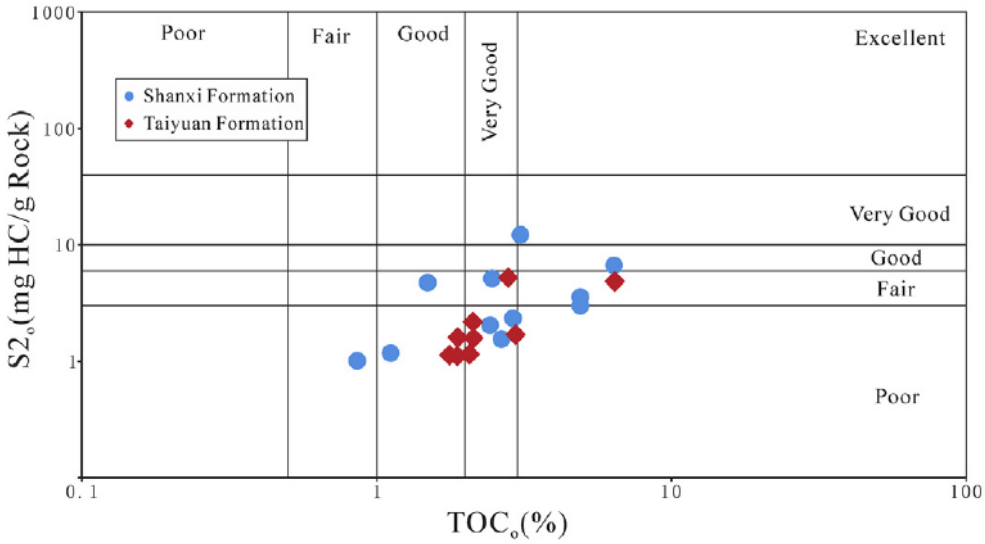

Figure 20. Original hydrocarbon generative potential ($S2_o$) versus initial total organic carbon (TOC_o) cross plot, indicating a poor to fair organic-richness and low original generative potential (from Dang et al., 2016).

2.3.5 Depositional environment

The deposition of the organic matter in the Taiyuan Formation was a result of a transgressive pulse during the Early Permian in the Southern North China Basin (Yu et al., 2005). The transgressive phase originated from the re-subsidence of the basin the Late Carboniferous after being uplifted during the Caledonian orogeny (Zhou et al., 2010). The formation consists of epicontinental shale, coal, limestone and sandstone deposits with a thickness between 30–175 metres (Yu et al., 2005; Zhou et al., 2010). After the deposition of the formation, regression took place in the basin due to the Early Permian collision of the North China and Siberian plates (Yu et al., 2005). This event contributed to the formation of the 50–130 metres thick, shallow water delta beds of the Shanxi Formation (Chen et al., 1997; Liu et al., 1999; Yu et al., 2005; Zhou et al., 2010; Wu et al., 2015). According to Dang et al. (2016), in the last stage of its regional tectonic development during the late Permian, the North China Basin was uplifted again. The uplift of the area resulted in regression, establishing terrestrial sedimentary conditions (Chen et al., 1997; Liu et al., 1999.; Yu et al., 2005; Zhou et al., 2010.

The average original hydrogen index (HI_o) calculated by Dang et al. (2016) based on the Jarvie et al. (2007) method (Table 6) indicates organic facies CD for the Taiyuan Formation (HI_o = 87 mg HC/g TOC) and organic facies C for the Shanxi Formation (HI_o = 144 mg HC/g TOC) (Jones, 1987). These values suggest an inner-shelf environment for the deposition of the organic matter of the formations, and indicate the dominance of terrestrial organic matter input (Jones, 1987). The depositional environment characteristics outlined based on the scheme of Jones (1987) are in agreement with the sedimentary conditions specific for the Early Permian in the Southern North China Basin (Yu et al., 2005; Zhou et al., 2010).

2.4 Wenchang Formation, Huizhou Depression, South China Sea

2.4.1 Geological setting

The Pearl River Mouth Basin is a rift basin, located in the South China Sea (Fig. 21a) and is divided into five tectonic units from north to south (Fig. 21b): the Northern Uplift Zone, the Northern Depression Zone, the Central Uplift Zone, the Southern Depression Zone and the Southern Uplift Zone (Jiang et al., 2015). The Huizhou Depression is situated in the central part of the Northern Depression Zone (Fig. 21c) with an area of 10.000 km^2 (Jiang et al., 2015).

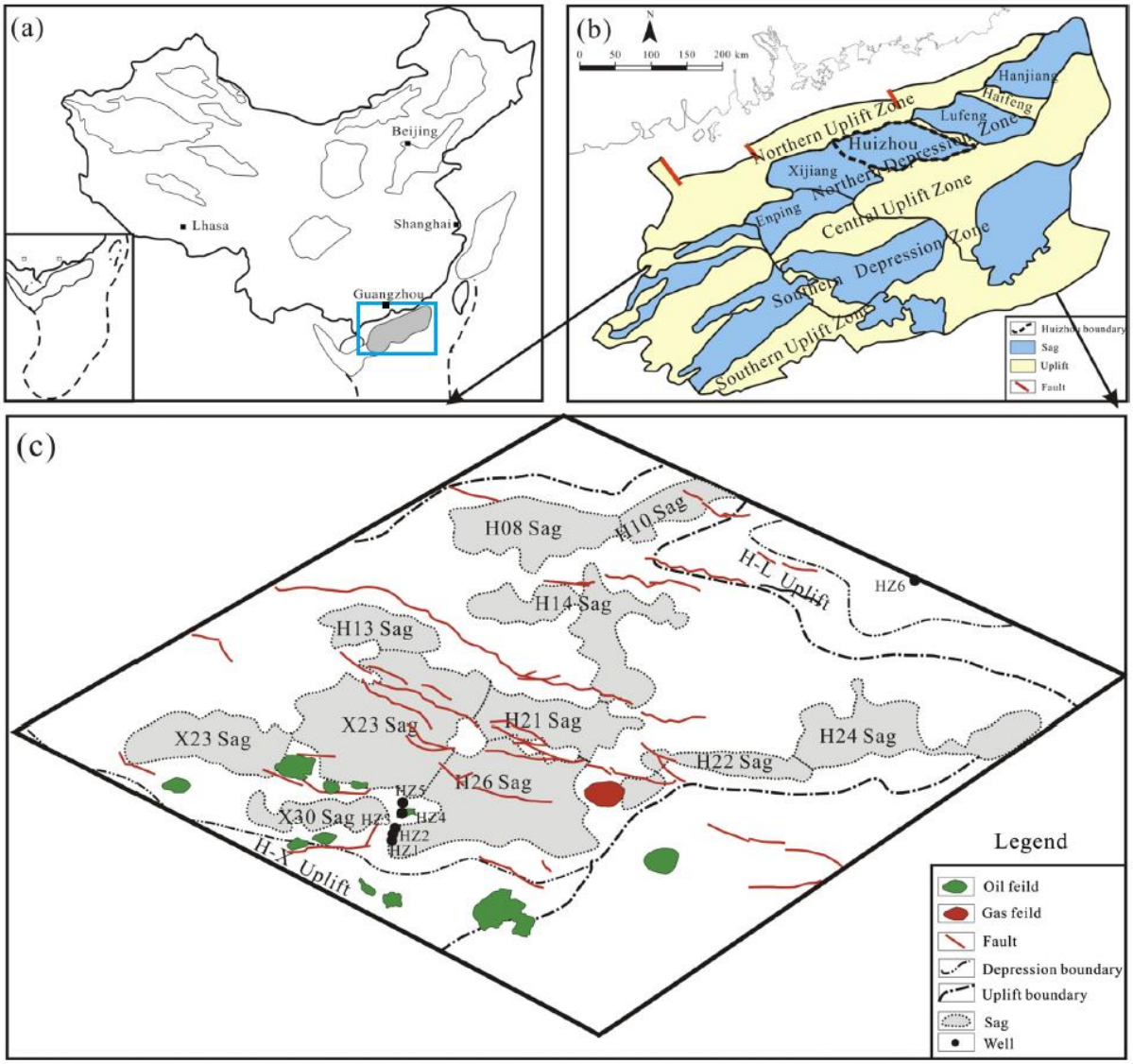

Figure 21. (a) Location (light blue rectangle) and (b) tectonic units of the Pearl River Mouth Basin, and (c) structural map of the Huizhou Depression (from Jiang et al., 2015).

The Huizhou Depression has large estimated hydrocarbon reserves and many discovered oil fields (Jiang et al., 2015). The primary source of these hydrocarbons is the Middle Eocene, shallow to semi-deep, organic-rich, lacustrine mudstones of the Wenchang Formation (Xu et al., 2012). The lithostratigraphy of the Huizhou Depression is shown in Fig. 22.

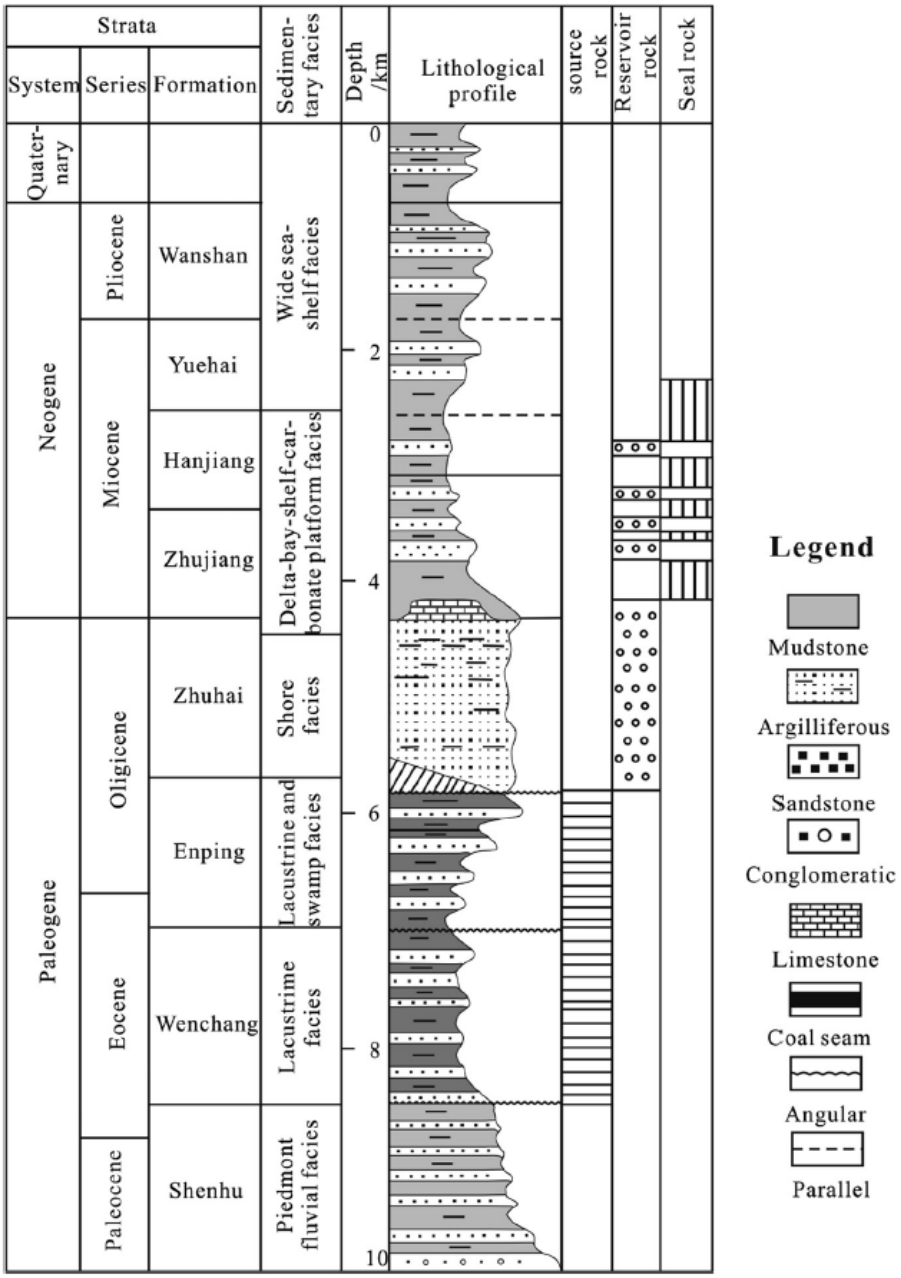

Figure 22. Lithostratigraphic column and petroleum system elements of the Huizhou Depression (from Jiang et al., 2015).

2.4.2 Geochemical characteristics

Seventy-two core samples were collected from five wells in the Huizhou Depression for Rock-Eval and geochemical analysis (Jiang et al., 2015). The results of the Rock-Eval measurements are shown in Tables 7 and 8.

Table 7. Geochemical parameters of samples 1–44 from the Wenchang Formation (WC). R_o = vitrinite reflectance (from Jiang et al., 2015).

Sample	Well	Formation	Depth (m)	TOC (wt.%)	T_{max} (˚C)	S1 (mgHC/gRock)	S2 (mgHC/gRock)	PI (%)	HI (mgHC/gTOC)	Ro (%)
1	HZ1	WC	3556.5	0.30	441	0.15	0.54	0.22	180.00	
2	HZ1	WC	3562.5	0.27	435	0.1	0.36	0.22	133.33	
3	HZ1	WC	3574.5	0.40	436	0.16	0.49	0.25	122.50	
4	HZ1	WC	3577.5	0.39	445	0.2	0.72	0.22	184.62	
5	HZ1	WC	3582.0	0.45	443	0.13	0.57	0.19	126.67	0.730
6	HZ1	WC	3589.5	0.36	436	0.16	0.58	0.22	161.11	
7	HZ1	WC	3595.5	0.35	441	0.11	0.42	0.21	120.00	
8	HZ1	WC	3688.5	0.41	438	0.34	0.72	0.32	175.61	0.714
9	HZ1	WC	3712.5	0.99	455	0.38	1.1	0.26	111.11	
10	HZ1	WC	3745.5	0.44	444	0.17	0.5	0.25	113.64	0.720
11	HZ1	WC	3768.0	2.26	443	1.81	5.14	0.26	227.43	
12	HZ1	WC	3805.5	2.59	451	2.21	6.03	0.27	232.82	
13	HZ1	WC	3844.5	1.02	449	0.65	1.28	0.34	125.49	
14	HZ1	WC	3847.0	0.76	452	0.18	1.14	0.14	150.00	0.725
15	HZ1	WC	3850.0	2.95	453	2.41	5.9	0.29	200.00	
16	HZ1	WC	3859.5	2.16	444	1.06	4.05	0.21	187.50	0.740
17	HZ1	WC	3862.5	1.92	450	0.77	3.8	0.17	197.92	0.760
18	HZ1	WC	3880.5	3.59	453	2.44	7.42	0.25	206.69	
19	HZ1	WC	3883.5	1.98	449	0.77	3.37	0.19	170.20	0.730
20	HZ1	WC	3888 2	2.38	448	1.71	4.38	0.28	184.03	0.730
21	HZ1	WC	3892.5	2.64	450	1.3	4.27	0.23	161.74	0.770
22	HZ1	WC	3898.5	2.22	450	1.77	4.65	0.28	209.46	0.760
23	HZ2	WC	3760.12	0.76	470	0.23	1.02	0.18	134.21	0.700
24	HZ2	WC	3768.12	0.46	444	0.13	0.92	0.12	200.00	
25	HZ2	WC	3770.12	0.37	419	0.12	0.57	0.17	154.05	0.710
26	HZ2	WC	3771.12	0.39	422	0.12	0.64	0.16	164.10	
27	HZ2	WC	3774.12	0.55	440	0.14	0.96	0.13	174.55	0.720
28	HZ4	WC	3715.5	0.86	450	0.12	0.39	0.24	45.35	
29	HZ4	WC	3718.5	0.80	443	0.11	0.78	0.12	97.50	0.681
30	HZ4	WC	3721.5	1.70	445	0.2	1.53	0.12	90.00	
31	HZ4	WC	3727.5	1.22	448	0.23	1.18	0.16	96.72	
32	HZ4	WC	3733.5	1.46	448	0.35	2.18	0.14	149.32	
33	HZ4	WC	3733.5	1.72	449	0.54	3.15	0.15	183.14	
34	HZ4	WC	3736.5	1.86	451	0.51	2.41	0.17	129.57	
35	HZ4	WC	3748.5	1.71	450	0.61	3.44	0.15	201.17	
36	HZ4	WC	3754.5	0.99	453	0.28	1.11	0.2	112.12	
37	HZ4	WC	3757.5	1.51	449	0.37	2.86	0.11	189.40	0.739
38	HZ4	WC	3763.5	2.17	452	0.46	5.02	0.08	231.34	
39	HZ4	WC	3766.5	2.89	448	0.69	9.73	0.07	336.68	0.751
40	HZ4	WC	3769.5	2.84	462	0.27	6.47	0.04	227.82	
41	HZ4	WC	3772.5	3.03	447	0.69	9.2	0.07	303.63	
42	HZ4	WC	3772.5	2.69	453	0.45	6.35	0.07	236.06	
43	HZ4	WC	3781.5	1.07	448	0.2	1.83	0.1	173.83	
44	HZ4	WC	3784.5	1.25	457	0.44	2.01	0.18	160.80	0.723

Table 8. Rock-Eval results and calculated parameters of samples 45–72 from the Wenchang Formation (WC). R_o = vitrinite reflectance (from Jiang et al., 2015).

Sample	Well	Formation	Depth	TOC	T_{max}	S1	S2	PI	HI	Ro
			(m)	(wt.%)	(˚C)	(mgHC/g Rock)		(%)	(mgHC/g TOC)	(%)
45	HZ4	WC	3787.5	0.52	446	0.47	0.81	0.37	155.77	
46	HZ4	WC	3790.5	1.36	449	0.29	2.7	0.1	198.53	
47	HZ4	WC	3802.5	1.25	445	0.12	1.28	0.09	102.40	
48	HZ4	WC	3826	1.08	447	0.12	1.31	0.08	121.30	
49	HZ4	WC	3838.5	1.28	447	0.18	2.81	0.06	219.53	
50	HZ4	WC	3856	1.01	445	0.09	1.33	0.06	131.68	
51	HZ4	WC	3856.5	1.28	448	0.13	1.79	0.07	139.84	
52	HZ4	WC	3874.5	1.47	445	0.18	2.46	0.07	167.35	
53	HZ4	WC	3891.5	0.96	446	0.08	1.34	0.06	139.58	
54	HZ4	WC	3895.5	0.74	443	0.1	1.23	0.08	166.22	
55	HZ4	WC	3907.5	1.13	448	0.12	1.68	0.07	148.67	
56	HZ4	WC	3919.5	1.00	446	0.11	1.55	0.07	155.00	
57	HZ4	WC	3931.5	0.77	446	0.06	0.93	0.06	120.78	
58	HZ4	WC	3946.5	0.70	446	0.07	1.09	0.06	155.71	
59	HZ5	WC	3976	1.23	438	0.36	2.98	0.11	242.28	
60	HZ5	WC	4066.5	0.67	442	0.28	2.11	0.12	314.93	
61	HZ5	WC	4096.5	0.89	445	0.38	2.21	0.15	248.31	
62	HZ5	WC	4096.5	2.14	455	0.52	2.73	0.16	127.57	
63	HZ5	WC	4102.5	1.97	448	0.71	3.71	0.16	188.32	0.774
64	HZ5	WC	4132.5	3.24	454	0.47	4.06	0.1	125.31	
65	HZ5	WC	4165.5	0.83	464	0.23	0.84	0.21	101.20	
66	HZ5	WC	4180.5	2.43	444	0.99	6.41	0.13	263.79	
67	HZ5	WC	4195.5	1.96	446	1.04	3.8	0.21	193.88	
68	HZ5	WC	4204.5	1.20	473	0.27	1.52	0.15	126.67	0.781
69	HZ5	WC	4224.5	1.64	454	0.61	2.03	0.23	123.78	
70	HZ6	WC	3312.5	1.32	442	0.19	1.9	0.09	143.94	0.656
71	HZ6	WC	3742.5	1.14	442	0.12	1.47	0.08	128.95	0.726
72	HZ6	WC	3972	1.42	443	0.16	1.99	0.07	140.14	0.754

According to Tables 7 and 8, the samples from the Wenchang Formation have a wide range of low to high total organic carbon (TOC) values (Jiang et al., 2015). The majority of the samples contain more than 0.5 wt.% organic carbon (Fig. 23), which indicates fair to good organic-richness (Peters & Cassa, 1994; Jiang et al., 2015). The pyrolysis S2 yield (Fig. 23) confirms the intepretation made on the basis of the TOC content in the formation (Peters & Cassa, 1994; Jiang et al., 2015). The S1 range shown in Tables 7 and 8 is however, suggests poor to fair organic-richness (Peters & Cassa, 1994; Jiang et al., 2015).

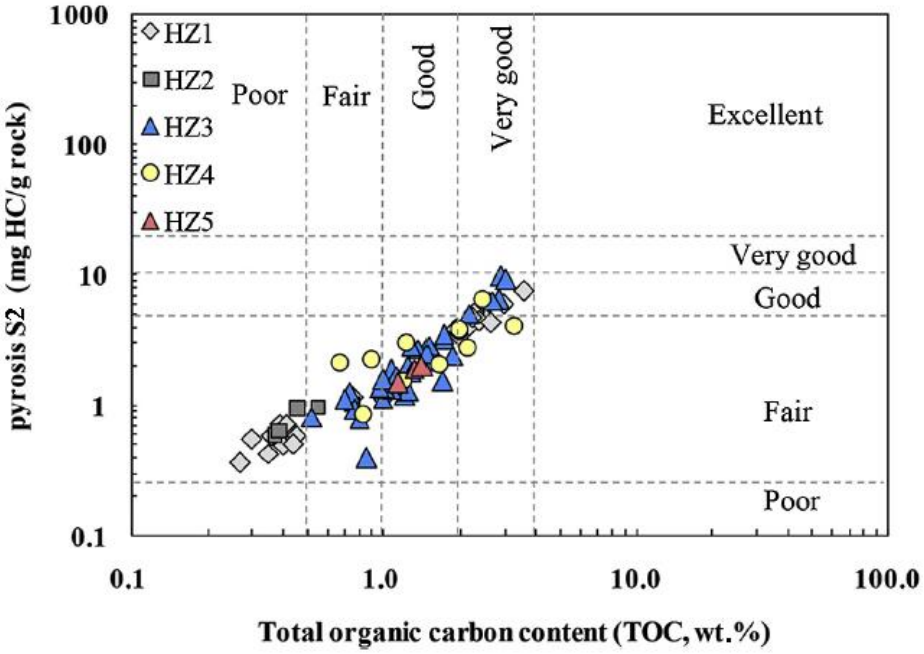

Figure 23. Pyrolysis S2 and total organic carbon (TOC) cross plot of the Wenchang Formation (from Jiang et al., 2015).

2.4.3 Organic matter type and maturity

The organic matter in the Wenchang Formation is classified as type II kerogen (Fig. 24a) with minor amounts of type I and type III kerogen (Tissot & Welte, 1984; Jiang et al., 2015). The majority of the samples with burial depth between 3500 and 4000 metres (Fig. 24b) contain

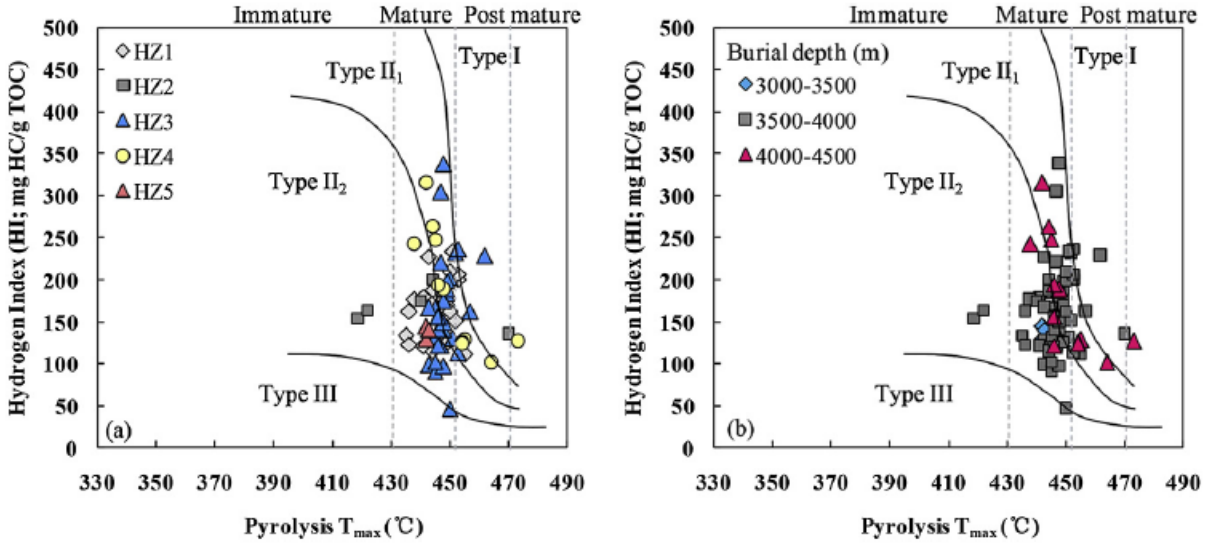

Figure 24. Hydrogen index (HI) versus T_{max} cross plot (a) with respect to well number, and (b) to depth, showing the kerogen type and maturity of the samples (from Jiang et al., 2015).

type II_1 and type II_2 kerogen (Jiang et al., 2015). Samples below 4000 metres depth mainly contain type II_1 kerogen (Jiang et al., 2015). Kerogen type II_1 is characterised by hydrogen index values higher than 300 mg HC/g TOC and represents lacustrine and marine organic matter. Kerogen type II_2 has hydrogen index values between 200–300 mg HC/g TOC (Hao, 1993; Nicholas et al., 2004).

The vitrinite reflectance values shown in Tables 7 and 8, exceed 0.6% and are below 0.8%, indicative of early to peak maturity (Peters & Cassa, 1994; Jiang et al., 2015). According to the T_{max} and production index (PI) ranges in the formation (Fig. 25), most of the samples in the Wenchang Formation are in the main stage of hydrocarbon generation and are thermally mature (Peters & Cassa, 1994; Jiang et al., 2015).

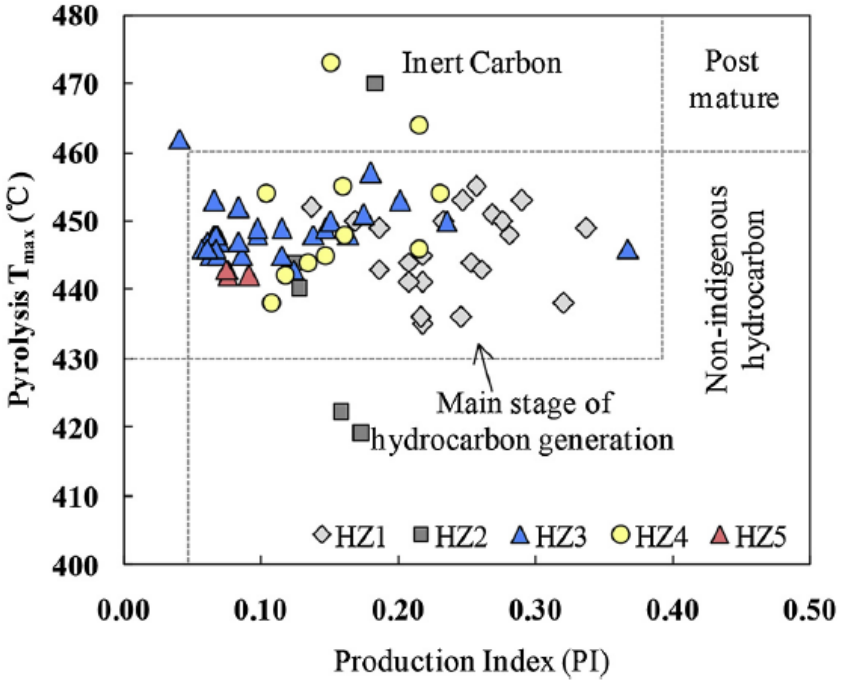

Figure 25. T_{max} versus production index (PI) cross plot showing the maturity and nature of hydrocarbon products of the Wenchang Formation with respect to well numbers (from Jiang et al., 2015).

2.4.4 Depositional environment

The depositional environment of the organic matter in the Wenchang Formation was interpreted on the basis of biomarker data by Jiang et al. (2015). The biomarker data is shown in Table 9 and the inferred depositional environment is discussed in the following paragraphs.

The sterane/hopane ratios of the samples shown in Table 9, indicate that the depositional environment of the organic matter in the Wenchang Formation was isolated from marine influence and was probably a lacustrine basin (Tissot & Welte, 1984; Jiang et al., 2015). The

Table 9. Biomarker intensities and ratios in the Wenchang Formation. Pr = pristane; Ph = phitane; TAR = Terrigenous Aquatic Ratio (from Jiang et al., 2015).

Well	Gamma-cerane	C30-hopane	Sterane	Hopane	Gamma-cerane/ C30-hopane	Sterane/ hopane	Pr/ Ph	Pr/ nC_{17}	Ph/ nC_{18}	TAR
HZ4	262278	1836701	1600545	8670110	0.14	0.18	2.02	0.66	0.31	1.13
HZ5	1341909	11966681	16608886	42678368	0.11	0.39	1.12	0.78	0.57	1.49
HZ6	2928606	76927709	66667881	515955789	0.04	0.13	1.67	0.45	0.21	0.85

terrigenous aquatic ratio (TAR) shows the dominance of terrestrial over marine organic matter (Jiang et al., 2015). Furthermore, the gammacerane/C-30 hopane ratio indicate a low salinity environment (Peters et al., 2005; Jiang et al., 2015). The moderate pristane/phitane (Pr/Ph) and the Pr/nC_{17} and Ph/nC_{18} ratios suggest that the organic matter in the formation was deposited in a weak oxidation–weak reduction environment (Peters et al., 2005; Bou Daher et al., 2015).

3. Methodology

The workflow of the five methods used in the study are discussed in this chapter. The limitations of the methods are also described.

For a better understanding, a standard notation was applied in the methods discussed below. The measured – present day – Rock-Eval hydrogen index is denoted by HI_{pd}, the back calculated initial hydrogen index is indicated by HI_o and TR stands for the transformation ratio. TOC_{pd} and TOC_o denote the measured and initial TOC values; PI_{pd} and PI_o are the present day and original production indices; $S2_{pd}$ and $S2_o$ represent the present day and initial hydrocarbon generative potential respectively.

3.1. Method of Peters et al. (1996)

Peters et al. (1996) applied mass balance equations to determine original total organic carbon (TOC_o) values, the fractional conversion of the organic matter (f, same as transformation ratio), the amount of expelled hydrocarbons ($S1_{expelled}$) and the expulsion efficiency (ExEf) of samples from the Jianghan Basin, China. Among these parameters, only TOC_o and the transformation ratio are comparable to the results of the other methods tested in this study. For this reason, the equations for obtaining $S1_{expelled}$ and expulsion efficiency are not presented in the description of the method.

To calculate the geochemical factors introduced in the previous paragraph, an assumption about the original hydrogen index (HI_o) needs to be made. Peters et al. (2005) mention the method of Baskin (1997) as an example of how to obtain HI_o. Baskin (1997) concluded that HI_o can be determined by the estimation of the original atomic H/C ratio.

The steps of the Peters et al. (1996) method are shown as follows.

3.1.1 Step 1: calculation of the transformation ratio

The execution of the Peters et al. (1996) method starts by determining the fractional conversion (transformation ratio) of organic matter to petroleum:

$$TR = 1 - \frac{HI_{pd}\{1200 - [HI_o/(1 - PI_o)]\}}{HI_o\{1200 - [HI_{pd}/(1 - PI_{pd})]\}}, \qquad \text{(Eq. 1)}$$

where HI_{pd} is the present day hydrogen index and HI_o is the original hydrogen index. PI_{pd} stands for the ratio of hydrocarbons already formed to the total hydrocarbons (calculated by S1/(S1+S2) based on Rock-Eval data; Espitalié et al., 1977). PI_o is the assumed original production index of thermally immature organic matter, equal to 0.02 (Peters et al., 1996).

3.1.2 Step 2: calculation of the original organic carbon content (TOC_o)

The original TOC (TOC_o) of the organic matter is determined by the following mass balance equation (Peters et al., 1996):

$$TOC_o = \frac{83.33(HI_{pd})(TOC_{pd})}{[HI_o(1-TR)(83.33-TOC_{pd}) + HI_{pd}(TOC_{pd})]}. \quad \text{(Eq. 2)}$$

The value of 83.33% represents the average carbon content of hydrocarbons (Burnham, 1989).

3.1.3 Mistakes in Peters et al. (2005)

The explanation of the theory and the derivation of the mass balance equations used in the Peters et al. (1996) method are given in Peters et al. (2005). The derived formula for TOC_o in the Appendix of Peters et al. (2005) contains a typo, a subtraction instead of summation in the second part of the denominator (equation 2 here, equation 4.5 in Peters et al., 2005). However, when the authors provide an example of their method, the same calculation is written and used in its correct form (equation 4.2 in the text of Peters et al., 2005).

3.2. Method of Jarvie et al. (2007)

The method of Jarvie et al. (2007) allows the estimation of several geochemical parameters such as original total organic carbon (TOC_o), original hydrogen index (HI_o), transformation ratio (TR) and the initial hydrocarbon generation potential ($S2_o$). The formulas of the method are modified from the mass balance equations of Peters et al. (1996) with the exception of the formula for HI_o.

The workflow of the Jarvie et al. (2007) method is as follows.

3.2.1 Step 1: calculation of the original hydrogen index (HI_o)

The approach presented in the paper of Jarvie et al. (2007) requires the calculation of the original hydrogen index (HI_o) as a first step based on the maceral composition from visual

kerogen assessment and by using the representative HI_o for the four kerogen types. The latter are determined from the results of Jones (1984) who provided a range of hydrogen indices for the main kerogen types. The initial hydrogen index (HI_o) is defined by the following equation:

$$HI_O = \left(\frac{\%\,typeI}{100} \times 750\right) + \left(\frac{\%\,typeII}{100} \times 450\right) + \left(\frac{\%\,typeIII}{100} \times 125\right) + \left(\frac{\%\,typeIV}{100} \times 50\right). \quad \text{(Eq. 3)}$$

3.2.2 Step 2: calculation of the transformation ratio (TR)

The next step in the method is to define the transformation ratio of the organic matter, which represents the change from the original (HI_o) to present day hydrogen index (HI_{pd}) (Jarvie et al., 2007):

$$TR = 1 - \frac{HI_{pd}\,[1200 - HI_o\,(1 - PI_o)]}{HI_o\,[1200 - HI_{pd}\,(1 - PI_{pd})]}. \quad \text{(Eq. 4)}$$

The value 1200 mg HC/g TOC stands for the maximum hydrogen index assuming the general carbon content of hydrocarbons to be 83.33% (Espitalié et al., 1984; Burnham, 1989).

3.2.3 Step 3: calculation of the original organic carbon content (TOC_o)

The original organic carbon content of the organic matter (TOC_o) is calculated on the basis of the initial hydrogen index (HI_o) and transformation ratio (TR):

$$TOC_o = \frac{HI_{pd}\left(\frac{TOC_{pd}}{1+k}\right)(83.33)}{\left[HI_o\,(1-TR)\left(83.33 - \left(\frac{TOC_{pd}}{1+k}\right)\right)\right] + \left[HI_{pd}\left(\frac{TOC_{pd}}{1+k}\right)\right]}, \quad \text{(Eq. 5)}$$

where 83.33% is the average carbon content in hydrocarbons (Burnham, 1989) and *k* is a correction factor (Jarvie et al., 2007). The correction factor is the product of the transformation ratio and pyrolysable carbon content of the organic matter ($k = TR \times C_p$) (P. Karcz, personal communication, 2016). The application of the correction factor is possible without having the measured values for pyrolysable carbon, which is beneficial in case of older datasets (Jarvie et al., 2007). Burnham (1989) described the *k* values for the three frequent kerogen types that can be used in these cases. According to Burnham (1989) and Jarvie et al. (2007), the increase in pyrolysable carbon at high maturity for type I kerogen is 50%, for type II, it is 15% and 0% for

type III. These provide a correction factor of 0.5 for type I kerogen, 0.15 for type II and 0 for type III kerogen respectively. In case the kerogen composition of the organic matter is heterogeneous, the correction factor of the predominant kerogen type in the organic matter is used (Jarvie et al., 2007).

3.2.4 Step 4: calculation of the initial hydrocarbon generative potential ($S2_o$)

The last step in the method is to calculate the initial hydrocarbon generative potential ($S2_o$):

$$S2_o = TOC_o \times 0.36/0.08333 \quad \text{(Eq. 6)}$$

The term $TOC_o \times 0.36$ represents the original pyrolysable carbon content of the organic matter (Jarvie et al., 2007) and 0.08333 is the general carbon content in hydrocarbons (83.33%; Burnham, 1989). The correction factor for high thermal maturity in the equation (0.36) is only valid for type II kerogen (Jarvie et al., 2007). The authors did not provide correction factors for the other kerogen types, which makes the results obtained by the equation for other kerogen types uncertain.

3.2.5 Mistakes in the original reference

3.2.5.1 TOC_o formula

The formula for TOC_o (equation 5) is described incorrectly in Jarvie et al. (2007). The equation has subtraction in the second part of the denominator instead of summation (equation 3 in Jarvie et al., 2007). The reason for the mistake in the equation is the result of presenting the modified form of equation 4.5 from the Appendix of Peters et al. (2005), instead of using equation 4.2 from the text of Peters et al. (2005), which is the correct formula (see chapter 3.1.3). In spite of the fact that Jarvie et al. (2007) present the wrong formula in their paper, the application of it in their study was carried out by the using the correct equation (P. Karcz, pers. comm., 2016).

3.2.5.2 Correction factor

The correction factor in equation 5 is a result of the increase in residual carbon at high maturity (Burnham, 1989). Jarvie et al. (2007) describe *k* as the product of the transformation ratio (TR) and the residual carbon fraction (C_R): $k = TR \times C_R$. However, the description and the formula for *k* is presented incorrectly in Jarvie et al. (2007) and can lead to wrong results and confusion about the calculation of the original TOC content of the organic matter. The correction factor is not the product of the transformation ratio and residual carbon, it is the result of the

multiplication of the transformation ratio (TR) and pyrolysable carbon content (C_P) of the rock: $k = \mathrm{TR} \times \mathrm{C_P}$ (P. Karcz, pers. comm., 2016). The difference between the TOC_o calculated by the wrong and correct formula of *k* is shown by the following example using data from Spitsbergen.

Karcz (2014) applied the method of Jarvie et al. (2007) to calculate various geochemical parameters, such as the transformation ratio of organic matter, the original hydrogen index and the initial TOC content of the Middle Triassic Passhatten Member (Bravaisberget Formation) in Spitsbergen. To demonstrate the differences by using the correct and wrong correction factor in the TOC_o formula (equation 5), the data of sample B1–96 are used. The measured (Karcz, 2014) and estimated values of the sample are given in Table 10:

Table 10. Measured Rock-Eval parameters for sample B1–96 from the Bravaisberget Formation (from Karcz, 2014) and the estimated transformation ratio and initial hydrogen index based on Jarvie et al. (2007).

Sample	**TOC_{pd}** (wt.%)	**HI_{pd}** (mg HC/g TOC)	**RC_{pd}** (%)	**PC_{pd}** (%)	**TR** (%)	**HI_o** (mg HC/g TOC)
B1-96	2.07	98	1.86	0.21	82	394

The transformation ratio presented in Table 10 for the sample is slightly different from the estimated value of Karcz (81%), however, a difference of 1% is acceptable as this can occur due to rounding (P. Karcz, pers. comm., 2016). The correct *k* factor for the sample is then 0.17 $(k = 0.82 \times 0.21)$, while the erroneously calculated factor is 1.53 $(k = 0.82 \times 1.86)$. Then by applying the correct *k* value in equation 5, the correct TOC_o value is 2.46 wt.%. In contrast, the TOC_o calculated by the wrong *k* value (1.53) will be equal to 1.13 wt.%. These calculations shows that the application of the incorrectly calculated *k* in the TOC_o formula results in lower values than by using the correct *k* value.

3.2.5.3 Transformation ratio formula

Jarvie et al. (2007) consider the equation of the transformation ratio to be the same as the formula for fractional conversion (f) of Peters et al. (2005), where the latter contains a division between the terms HI_o and '$1–PI_o$' in the numerator as well as between HI_{pd} and '$1–PI_{pd}$' in the denominator (equation 1). In contrast, the formula of Jarvie et al. (2007) shows a multiplication between these terms (equation 4). Therefore the application of the two equations on the same

dataset will result in different computed transformation ratio values, which will yield different original TOC results as the formula of TOC_o (equation 5) is dependent on the conversion stage of organic matter. Moreover, Karcz (pers. comm., 2016) mentioned that Jarvie et al. (2007) did not apply the complete transformation ratio formula on their dataset, the term containing '$1-PI_o$' in the numerator and '$1-PI_{pd}$' in the denominator were neglected. Using the equation this way is linked to the assumption that '$1-PI_o$' and '$1-PI_{pd}$' will give values close to 1 because the difference between PI_{pd} and PI_o is generally small. As a result, these parts of the equation will have very small or negligible impact on the transformation ratio (P. Karcz, pers. comm., 2016).

The validity of these assumptions was tested on data from the Bazhenov Formation in Western Siberia in this study and the results are presented below. The measured (Galimov et al., 1988) and estimated geochemical values (Peters et al., 2005) of the formation are given in Table 11:

Table 11. Measured and calculated geochemical parameters of the Bazhenov Formation, Western Siberia (from Galimov et al., 1988 and Peters et al., 2005).

Sample depth (m)	**Borehole identifier**	**HI_{pd}** (mg HC/g TOC)	**PI_{pd}** (%)	**PI_o** (%)	**HI_o** (mg HC/g TOC)
2926.3	312	90	0.68	0.02	500

The calculated transformation ratios obtained by using the approach of Peters et al. (2005) (a) and Jarvie et al. (2007) (b) give the following results:

(a) $$TR = 1 - \frac{HI_{pd}\{1200 - [HI_o/(1-PI_o)]\}}{HI_o\{1200 - [HI_{pd}/(1-PI_{pd})]\}} = 1 - \frac{90\left[1200 - 500/(1-0.02)\right]}{500\left[1200 - 90/(1-0.86)\right]} = 86.49\%$$

(b) $$TR = 1 - \frac{HI_{pd}\,[1200 - HI_o\,(1-PI_o)]}{HI_o\,[1200 - HI_{pd}\,(1-PI_{pd})]} = 1 - \frac{90(1200-500)}{500(1200-90)} = 88.65\%.$$

The discrepancy between the two methods is 2.16%. In case the calculated transformation ratio values of these two methods are used in the corresponding TOC_o equations (equations 2 and 5 respectively), the difference between the estimated TOC_o values will be negligible (Fig. 26).

However, the mixing of the methods will result in greater differences in the calculated TOC_o than when they are used separately. To illustrate how much difference there will be between the methods in terms of the TOC_o value, a range of 0−15 wt.% was assigned to TOC_{pd}. First, a prediction of TOC_o is shown in Fig. 27, when the calculated transformation ratio values of the Peters et al. (1996; a) and Jarvie et al. (2007; b) methods are used in the TOC_o formula of

Peters et al. (1996) (equation 2).

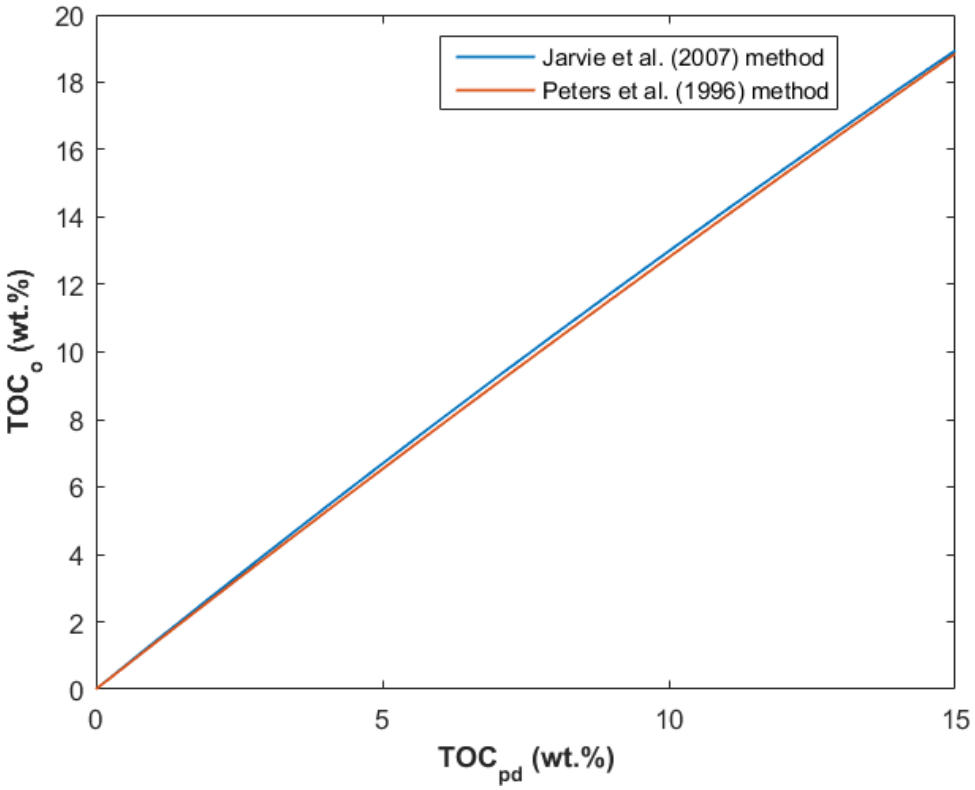

Figure 26. Differences between the TOC_o back calculation of the Peters et al. (1996) and Jarvie et al. (2007) methods. The two methods operate with different transformation ratio values which will cause only minor variation in the resulting TOC_o.

The difference between the estimated TOC_o values due to the particular transformation ratio values is 2.66 wt.% for the Bazhenov sample. It can also be concluded from Figure 27, that the greater TOC_{pd} is, the larger the difference is between the calculated TOC_o values. This is the result of the different transformation ratio estimations only.

The same procedure was followed when examining how TOC_o values change when the same transformation ratio values (calculated previously by the Peters et al., 1996 and Jarvie et al., 2007 methods) are used in the TOC_o formula of Jarvie et al. (2007). Furthermore, to account for the correction factor in equation 5 for TOC_o, a *k* value of 0.15 was applied due to the type II kerogen nature of the organic matter in the Bazhenov Formation (Jarvie et al., 2007; Lopatin et al., 2003).

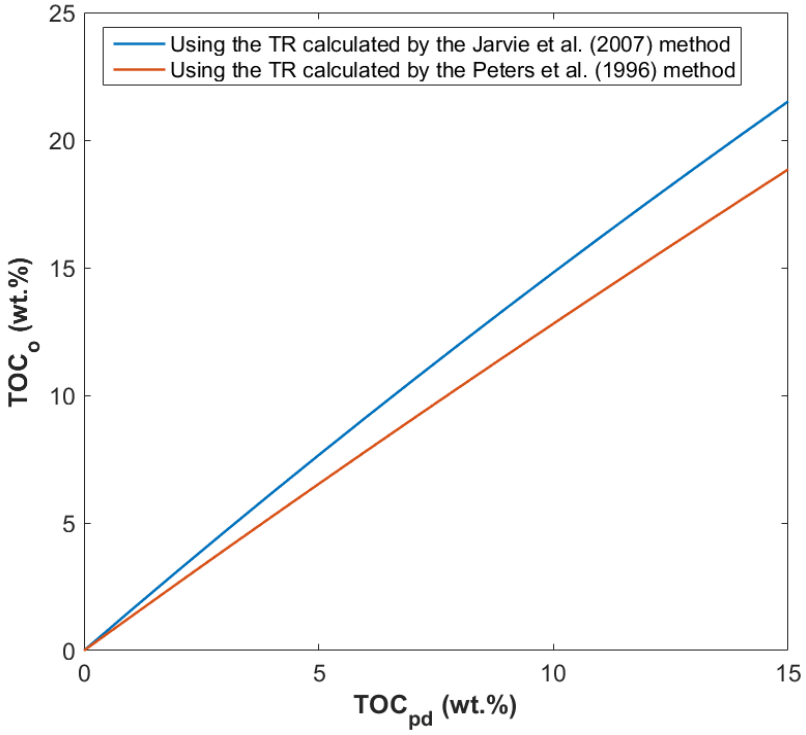

Figure 27. The difference between the back calculated TOC_o values when the transformation ratios of the Peters et al. (1996) and Jarvie et al. (2007) methods are used in the TOC_o formula of Peters et al. (1996).

In this case, the two TOC_o values differ by 2.43 wt.% as shown in Fig. 28. The figure suggests the same trend as described before: the results will be more diverse as TOC_{pd} increases. Furthermore, the results of the Jarvie et al. (2007) method are the largest in all cases. In conclusion, the exact application of the transformation ratio formula of Jarvie et al. (2007) is defined incompletely and therefore it should be used with caution. When mixing of the two methods occurs to avoid the application of the inappropriately described formula, the result might be an overestimation of the original quantity of organic material.

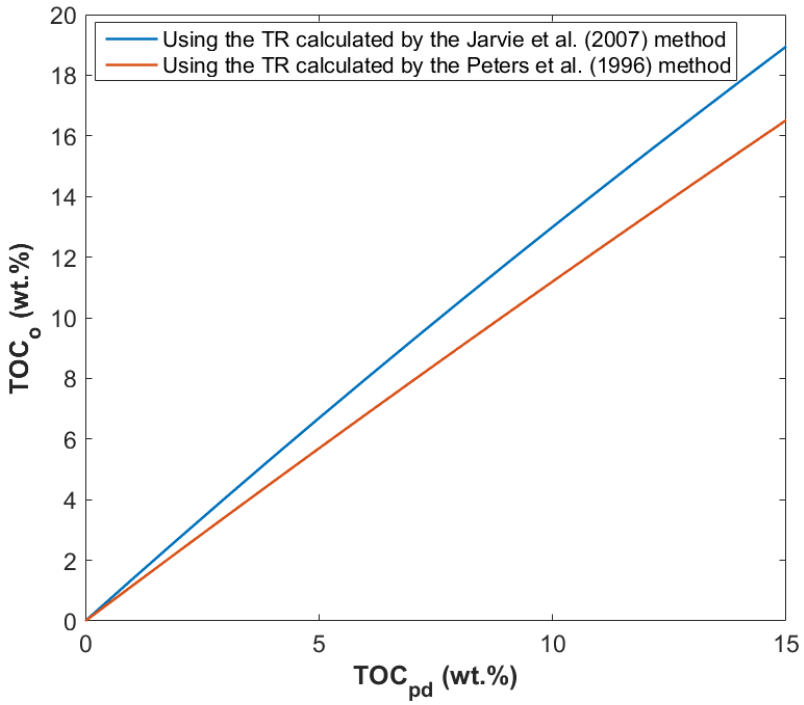

Figure 28. The difference between the back calculated TOC_o values in case the transformation ratios calculated by the Peters et al. (1996) and Jarvie et al. (2007) methods are used in the TOC_o formula of Jarvie et al. (2007).

3.3. Method of Jarvie (2012)

Jarvie (2012) constructed a quick and easily applicable method to calculate the original TOC (TOC_o), the original generative- (GOC_o) and non-generative organic carbon content ($NGOC_o$) and the initial hydrocarbon generative potential ($S2_o$) of the organic matter. The steps of the method are explained in the following subchapters.

3.3.1 Step 1: calculation of the transformation ratio

The first step of the Jarvie (2012) method is to determine the transformation ratio:

$$TR = (HI_o - HI_{pd})/HI_o. \quad \text{(Eq. 7)}$$

3.3.2 Step 2: calculation of the original organic carbon content (TOC_o)

To obtain TOC_o, first the fraction of organic carbon (OC) in S1+S2 needs to be calculated:

$$OC = 0.085 \times (S1_{pd} + S2_{pd}). \quad \text{(Eq. 8)}$$

Then, the present day bitumen and kerogen free TOC ($TOC_{pdbkfree}$) needs to be obtained:

$$TOC_{pdbkfree}\ (wt.\%) = TOC_{pd} - \%OC. \quad \text{(Eq. 9)}$$

Moreover, TOC_{pd} needs to be adjusted due to added carbonaceous char from bitumen and/or oil cracking to calculate the non-generative carbon corrected TOC ($TOC_{NGOCcorrection}$) :

$$TOC_{NGOCcorrection}\ (wt.\%) = (HI_o \times 0.0008). \quad \text{(Eq. 10)}$$

Another correction has to be carried out for TOC_{pd} due to the amount of carbon in kerogen and bitumen and/or in oil to obtain $TOC_{pdNGOCadjusted}$:

$$TOC_{pdNGOCadjusted}\,(wt.\%) = TOC_{pdbkfree} - TOC_{NGOCcorrection}. \quad \text{(Eq. 11)}$$

Based on the study of Jarvie (2012) on rock extract and oil fractionation data of marine organic matter and their sourced oils, the carbon content in hydrocarbons is 85%. The maximum original hydrogen index (HI_o) can be estimated by its reciprocal, 1/0.085 or 1177 mg HC/g TOC. Using this value, the generative organic carbon content (%GOC) in the organic matter can be calculated by:

$$\%GOC = HI_o/1177. \quad \text{(Eq. 12)}$$

Jarvie (2012) emphasizes that to calculate the correct volumes of generated hydrocarbons in a certain area in the presence of multiple organofacies, the subdivision of the different organofacies within a rock is essential. For example, if a shale unit consists of two organofacies, comprising 50-50% of the rock with different HI_o values (e.g. the first organofacies has an HI_o of 350 mg HC/g TOC while the second yields an HI_o of 450 mg HC/g TOC), equation 12 can be written as (Jarvie, 2012):

$$\begin{aligned} GOC &= 0.50 \times (350/1177) + 0.50 \times (450/1177) \\ &= 0.34 \text{ or } 34\% \text{ reactive organic carbon.} \end{aligned} \quad \text{(Eq. 13)}$$

This is followed by the estimation of the original TOC (TOC_o; Jarvie, 2012):

$$TOC_o\,(wt.\%) = TOC_{pdNGOCadjusted}/(1 - GOC). \quad \text{(Eq. 14)}$$

3.3.3 Step 3: calculation of the initial hydrocarbon generative potential ($S2_o$)

The fraction of the original generative organic carbon has to be determined (Jarvie, 2012):

$$GOC_o\ (wt.\%) = TOC_o \times GOC. \quad \text{(Eq. 15)}$$

Finally, the original generation potential is defined (Jarvie, 2012):

$$S2_o\,(\text{mg HC/g rock}) = (GOC_o/0.085). \quad \text{(Eq. 16)}$$

3.4 Method of Banerjee et al. (1998)

The approach of Banerjee et al. (1998) is based on nonlinear curve fitting with the form of the following exponential equation:

$$Y = 1/(a \times \exp(b \times X) + c). \quad \text{(Eq. 17)}$$

Constants *a*, *b* and *c* are found by the fitting algorithm. The method uses the relationship between the hydrogen index and T_{max} to determine the original hydrogen index and transformation ratio of a data set (Banerjee et al., 1998). The type of kerogen within a rock is a function of its organic compounds and the depositional environment (Banerjee et al., 1998). The relationship between the hydrogen index, T_{max} and kerogen type allows for the characterization of each kerogen type based on a HI−T_{max} plot as all the particular types show a distinctive maturation path on it (Banerjee et al., 1998).

The transformation ratio curves for different source rock units with various organic matter compositions can also be constructed which indicate the limits and rates of hydrocarbon generation for different types of kerogen (Banerjee et al., 1998).

3.3.1 Workflow of the method

Banerjee et al. (1998) used the typical HI–T_{max} trend lines of kerogen types I, II and III from Bordenave (1993) to modify equation 17 for their curve fitting algorithm to:

$$HI = 1/(a \times \exp(b \times (T_{max} - 435)) + c), \quad \text{(Eq. 18)}$$

where *a*, *b* and *c* are constants, HI is in mg HC/g TOC and T_{max} is in ºC.

The intersection of the trend line with the HI axis gives the original hydrogen index (HI_o). The hydrogen index and T_{max} characterize the HI−T_{max} trend lines of the particular kerogen types while constants *a* and *b* define the rate of HI decay with respect to T_{max} (Banerjee et al., 1998).

The authors highlighted that where T_{max} approaches 435 ºC, the term $(a \times \exp(b \times (T_{max} - 435))$ of equation 18 approaches zero and HI tends to become equal to 1/*c*. Then, constant *c* is equal to $1/HI_o$ and thus equation 18 can be written as (Banerjee et al., 1998):

$$HI = 1/(a \times \exp(b \times (T_{max} - 435)) + 1/HI_o \quad \text{(Eq. 19)}$$

Once HI is known, the conversion fraction of the organic matter to petroleum (transformation ratio, TR) can be calculated (Banerjee et al., 1998):

$$TR = 1 - HI/HI_o \qquad \text{(Eq. 20)}$$

Combining equations 19 and 20 yields (Banerjee et al., 1998):

$$TR = (HI_o \times a \times \exp(b \times (T_{max} - 435)))/(HI_o \times a \times \exp(b \times (T_{max} - 435)) + 1). \qquad \text{(Eq. 21)}$$

3.3.2 Applicability of the method

Banerjee et al. (1998) tested their method on the three HI–T_{max} curves presented by Bordenave (1993) for type I, type II and type III kerogens to check the validity of equation 19.

Constants *a* and *b*, the computed linear correlation coefficient and the obtained original hydrogen index (HI_o) values for the three kerogen types are indicated in Fig. 29. The fitted curves provided by the method of Banerjee et al. (1998) gave high degrees of correlation ($r^2 > 0.7$) for the maturation path lines of kerogen types I, II and III proving that equation 19 is able to represent the HI decay with respect to T_{max} throughout the complete maturation path (Banerjee et al., 1998).

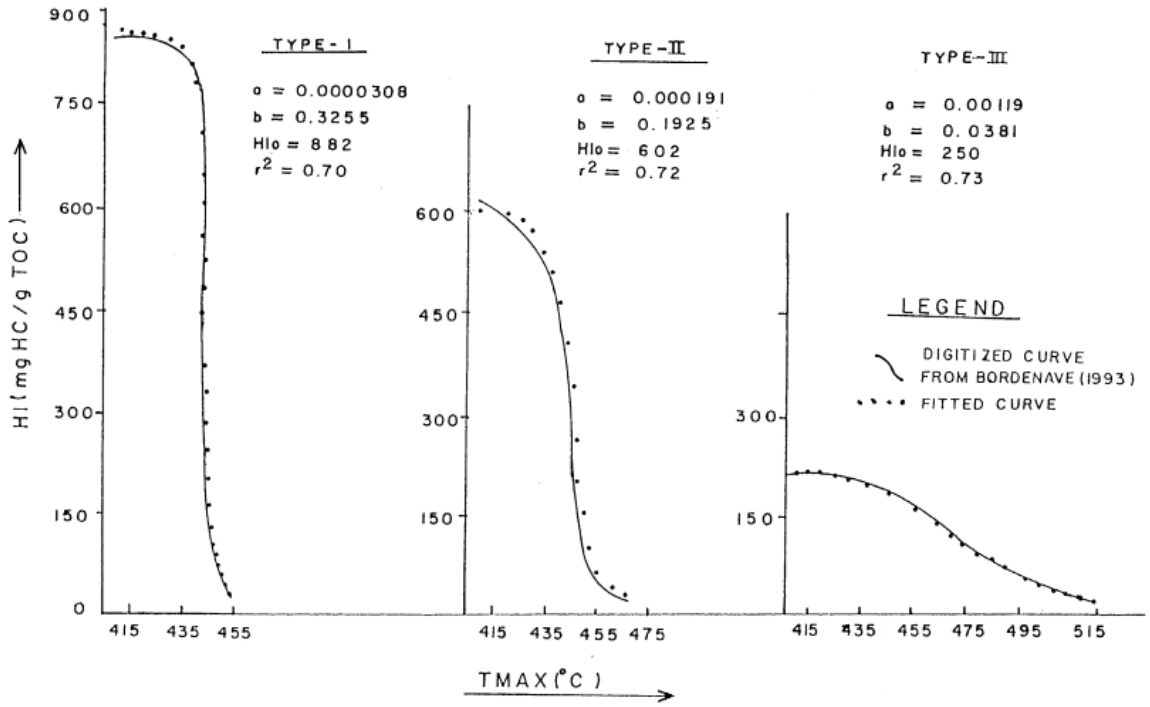

Figure 29. The hydrogen index (HI) versus T_{max} trend lines for kerogen types I, II and III (Bordenave, 1993). The original hydrogen index (HI_o) and constants *a* and *b* are given by curve fitting (from Banerjee et al., 1998). r^2 = linear correlation coefficient.

Banerjee et al. (1998) highlighted that the T_{max} boundary for the mature stage for type I kerogen is 445 ºC, not 435 ˚C which is used in the term 'T_{max}–435' in equation 23 (Banerjee et al., 1998). As a result, the fitted curve of the authors deviates from the maturation profile of type I kerogen in the study of Bordenave (1993) at the boundary of thermal maturity. The authors emphasize that using a T_{max} of 435 ºC to represent the marginally mature stage of organic matter has been done for generalisation purposes and for mathematical simplicity. They also point out that the hydrogen index can increase in the case of type III kerogen due to CO_2 loss at the boundary of maturation. Although the shape of the function used by Banerjee et al. (1998) is not able to account for the increase of HI at the marginally mature stage, this does not influence the outcome of the method because the fitted curve for type III kerogen starts to deviate from the one published by Bordenave (1993) at a temperature when the organic matter is immature. This means that at the temperature values where the fitted curve deviates from the one of Bordenave (1993), the hydrogen index equals the original hydrogen index of the organic matter (Banerjee et al., 1998).

Banerjee et al. (1998) tested their method on Rock-Eval data of Snowdon (1995) from the Second White Speckled Formation, Alberta Basin, Canada. The dataset showed great variability regarding geochemical parameters, which resulted in low correlation in the curve fitting method (Banerjee et al., 1998). For this reason, the samples were divided into four separate groups (I, II, III and IV) by Banerjee et al. (1998) on the basis of the oxygen index (OI) versus T_{max} (Fig. 30) and the S2 versus TOC plot (not shown in the publication). The curve fitting method was applied to the four groups (Fig. 31), showing high linear correlation coefficient for groups I-III (Banerjee et al., 1998). In contrast, the trend line on the HI–T_{max} plot of group IV indicates low correlation between the data points (Banerjee et al., 1998).

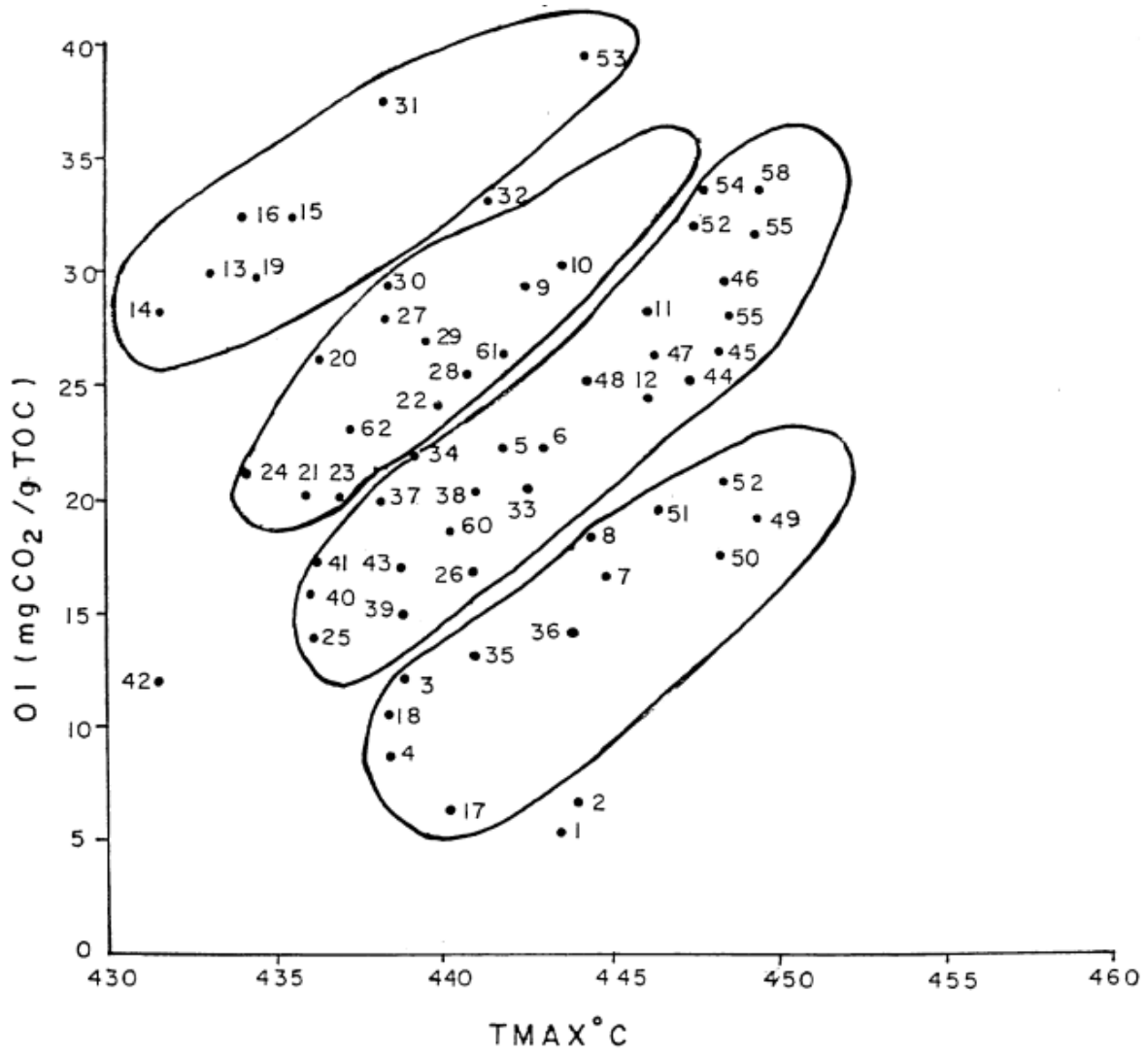

Figure 30. Oxygen index (OI) versus T_{max} plot showing the separation of the four groups by Banerjee et al. (1998) of core data from the Second White Speckled Formation (Snowdon, 1995).

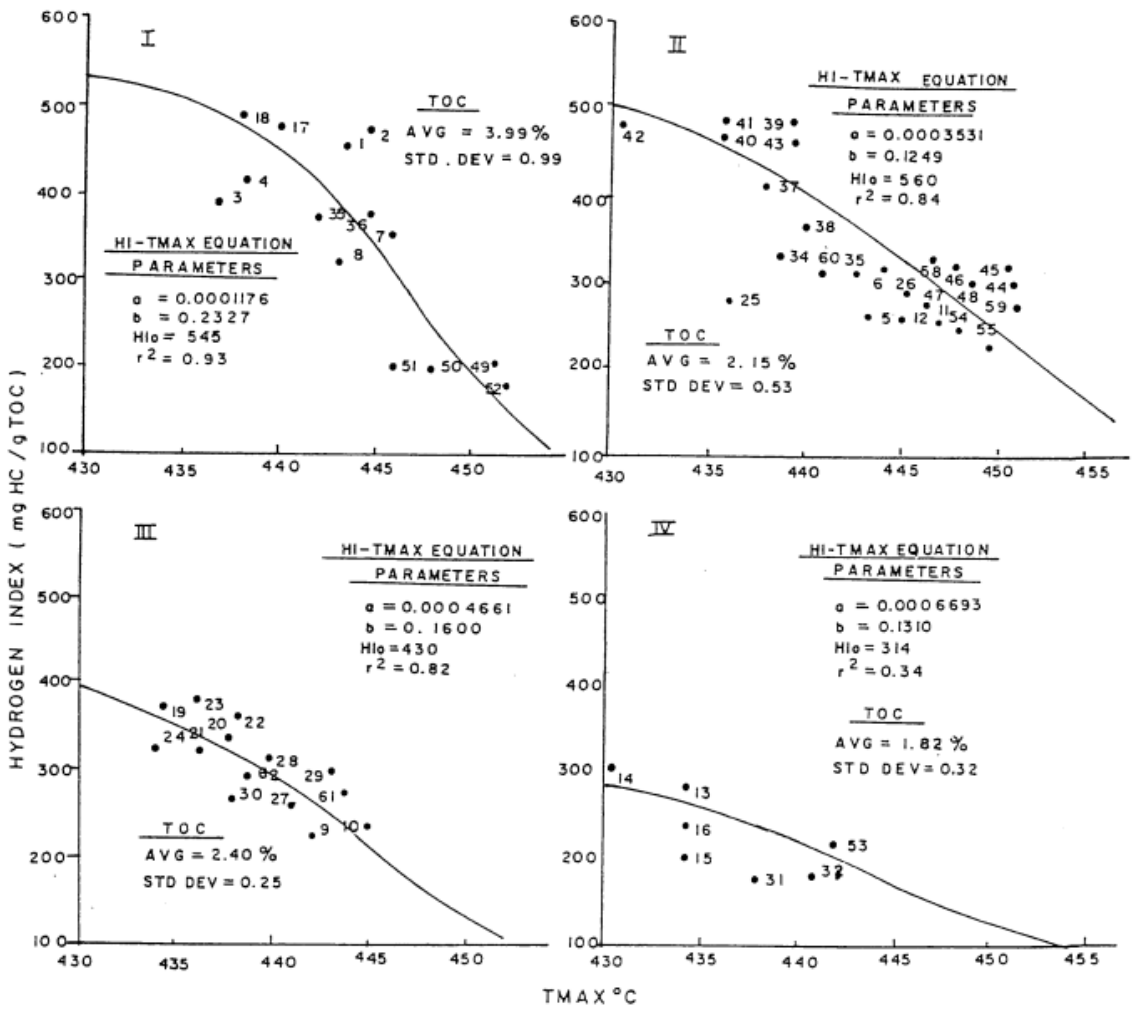

Figure 31. Hydrogen index (HI) versus T_{max} plot showing the trend line, the linear correlation coefficient (r^2), the calculated original hydrogen index (HI_o) and constants *a*, *b* for each group (from Banerjee et al., 1998).

3.3.3 Limitations

A limitation of the method lies in the separation of the four groups. According to Banerjee et al. (1998), the data of the unextracted samples were used to define groups I–IV in the Second White Speckled Formation. However, the oxygen index versus T_{max} plot of the samples does not appear to be the same as the one shown in the publication (Fig. 31). Some samples, for example sample 42 has an oxygen index of 17 mg CO_2/g TOC and a T_{max} of 430 ˚C (Banerjee et al., 1998; Snowdon, 1995). Moreover, when referring to the plot of Banerjee et al. (1998), one can notice that the sample appears to have a higher T_{max} and lower oxygen index compared to the published data by Snowdon (1995). The original data presented by Snowdon (1995) were plotted for a better comparison (Fig. 32). Furthermore, Banerjee et al. (1998) analysed 62

samples but none of the cross plots published by the authors show the complete sample set. In addition, the figures in the publication in some cases seem to contain the same sample numbers for different data points. An example of this can be seen in Fig. 31, where sample no. 35 is presented in both group I and II.

The issues discussed above reduce the reliability of the study as it is problematic to find out which sample belongs to which group exactly and for this reason, the method is difficult to apply.

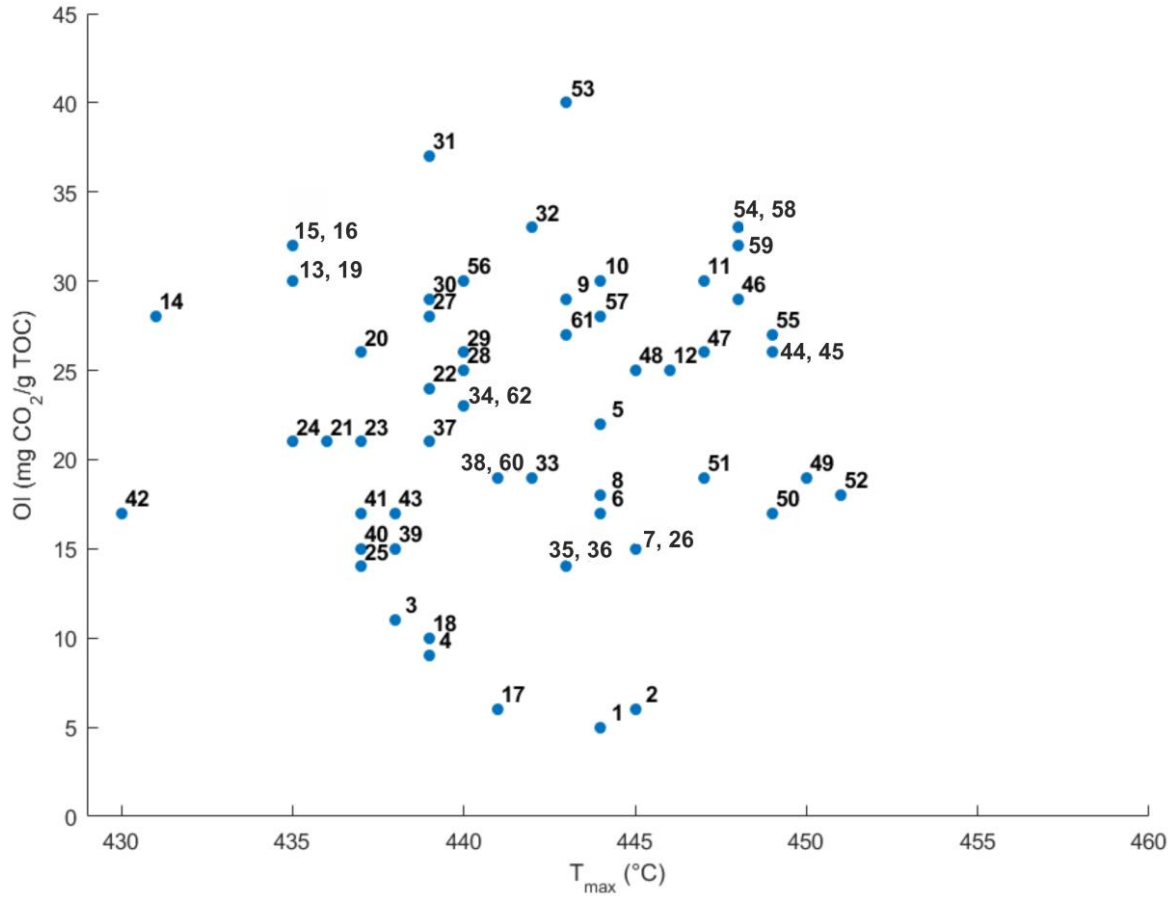

Figure 32. Oxygen index (OI) versus T_{max} plot of the Second White Speckled Formation samples (after Snowdon, 1995). The oxygen index and T_{max} values for some samples (for example for sample 42) appear to be different from what is published in Banerjee et al., (1998; fig. x in the text). Multiple sample numbers were removed and corrected. The data points separated by comma have the same oxygen index and T_{max} values.

3.5 Method of Dahl et al. (2004)

The method of Dahl et al. (2004) incorporates hydrocarbon potential (S2) and total organic carbon (TOC) data into an algorithm to assess the average amounts of oil-prone, gas-prone and inert organic material. Dahl et al. (2004) emphasize that aim of the method is to estimate the average gas and/or oil potential of a sample set, not of individual samples. For this reason, the method calculates with mean values to smooth the deviations in the measured values for curve fitting. The basis of the method relies on the TOC versus S2 cross plot (as in Clayton & Ryder, 1984 and Langford & Blanc-Valleron, 1990) considering TOC to be a linear function of S2 and HI as the slope of the curve. According to Cornford (1994) and Cornford et al. (1998), the average hydrogen index of the organic matter can be determined from the regression line of a TOC versus S2 cross plot. Moreover, the intersection of the regression line at the TOC axis yields the average inert organic carbon content. The steps of the practical application of the method are shown in Fig. 33 and discussed below.

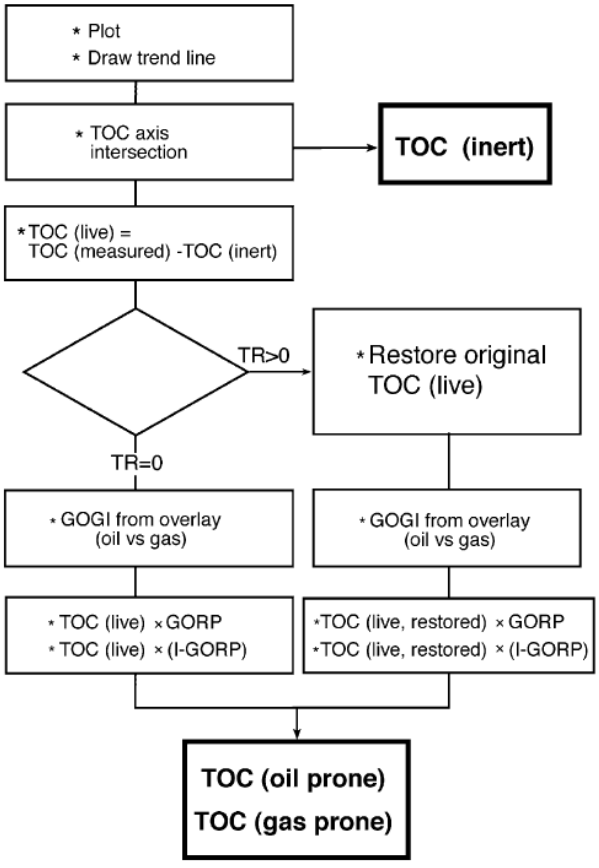

Figure 33. Workflow of the Dahl et al. (2004) method. The algorithm proposed by the authors starts with the calculation of the inert component (TOC(inert)). After that, TOC(live) is estimated. Then, based on the transformation ratio value of the studied section, the method follows two different sets of calculations to obtain the end-member constituents.

3.5.1 Kerogen end-member approach

The Dahl et al. (2004) method regards the organic matter to be composed of three kerogen end-members with similar features to the organic facies described in Jones (1987). Jones (1987) defined seven types of organic facies on the basis of maceral composition, Rock-Eval measurements at R_o ~ 0.5, H/C and O/C ratios. The organic facies are named types A, AB, B, BC, C, CD and D and are assigned to a certain depositional environment (Jones, 1987). Furthermore, the most likely hydrocarbon products (oil and gas) generated by each organic facies are also described (Jones, 1987). Organic Facies A consists of marine organic matter composed of algae and bacteria, Organic Facies C is inertinite dominated, while Organic Facies D is composed of inertinite (Jones, 1987). Organic Facies A is deposited under persistent anoxic conditions, while Organic Facies D is highly oxidised (Jones, 1987).

Dahl et al. (2004) suggest defining the various end-members by organic petrography, Rock-Eval pyrolysis, combined pyrolysis, gas chromatography as well as by elemental composition analysis to ensure that the outcome of the method will not be misleading and is fully controlled. Dahl et al. (2004) modified Organic Facies B, C and D of Jones (1987) and applied these and end-members in their method. Dahl et al. (2004) hypothetically removed the possible inertinite and vitrinite components of Organic Facies B to obtain the oil-prone end-member, HI(oil). Based on the study of Jones (1987), Dahl et al. (2004) selected the hydrogen index value of 700 mg HC/g TOC as representative value to be used in the method. For the gas-prone end-member, HI(gas), Dahl et al. (2004) suggested the value of 250 mg HC/g TOC on the basis of the hydrogen index range defined for Organic Facies C in Jones (1987). The inert end-member (Organic Facies D of Jones, 1987) has a hydrogen index value of 0 mg HC/g TOC (Dahl et al., 2004).

3.5.2 Step 1: Determination of the amount of inert and pyrolysable organic material

The first step in the method is the determination of the inert component. The amount of inert organic material (TOC(inert)) in the organic matter is given by the intersection point (*b*) of the regression line of the sample population on an S2–TOC plot,

$$\mathrm{TOC} = \mathrm{aS2} + \mathrm{b}, \qquad \text{(Eq. 22)}$$

at the TOC axis (Dahl et al., 2004). The regression lines passes through the origin, $b = 0$, if no inert material is present in the organic matter. In most cases, the regression line crosses the

positive TOC axis with an offset from the origin due to the presence of residual organic matter (Cornford, 1994).

After determining the percentage of the inert component, the pyrolysable quantity of organic matter, TOC(live), can be determined by the following formula:

$$\mathrm{TOC(live)} = \mathrm{TOC_{pd}} - \mathrm{TOC(inert)}. \quad \text{(Eq. 23)}$$

3.5.3 Step 2: obtaining the hydrogen index of the "live" organic matter

The phrase, "live organic material" means the pyrolysable fraction of organic matter and can be calculated in two ways. The first approach for the estimation of the hydrogen index of the pyrolysable organic material originates from the definition of the hydrogen index (Dahl et al. 2004):

$$\mathrm{HI} = 100\mathrm{S2_{pd}}/\mathrm{TOC_{pd}}. \quad \text{(Eq. 24)}$$

Based on equation 24, the slope of an S2 versus TOC curve can be written as:

$$\mathrm{a} = \mathrm{TOC_{pd}}/\mathrm{S2_{pd}} = 100/\mathrm{HI}, \quad \text{(Eq. 25)}$$

Then, HI(live) can be calculated by the following equation:

$$\mathrm{HI(live)} = 100/\mathrm{a}. \quad \text{(Eq. 26)}$$

When $b = 0$ and the regression line intersects the origin, the hydrogen index is determined from the arithmetic mean. In case the regression line does not intersect the origin, the derived hydrogen index is different from the arithmetic mean of the hydrogen index value calculated from the same dataset. Therefore, the authors established another formula to estimate the hydrogen index of the pyrolysable organic matter, HI(live), by subtracting the amount of inert organic material, TOC(inert), from the total organic carbon content of the sample set, $\mathrm{TOC_{pd}}$:

$$\mathrm{HI(live)} = 100\mathrm{S2_{pd}}/(\mathrm{TOC_{pd}} - \mathrm{TOC(inert)}). \quad \text{(Eq. 27)}$$

The authors point out that that the values of $\mathrm{TOC_{pd}}$ and TOC(inert) will always be positive and that $\mathrm{TOC_{pd}}$ > TOC(inert), therefore HI(live) will always be greater than the arithmetic mean, HI(mean). This suggests that the source rocks containing inert organic material will have lower hydrogen indices than the real hydrogen index value of the samples delineated by HI(live). Consequently, the method results in higher HI values than those from Rock Eval pyrolysis.

3.5.4 Step 3: Composition of active kerogen

After determining the average hydrogen index of the pyrolysable organic material in the studied section, the composition of the active kerogen needs to be calculated. This process is based on the assumption that kerogens can be divided into oil-prone and gas-prone end-members with associated hydrogen indices, HI(oil) and HI(gas) respectively (Dahl & Yukler, 1991). Then, the oil fraction (*m*) and gas fraction (*n*) can be estimated by the following equation (Dahl et al., 2004):

$$\mathrm{HI(live)} = \mathrm{HI(oil)}m + \mathrm{HI(gas)}n \qquad \text{(Eq. 28)}$$

Due to mass balance,

$$m + n = 1. \qquad \text{(Eq. 29)}$$

Espitalié & Bordenave (1993) ascertained that the hydrogen index is reduced upon maturation which is expressed by an increase in the transformation ratio. This was incorporated into the study of Dahl et al. (2004) who introduced a modified formula of equation 28 which accounts for the change in organic matter quality due to hydrocarbon generation:

$$\mathrm{HI} = \mathrm{HI(oil)}(1-\mathrm{TR})m + \mathrm{HI(gas)}(1-\mathrm{TR})n. \qquad \text{(Eq. 30)}$$

As a next step, the mean TOC needs to be divided into oil-and gas-prone organic carbon. In order to perform this, the GORP (gas to oil ratio potential) was established:

$$\mathrm{GORP} = n/(m+n). \qquad \text{(Eq. 31)}$$

Dahl et al. (2004) constructed different overlays that can be superimposed on the S2−TOC plot for transformation ratio values of 0%, 30% and 40%. This provides the possibility to estimate the relative compositions of oil- and gas-prone kerogens (GORP) directly from the plot and apply it in the calculations but overlays for other transformation ratios can also be generated (see chapter 3.5.10).

After selecting the proper GORP value, the oil and gas producing constituents, TOC(gas) and TOC(oil) are given by:

$$\mathrm{TOC(oil)} = \mathrm{TOC(live)}(1-\mathrm{GORP}), \qquad \text{(Eq. 32)}$$

$$\mathrm{TOC(gas)} = \mathrm{TOC(live)GORP}. \qquad \text{(Eq. 33)}$$

The oil and gas generation potential can also be estimated:

$$S2(\text{oil}) = S2_{pd}(1 - \text{GORP}), \quad \text{(Eq. 34)}$$

$$S2(\text{gas}) = S2_{pd} \times \text{GORP}. \quad \text{(Eq. 35)}$$

3.5.5 Step 4: Petroleum potential restoration (TOC_o, $S2_o$, HI_o)

The formulas described above for TOC(live), HI(live), kerogen end-member constituents and oil and gas generation potential are used to obtain the hydrogen index and TOC of the pyrolysable organic material in the organic matter and to split the organic matter into oil- and gas-prone proportions when the organic matter is immature.

In case the organic matter has been transformed, the original hydrocarbon potential of the organic material needs to be restored (Dahl et al., 2004). The methodology for the back calculation of the original hydrocarbon potential is given in subchapters 3.5.5 and 3.5.6.

To obtain the initial hydrocarbon generative potential ($S2_o$), the following equation is used (Dahl et al., 2004):

$$S2_o = S2_{pd}/(1 - TR). \quad \text{(Eq. 36)}$$

The original TOC restoration is carried out by determining the amount of organic matter lost in the hydrocarbon generation process by (Dahl et al., 2004):

$$S2(\text{lost}) = S2_o - S2_{pd}, \quad \text{(Eq. 37)}$$

Then, S2(lost) is multiplied by a constant α (described in chapter 3.5.8) to obtain TOC(lost):

$$TOC(\text{lost}) = S2(\text{lost})\alpha \quad \text{(Eq. 38)}$$

As a next step, TOC(lost) has to be summed with TOC_{pd} to determine the original TOC content of the rock (TOC_o; Dahl et al., 2004):

$$TOC_o = TOC_{pd} + [S2_{pd}\,TR/(1 - TR)]\alpha. \quad \text{(Eq. 39)}$$

TOC_o is different from the value of TOC(live) which makes the calculation of a restored hydrogen index necessary (instead of using HI(live)) to determine the kerogen end-member constituents (Dahl et al., 2004). The restored hydrogen index (HI_o) represents the original hydrogen index of the organic matter:

$$HI_o = 100 \times S2_o / (TOC_o - TOC(inert)). \quad \text{(Eq. 40)}$$

3.5.6 Step 5: Restoration of the kerogen end-member constituents and their generative potential

The proportions of gas- and oil-prone kerogens need to be estimated by replacing TOC_{pd} with TOC_o in equations 23 and 32–33:

$$TOC(live, restored) = TOC_o - TOC(inert), \quad \text{(Eq. 41)}$$

$$TOC(oil, restored) = TOC(live, restored) \times (1 - GORP), \quad \text{(Eq. 42)}$$

$$TOC(gas, restored) = TOC(live, restored) \times GORP. \quad \text{(Eq. 43)}$$

The restored oil and gas generation potentials also need to be calculated by replacing $S2_o$ with $S2_{pd}$ in equations 34–35:

$$S2(oil, restored) = S2_o (1 - GORP), \quad \text{(Eq. 44)}$$

$$S2(gas, restored) = S2_o \times GORP. \quad \text{(Eq. 45)}$$

3.5.7 Step 6: Matrix effect correction

The mineral matrix can reduce the S2 pyrolysis yield during Rock-Eval analysis, underestimating the hydrogen index value and organic matter quality (Peters, 1986). The intensity of matrix retention is mainly defined by T_{max} and the proportion of heavy hydrocarbons but the mineralogy, the quantity of organic matter and the level of organic enrichment of the studied samples also influence the process (Espitalié et al., 1980; Katz, 1983). Ideally, the regression line through a sample population on an S2 versus TOC plot intersects at the origin. However, due to the presence of inert carbon in the organic matter and matrix retention effect, the trend line intersects the positive TOC axis with an offset from the origin (Espitalié et al., 1980; Langford & Blanc-Valleron, 1990; Cornford, 1994). The negative intersection of the regression line at the S2 axis indicates the average magnitude of retained pyrolysable material due to the mineral matrix effect. The amount of retained S2 (referred to as S2(retained)) can be used to correct for this effect (Dahl et al., 2004).To eliminate the effects of matrix retention on the results obtained by the Dahl et al. (2004) method, the following calculations need to be carried out.

The correction for matrix retention in mature organic matter is shown below in equations 46–52. The matrix effect correction is not implemented in the code given in Appendix F, the calculations were carried out manually.

First, S2(retained) has to be multiplied by the stoichiometric factor (α) to estimate the retained organic carbon, TOC(retained):

$$\mathrm{S2(retained)} \times \alpha = \mathrm{TOC(retained)}. \quad \text{(Eq. 46)}$$

Then, TOC(live, restored) needs to be corrected for the matrix effect to obtain TOC(live, restored, corrected):

$$\mathrm{TOC(live, restored, corrected)} = \mathrm{TOC_0} - \mathrm{TOC(inert)} + \mathrm{TOC(retained)}. \quad \text{(Eq. 47)}$$

Next, the proportions of oil- and gas-prone kerogens are corrected for matrix retention by computing TOC(oil, restored, corrected) and TOC(gas, restored, corrected):

$$\mathrm{TOC(oil, restored, corrected)} = \mathrm{TOC(live, restored, corrected)} \times (1 - \mathrm{GORP}), \quad \text{(Eq. 48)}$$

$$\mathrm{TOC(gas, restored, corrected)} = \mathrm{TOC(live, restored, corrected)} \times \mathrm{GORP}. \quad \text{(Eq. 49)}$$

Then, the original hydrocarbon generative potential has to be corrected for matrix effect to obtain $S2_o$(corrected):

$$\mathrm{S2_0(corrected)} = \mathrm{S2(restored)} + \mathrm{S2(retained)}. \quad \text{(Eq. 50)}$$

Finally, the hydrocarbon generative potentials of the kerogen end-members are corrected for matrix retention by calculating S2(oil, restored, corrected) and S2(gas, restored, corrected):

$$\mathrm{S2(oil, restored, corrected)} = \mathrm{S2_0(corrected)} \times (1 - \mathrm{GORP}), \quad \text{(Eq. 51)}$$

$$\mathrm{S2(gas, restored, corrected)} = \mathrm{S2_0(corrected)} \times \mathrm{GORP}. \quad \text{(Eq. 52)}$$

3.5.8 Stoichiometric factor

As mentioned in subchapter 3.5.5, Dahl et al. (2004) introduced constant α (a stoichiometric factor) in their algorithm. This parameter is used as a constant in their method for simplicity, although in reality it changes with maturation of the kerogen. Parameter α is dependent on the gross elemental composition of the hydrocarbon products generated from an ideal kerogen and it is determined using the following formula:

$$\alpha = 0.1C/(C + gH), \quad \text{(Eq. 53)}$$

where C and H stand for the atomic weights of carbon and hydrogen, while g represents the number of hydrogen atoms. Taking a sulphur gross composition CH_2 into account, α is equal to 0.086, meaning that 86 wt.% of petroleum consists of carbon (Dahl et al., 2004), while the research conducted by Espitalié et al. (1987) suggests an α of 83 wt.% carbon content in petroleum. As a result of the different proposed carbon contents for hydrocarbons, the estimation of the most applicable value for α is problematic. Dahl et al. (2004) considered the values described in the literature and used in practice as well as the extreme values of the parameter. The lowest value for α is given by the elemental composition of methane (which is the most hydrogen-rich petroleum that can be generated), which yields α = 0.075. The maximum value for α is determined by letting the hydrogen amount in equation 53 to get as close to zero as possible, which gives an α = 0.1 (Dahl et al., 2004).

Dahl et al. (2004) also considered the amounts of atomic nitrogen, sulphur and oxygen produced in the generated petroleum to obtain the most accurate value for α:

$$\alpha = 0.1\mathrm{C}/(\mathrm{C} + p\mathrm{H} + q\mathrm{N} + r\mathrm{S} + s\mathrm{O}), \quad \text{(Eq. 54)}$$

where p, q, r and s represent the relative numbers of hydrogen, nitrogen, sulphur and oxygen atoms. According to Dahl et al. (2004), considering a sulphur composition suggested by Tissot and Welte (1978) for average oils in equation 54, α will be equal to 0.084, which forms a basic input value for the algorithm.

3.5.9 Adjustments to the method

The original workflow of obtaining GORP does not reflect the exact gas to oil potential of a section as it is estimated on the basis of an overlay. To ease the process of obtaining a GORP value for a sample set and to increase the accuracy of this value and the results dependent on it, an additional equation was added to the code of the method. This makes the calculation of GORP automatic and more precise. The equation was derived from the combination of equations 25 and 28, which yields:

$$\mathrm{HI(oil)} \times m + \mathrm{HI(gas)} \times n = \frac{100}{\mathrm{a}(1 - \mathrm{TR}).} \quad \text{(Eq. 55)}$$

Combining equations 29 and 55 gives:

$$\mathrm{HI(oil)} \times m + \mathrm{HI(gas)} \times (1 - m) = \frac{100}{\mathrm{a}(1 - \mathrm{TR}).} \quad \text{(Eq. 56)}$$

This can be rewritten as:

$$m\big(\mathrm{HI(oil)} - \mathrm{HI(gas)}\big) = -\mathrm{HI(gas)} + \frac{100}{\mathrm{a}(1-\mathrm{TR})}. \qquad \text{(Eq. 57)}$$

Then, equation 57 can be changed to:

$$m = \frac{\dfrac{100}{\mathrm{a}(1-\mathrm{TR})} - \mathrm{HI(gas)}}{\mathrm{HI(oil)} - \mathrm{HI(gas)}}. \qquad \text{(Eq. 58)}$$

Finally, on the basis of equation 29, the formula for GORP can be obtained:

$$\mathrm{GORP} = 1 - (100/(\mathrm{a}(1-\mathrm{TR})) - \mathrm{HI(gas)})/(\mathrm{HI(oil)} - \mathrm{HI(gas)}), \qquad \text{(Eq. 59)}$$

where 'a' is the slope of the trend line through the sample population on an S2–TOC plot, TR is the transformation ratio and HI(gas) and HI(oil) represent the hydrogen indices of the associated end-members (Dahl et al., 2004).

Moreover, two other formulas were also added to the code to calculate a transformation ratio range for each studied section, in which the method works. In case the transformation ratio input is out of the proper transformation ratio range, the code gives a warning message, showing the minimum and maximum transformation ratio that can be used in the particular section for the method to work. To obtain the equation for the minimum boundary of the transformation ratio range which can be applied in a section, m = 0 is used in equation 57. This yields:

$$\frac{100}{\mathrm{a}(1-\mathrm{TR})} = \mathrm{HI(gas)}. \qquad \text{(Eq. 60)}$$

This can be rewritten as:

$$1 - \mathrm{TR} = \frac{100}{\mathrm{a}(\mathrm{HI(gas)})}. \qquad \text{(Eq. 61)}$$

Finally, equation 61 is changed to:

$$\mathrm{TR} = 1 - 100/(\mathrm{slope} \times \mathrm{HI(gas)}). \qquad \text{(Eq. 62)}$$

The maximum value of the transformation ratio range in which the Dahl et al. (2004) method works for a section is found by using m = 1 in equation 57. This yields:

$$\frac{100}{\mathrm{a}(1-\mathrm{TR})} = \mathrm{HI(oil)}. \qquad \text{(Eq. 63)}$$

Rewriting equation 63 gives:

$$1 - \mathrm{TR} = \frac{100}{\mathrm{a(HI(oil))}}. \qquad \text{(Eq. 64)}$$

Then, equation 64 can be changed to:

$$\mathrm{TR} = 1 - 100/(\mathrm{slope} \times \mathrm{HI(oil)}). \qquad \text{(Eq. 65)}$$

3.5.10 Overlays

The overlays depend on maturity due to the change in the S2 and TOC values with increasing maturity as well as on the kerogen end-members used in the method (Dahl et al., 2004). Overlays for different transformation ratios can be prepared by inserting the ideal end-member values, the transformation ratio values of the end-members and the fractions of oil- and gas-prone kerogen (*m* and *n*) into equations 28–30, which enables the calculation of the hydrogen index values of the end-members (Dahl et al., 2004). Then, the computed hydrogen indices need to be converted to lines in an S2 versus TOC cross plot to obtain the overlays, where S2 is the x-axis and TOC is the y-axis (Dahl et al., 2004). The spacing between the overlay lines and the angle of the slope increases with maturation (Dahl et al., 2004).

3.5.11 Limitations

3.5.11.1 Transformation ratio assumption

To be able to use the method, the transformation ratio for the studied section needs to be defined as this forms an initial input to the method. In the study of Dahl et al. (2004) the mean production index (PI) value was used as a basis for this purpose. After determining the mean PI for the section, the authors estimated the kerogen end-members on the basis of the overlay with the closest value to the mean production index. For example, when restoring the hydrocarbon potential of the Volg-2 sequence in the Jeppe-1 well in the Danish Central Graben, Dahl et al. (2004) used the overlay constructed for the transformation ratio of 40%, which is close to the mean production index of the section, 46%. In contrast, for some sections it is better to use other methods first which can yield a transformation ratio value for the organic matter (such as the approach of Peters et al., 1996; Jarvie et al., 2007 and Jarvie, 2012). However, these methods already operate with other assumptions which might influence the outcome. As will be shown in the results, the production index is too low compared to the transformation ratio of the organic matter in one data set (Wenchang Formation, chapter 4.5) so it is more beneficial to use the transformation ratio calculated by other methods as an input. In another case, the method

provides similar results using the mean production index value to when the transformation ratio values calculated by other methods are used as inputs (see chapter 4.3.1).

3.5.11.2 GORP estimation

The estimation of the gas to oil ratio potential of the sample set is carried out visually in Dahl et al. (2004). This means that the authors have generated overlays for transformation ratios of 0, 30% and 40% and when the fractional conversion of the organic matter falls within this range, the data can be plotted on an S2–TOC plot and the proper GORP can be read off by applying the relevant transformation ratio overlay on the plot. This method however, gives different results than when the GORP is calculated automatically (as suggested in chapter 3.5.9) and might yield different kerogen-end member and generative potential values.

The authors use exact fitting of the data points to obtain the hydrogen index of the immature organic matter, which does not take into account the deviation of the data points from the overlay range. In case the data points are too scattered and the linear correlation coefficient is too low, the method yields imprecise results and it is not applicable (see chapter 4.4).

3.5.11.3 Depositional environment

Based on their experience of testing the method in various geological settings, Dahl et al. (2004) highlight that great fluctuations in the terrestrially derived waxy components limit the applicability of the method. An additional limitation is caused by the rapid change in the chemical composition of kerogen, resulting from depositional environments where the oxygenation of bottom water changes quickly on a geological time scale or in places where the depositional rate of clastic material is high (Dahl et al., 2004). The fast changes in the composition of organic matter and facies will give chaotic S2−TOC plots (Dahl et al., 2004). Chaotic S2–TOC cross plots should also be expected where rapid vertical shifts in the kerogen blends occur (Dahl et al., 2004). The limitations experienced with certain chemical compositions of organic matter described by Dahl et al. (2004) are not reflected in the equations as the method gives results regardless of the type of the studied organic matter.

3.5.11.4 Mistakes in the original reference

The GORP equation is written incorrectly in Dahl et al. (2004). In the study of Dahl et al.

(2004), GORP represents the gas to oil ratio potential, however, equation 8 in Dahl et al. (2004) indicates that GORP stands for the oil to gas ratio potential. The wrong GORP equation is shown below:

$$\mathrm{GORP} = m/(m+n). \qquad \text{(Eq. 59)}$$

In spite of the incorrectly published formula, the term GORP is used correctly in the study of Dahl et al. (2004).

3.6 Geochemical classifications

3.6.1 Classification of Peters & Cassa (1994)

The classification of Peters & Cassa (1994) is widely used in the literature to carry out geochemical screening on the studied organic matter. The back calculated values by the tested methods include TOC_o and $S2_o$, which can be used to determine the organic-richness and the hydrocarbon generative potential of the immature organic matter. To compare the organic-richness and hydrocarbon generative potential interpretations suggested by the different methods, the classification of Peters & Cassa (1994) was used. The ranges defined by Peters & Cassa (1994) for TOC and S2 are shown in Table 12 below.

Table 12. Organic-richness classification of the organic matter (from Peters & Cassa, 1994).

Organic-richness	**TOC**	**S2**
	wt.%	mg HC/g Rock
Poor	<0.5	<2.5
Fair	0.5–1	2.5–5
Good	1–2	5–10
Very good	2–4	10–20
Excellent	>4	>20

The different back calculation methods computed transformation ratio values, which were used to interpret the maturity stage of the organic matter. The classification for the maturity interpretation and the comparison of the interpretation made on the basis of the results and what is suggested by the T_{max} values measured in the data sets is from Peters & Cassa (1994) and is shown in Table 13 below.

Table 13. Maturity classification of the organic matter (from Peters & Cassa, 1994). R_o = vitrinite reflectance, T_{max} = maximum temperature.

Maturity	**T_{max}**	**Production index**
	˚C	S1/(S1+S2)
Immature	<435	<0.10
Early mature	435–445	0.10–0.15
Peak mature	445–450	0.25–0.40
Late mature	450–470	>0.40
Postmature	>470	–

3.6.2 Classification of Jones (1987)

The hydrogen index classification of Jones (1987) was used to define the depositional environment interpretations in the results on the basis of the back calculated original hydrogen index values. Jones (1987) describes the general TOC content as well for most of the organic facies but highlights that for the majority of the organic facies, the TOC values are highly variable. This means that the TOC content of the organic facies is not as reliable indicator of the depositional environment as the hydrogen index (Jones, 1987). For this reason, the characteristic TOC values of the organic facies are not shown here but are discussed in the results where applicable. The scheme of Jones (1987) is shown in Table 14 below.

Table 14. Organic facies classification of Jones (1987).

Organic facies	**HI**
	mg HC/g TOC
A	>850
AB	650–850
B	400–650
BC	250–400
C	125–250
CD	50–125
D	<50

4. Results

The original total organic carbon content, initial hydrogen index and generative potential and the transformation ratio back calculated by the tested methods are compared in the following subchapters. Furthermore, the depositional environment interpretations inferred from the results are compared to the interpretations of the sedimentary conditions presented in the publications analysing the tested data sets.

Among the successfully tested methods, only the Dahl et al. (2004) and Jarvie et al. (2007) methods provide an estimate of the original hydrogen index (HI_o) which is an indicator of the initial depositional environment (Jones, 1987). Furthermore, all methods calculate the original organic carbon content of the studied samples, which, in combination with the HI_o can yield information about the depositional environment (Jones, 1987). For this reason, the interpretation of the sedimentary conditions was carried out on the basis of the initial hydrogen index given by these two methods and on the basis of the TOC_o values calculated by all methods according to the organic facies classification of Jones (1987).

To be able to compare the different methods, the original hydrogen index value calculated on the basis of the Jarvie et al. (2007) method was used as input to the Peters et al. (1996) and Jarvie (2012) methods. The Dahl et al. (2004) method requires a transformation ratio input value which is given by the Peters et al. (1996), the Jarvie et al. (2007) and the Jarvie (2012) methods. As the latter three methods yield different transformation ratio values, each was tested as input in the Dahl et al. (2004) approach. This was carried out to observe whether the results are dependent on the transformation ratio input and how sensitive the method is to the initial input. The Dahl et al. (2004) method was also tested with the mean production index values of each data set which is a slight modification of the original workflow carried out by Dahl et al. (2004). The aim of testing the mean production index values as inputs is to observe how the results change compared to when the transformation ratio is used as input. The reason for this is that the mean production index value is sometimes significantly lower than the transformation ratio values calculated by the mass balance equations. This means that applying the average production index value of a section or the transformation ratio values computed by the mass balance based methods yield different results, which lead to different interpretation about the the organic-richness and quality of the organic matter.

The original organic carbon content (TOC_o) calculation is included in all methods while the initial hydrocarbon generative potential ($S2_o$) calculation is only included in the Dahl et al. (2004), Jarvie et al. (2007) and Jarvie (2012) methods. Among the results of the Dahl et al. (2004) method, the HI_o and $S2_o$ values are shown both before and after matrix correction to see how these parameters change after the corrections and to observe whether the lack of matrix corrections affects the interpretation of the results. The TOC_o calculated by the Dahl et al. (2004) method does not change due to matrix correction, only TOC(oil), TOC(gas) and TOC(inert) vary. After correcting for matrix retention, TOC(oil) and TOC(gas) increase and TOC(inert) decreases. These values will not be shown because they cannot be compared to the results of the other methods and TOC_o is not affected by the change in these parameters.

4.1 Reproduction of the Banerjee et al. (1998) method

To test the method of Banerjee et al. (1998) the data of Snowdon (1995) were used. The sample numbers presented in this chapter are the same as in Table 1 of Banerjee et al. (1998). As discussed in chapter 3.3.3, the subdivision of groups I–IV in the sample population carried out by Banerjee et al. (1998) lacks an appropriate description which makes the method hard to reproduce. For this reason, the subdivision of the samples into groups was carried out in this study by comparing the original figures of Banerjee et al. (1998, Figs. 2 and 3) with each other. Then, Fig. 30 was compared to Fig. 32, showing the correct oxygen index versus T_{max} plot of the samples. The results of the obtained subdivision of groups I–IV and the calculated original hydrogen index and constants *a*, *b* based on the method of Banerjee et al. (1998) are shown below.

The results calculated for the first group (Fig. 34) are different from the results of Banerjee et al. (1998, fig. 3); illustrated in fig. 31 in the text. The original hydrogen index (HI_o) was estimated to be 81 mg HC/g TOC, which is lower than the one calculated by Banerjee et al. (1998), 545 mg HC/g TOC. Constants *a* and *b* estimated by curve fitting have negative values, in contrast, the same constants were calculated to be positive in Banerjee et al. (1998).

The correlation coefficient is also lower compared to the value for group I in Banerjee et al. (1998) and the shape of the trend line appears to be different as well from the one published by Banerjee et al. (1998).

For group II (Fig. 35), the calculated original hydrogen index is slightly lower (549 mg HC/g TOC) than the one estimated by Banerjee et al. (1998; 560 mg HC/g TOC). The calculated

values of constants *a* and *b* are close to the values published by Banerjee et al. (1998, Fig. 3), shown in Fig. 31 in the text, however, constant *a* is underestimated while constant *b* is overestimated. The correlation coefficient is also close to the one obtained by Banerjee et al. (1998). The trend line calculated in this study has a similar shape as the trend line of Banerjee et al. (1998) but the current trend line in this study intersects the hydrogen index axis at a higher value than the trend line of Banerjee et al. (1998).

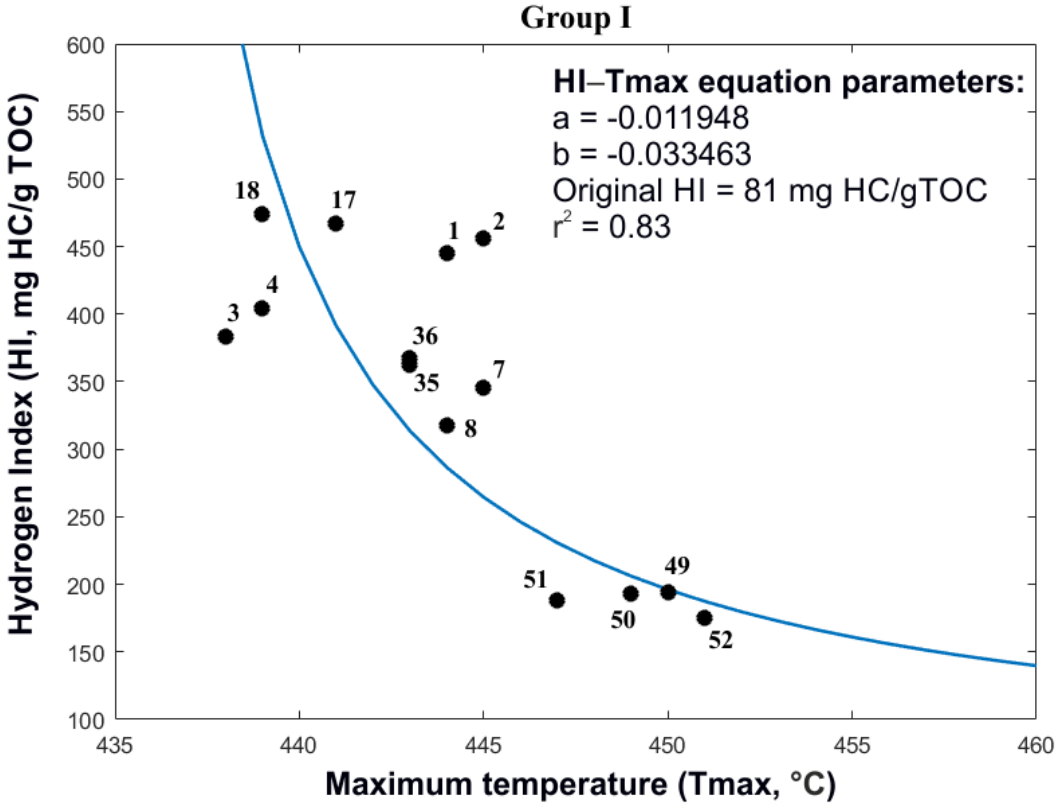

Figure 34. Hydrogen index versus T_{max} cross plot of group I showing the calculated parameters from curve fitting and the trend line. r^2 = linear correlation coefficient.

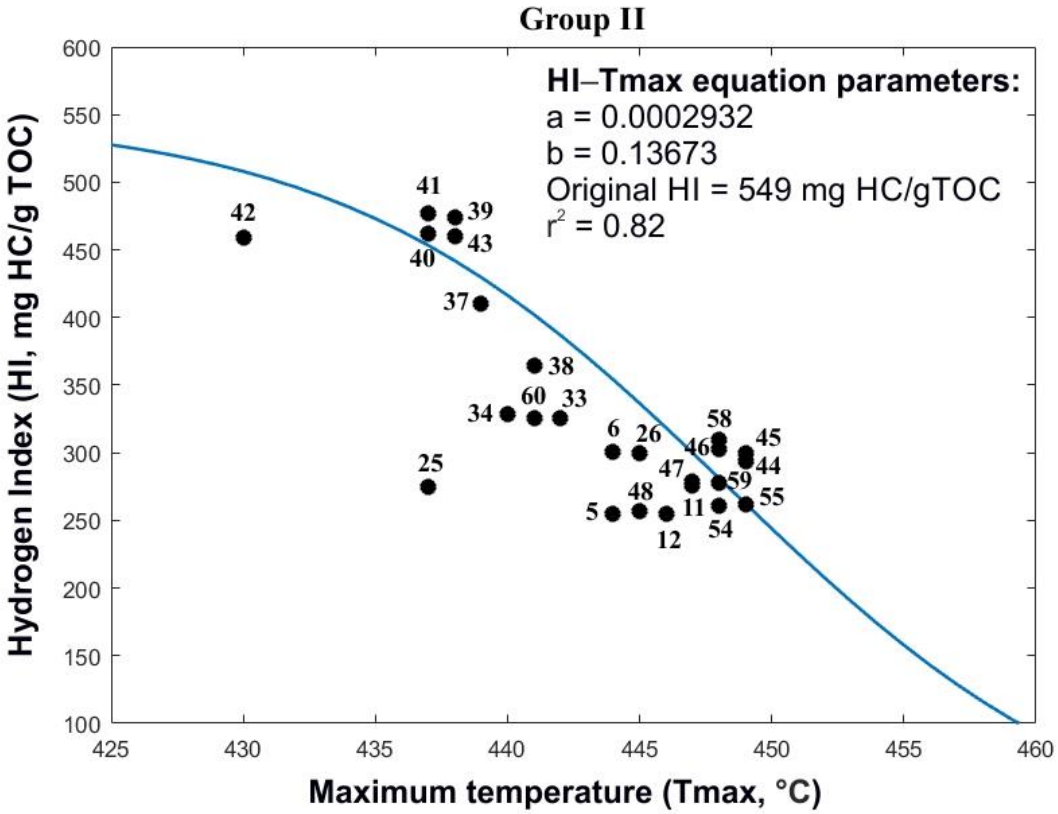

Figure 35. Hydrogen index versus T_{max} cross plot of group II showing the the values of constants *a*, *b*, the orignal hydrogen index and the correlation coefficient obtained by curve fitting. The trend line is also shown. r^2 = linear correlation coefficient.

Constants *a* and *b* were calculated to be negative for group III (Fig. 36), while they have positive values in the study of Banerjee et al. (1998). The estimated original hydrogen index is underestimated with a value of 81 mg HC/g TOC instead of 430 mg HC/g TOC as shown in Banerjee et al. (1998). The shape of the trend line is different from the one presented by Banerjee et al. (1998). Moreover, the intersection point of the trend line at the hydrogen index axis is higher than the one published in Banerjee et al. (1998).

The closest results to Banerjee et al. (1998) including the calculated values for constants *a* and *b* and the original hydrogen index were observed for group IV (Fig. 37). Constant *a* is slightly overestimated and constant *b* is underestimated.

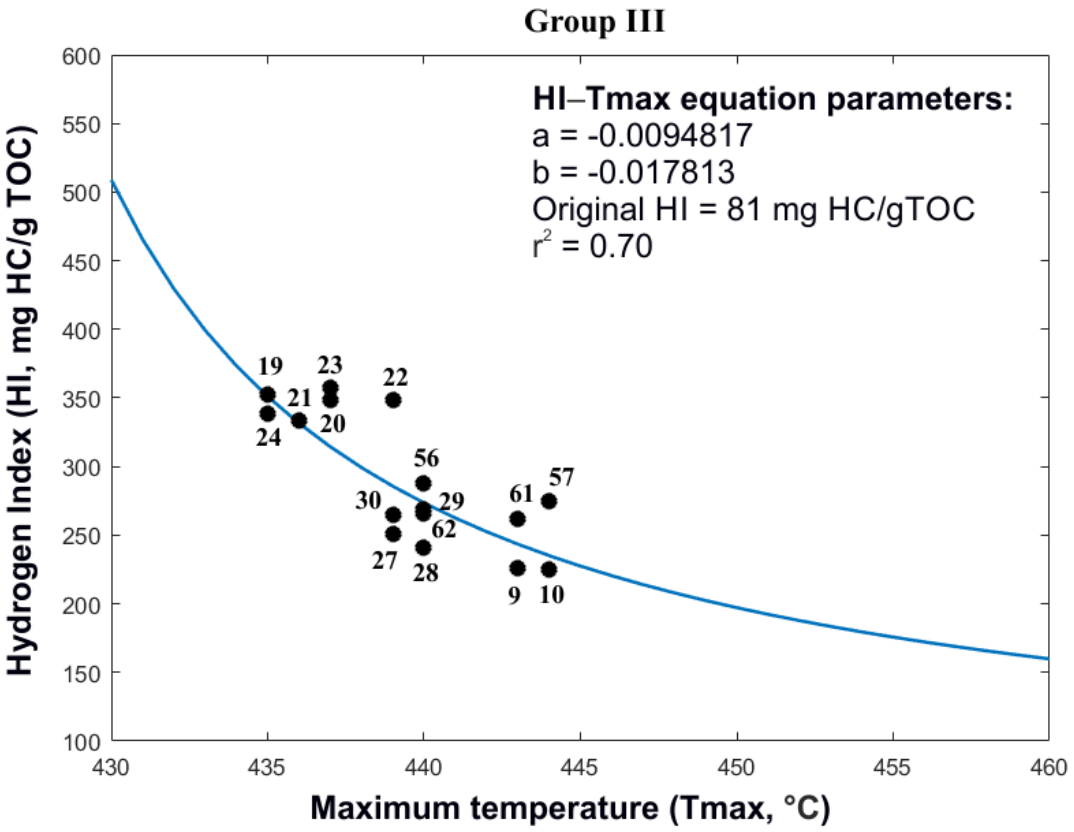

Figure 36. Hydrogen index versus T_{max} cross plot of group III showing the parameters obtained by curve fitting and the trend line.

The estimated orignal hydrogen index only differs by 1 mg HC/g TOC from the one calculated by Banerjee et al. (1998). The difference is also low between the published (Banerjee et al., 1998) and calculated (this study) correlation coefficient values: r^2 = 0.34 and r^2 = 0.33 respectively. The shape and the intersection point of the trend line shown in this study have only minor differences compared to the trend line shown in Banerjee et al. (1998).

It can be observed from the calculated values and trend lines shown in Figs. 34 and 36 that the shape of the trend lines and the intersection points of the trend lines at the hydrogen index axis for groups I and III deviate the most from the ones shown in Banerjee et al. (1998). Furthermore, these two groups yielded the least accurate results among the four groups, which is probably related to the inaccurate trend lines for groups I and III as the results rely on curve fitting. To reproduce the Banerjee et al. (1998) method, two MATLAB codes were used. One of the codes uses the curve-fitting procedure of MATLAB (Appendix D), the other code is the implementation of the code given by Banerjee et al. (1998) into the MATLAB programming language (Appendix E). The Banerjee et al. (1998) method is hard to apply in both implementations because the method is very sensitive to the initial input values. Furthermore,

the method requires a lot of manual manipulation as a change even in he values of one data point can influence the results. This makes the results obtained by the method uncertain. Conclusively, the method was not tested in any of the data sets.

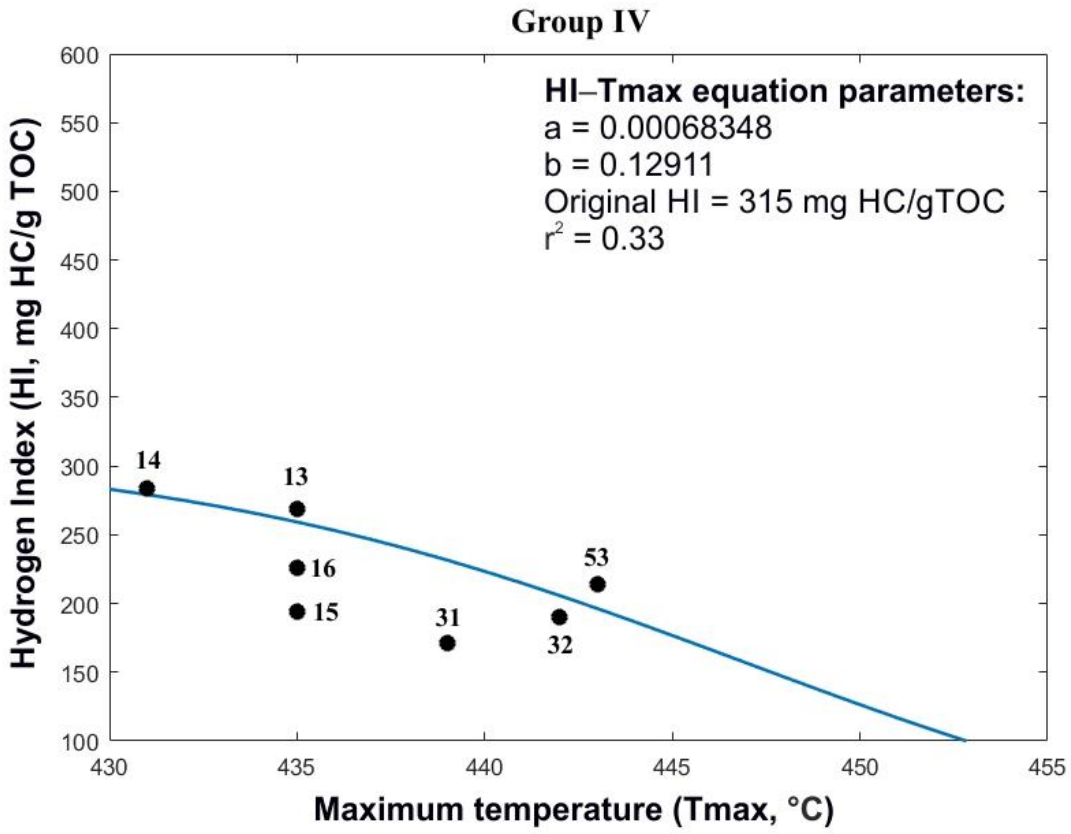

Figure 37. Hydrogen index versus T_{max} cross plot of group III showing the trend line and the parameters obtained by curve fitting.

4.2 Passhatten Member, Spitsbergen

4.2.1 Results obtained with prior knowledge about the origin of the organic matter

The maceral volume percentages and the study of the origin of the organic matter in the Passhatten Member published by Karcz (2014) were used to apply the original hydrogen index calculation of the Jarvie et al. (2007) method. Assigning the maceral groups to the right kerogen type in equation 3 is a crucial step as the original hydrogen index given by the Jarvie et al. (2007) method was used as an input to the Peters et al. (1996) and Jarvie (2012) methods. Based on visual kerogen assessment and by taking the marine origin of the organic matter into consideration, Karcz (2014) assigned the volume percentage of liptinite to type I kerogen, inertinite to type II kerogen (not to type IV as should be done without the visual classification)

and the percentage of vitrinite in the organic material to type III kerogen. This classification was used in equation 3 to obtain the original hydrogen index values of the samples. The kerogen classification described in this paragraph was not mentioned explicitly in the publication of Karcz (2014), it was determined from the calculated results presented in the paper.

4.2.1.1 Transformation ratios

Fig. 38 shows the results of the transformation ratio calculations as box and whisker plots. Box and whisker plots enable the comparison of the calculated values yielded by the different back calculation methods. The middle line in the box is the median (50% of the values are larger than the median, 50% are lower), the lower line of the box is the first quartile Q_1 (25% of the values are smaller than Q_1), the upper line of the box is the third quartile Q_3 (25% of the calculated values are larger than Q_3). The whisker lengths are 1.5 times the range between Q_3 and Q_1.

The transformation ratios given by the Jarvie et al. (2007) and Peters et al. (1996) methods are similar, 87% and 86% on average (Fig. 38). The Jarvie (2012) method yielded a lower average transformation ratio, 80% (Fig. 38). These values were used as inputs to the Dahl et al. (2004) method to see how the calculated HI_o, TOC_o and $S2_o$ values vary depending on the initial input.

In case of using 86% and 87% transformation ratios as inputs into the Dahl et al. (2004) method, the code showed a warning message that based on equation 65, the transformation ratio should be lower than 82% for the method to work. This means that the maximum transformation ratio equation and the equations computing the overlays contradict: the transformation ratio equation calculates a maximum boundary in which the method works but in spite of this, the method yields results on the basis of the overlay.

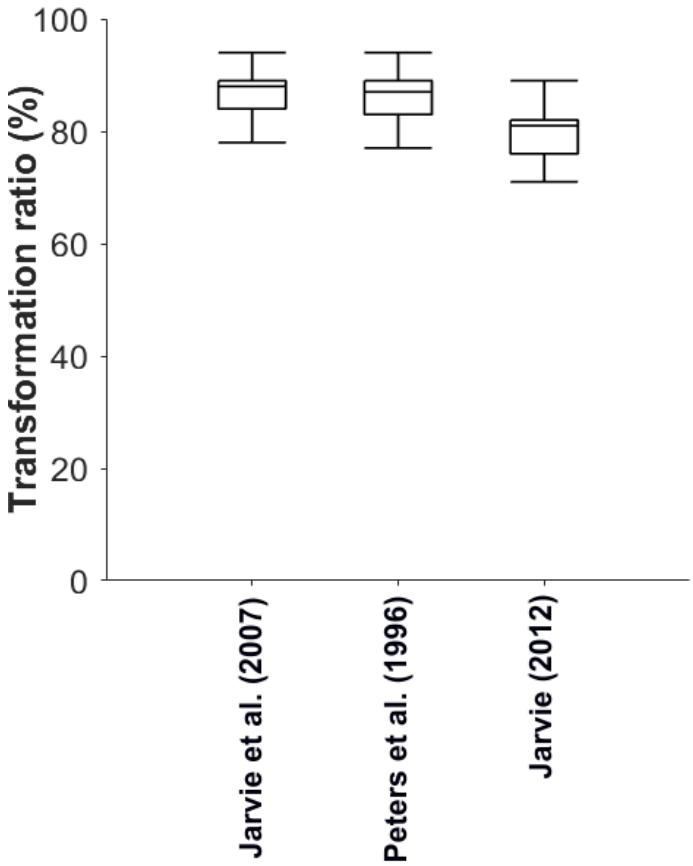

Figure 38. Transformation ratio estimates of the Passhatten Member calculated by the different methods.

4.2.1.2 Original hydrogen index (HI_o)

The Jarvie et al. (2007) method yielded an original hydrogen index value of 481 mg HC/g TOC (Fig. 39). The original hydrogen index value given by the Dahl et al. (2004) method is different for each transformation ratio (Fig. 39). In case a transformation ratio of 80% is used as input to the method, the corrected and uncorected HI_o values are lower than the mean HI_o value calculated by the Jarvie et al. (2007) method (Fig. 39). When the transformation ratios of 86% and 87% were applied as inputs to the Dahl et al. (2004) method, the computed corrected and uncorrected original hydrogen index values are higher than the mean HI_o calculated by the Jarvie et al. (2007) method (Fig. 39).

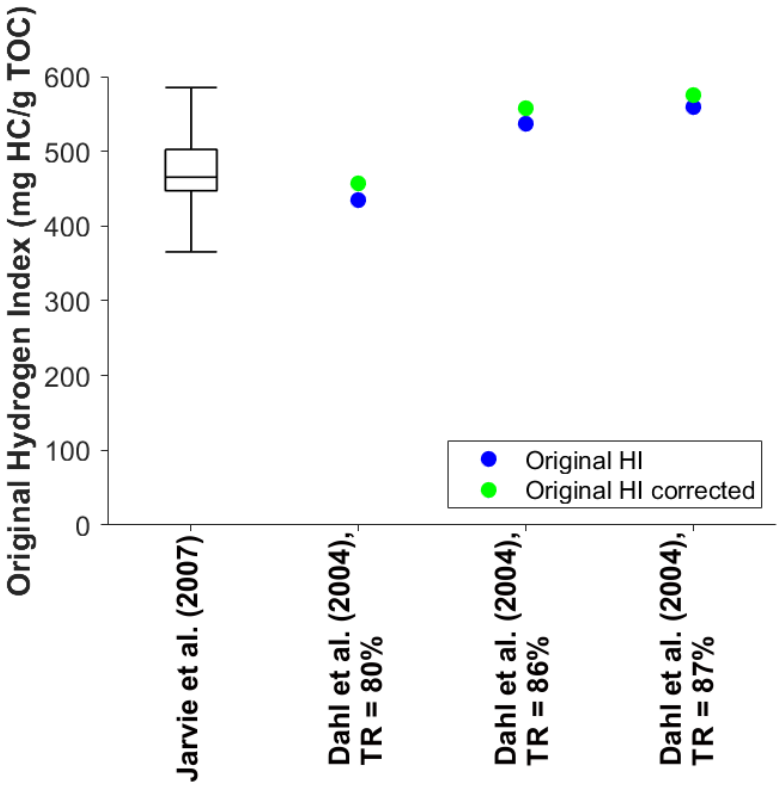

Figure 39. Original hydrogen index values calculated by the different methods for the Passhatten Member. The different transformation ratio values (TR) used as inputs into the Dahl et al. (2004) method are also indicated. HI = Hydrogen index.

Furthermore, the corrected and uncorrected values of the Dahl et al. (2004) method are very similar.

4.2.1.3 Gas to oil ratio potential (GORP)

Applying the transformation ratio of the Jarvie (2012) method (80%) in the Dahl et al. (2004) method yielded a GORP of 0.2 based on equation 59. This suggests mainly oil-prone organic matter in the Passhatten Member (Fig. 40). In contrast, the transformation ratio output of the Peters et al. (1996) method (86%) provided a GORP of –0.4 while the transformation ratio given by the Jarvie et al. (2007) method (87%) resulted in a GORP of –0.5 on the basis of equation 59. The negative GORP values are the result of the data points being located outside of the overlay range (Fig. 41), which shows the inapplicability of equation 59 in these cases. To account for the scattered data points, the GORP was manually set to 0.2, following the methodology for the GORP estimation of Dahl et al. (2004). The GORP value of 0.2 indicates oil-prone organic matter in the Passhatten Member as suggested by the study of Karcz (2014) as well.

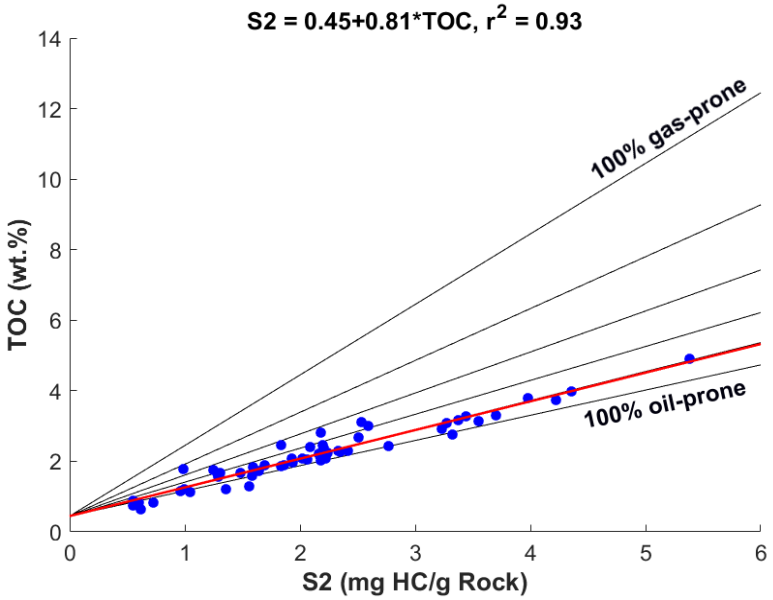

Figure 40. S2–TOC cross plot of the Passhatten Member samples when the transformation value of 80% is used in the Dahl et al. (2004) method. The regression line (red), the generated overlay (black lines), the equation of the trend line and the linear regression coefficient (r^2) are also shown.

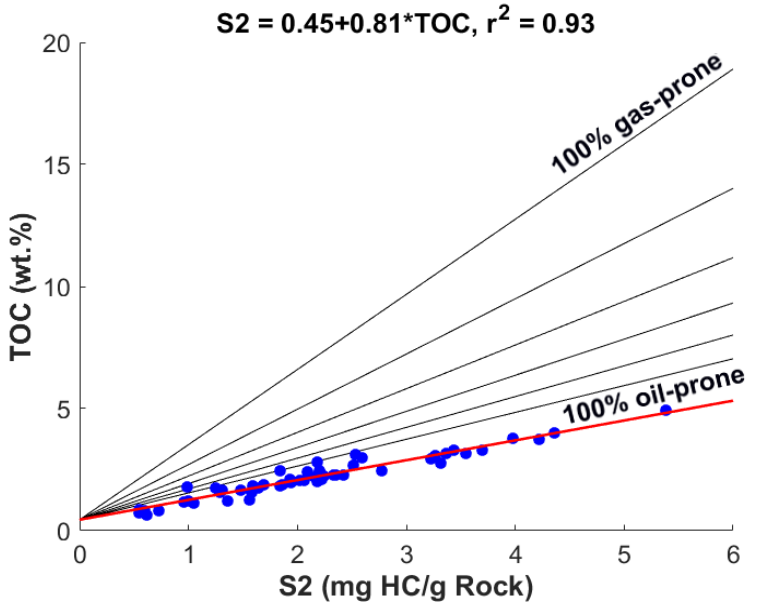

Figure 41. S2–TOC cross plot of the Passhatten Member data. The majority of the data points fall out of the overlay range when the transformation ratio values of 86% and 87% are used as input into the Dahl et al. (2004) method. The regression line (red), the generated overlay (black lines), the trend line equation and the linear correlation coefficient (r^2) are also shown. The trend line equation and the linear correlation coefficients are the same as shown in the previous figure but the different transformation ratio inputs used here show the section to be more oil-prone.

4.2.1.4 Original organic carbon content (TOC_o)

All methods gave comparable values with respect to the mean original organic carbon content (TOC_o; Fig. 42). It can be observed in Figure 42 that the highest mean values were given by the Dahl et al. (2004) method. The lowest mean TOC_o values were calculated by the Jarvie (2012) method. Furthermore, the mean original TOC values estimated by the Jarvie et al. (2007) and Jarvie (2012) methods show only a minor difference.

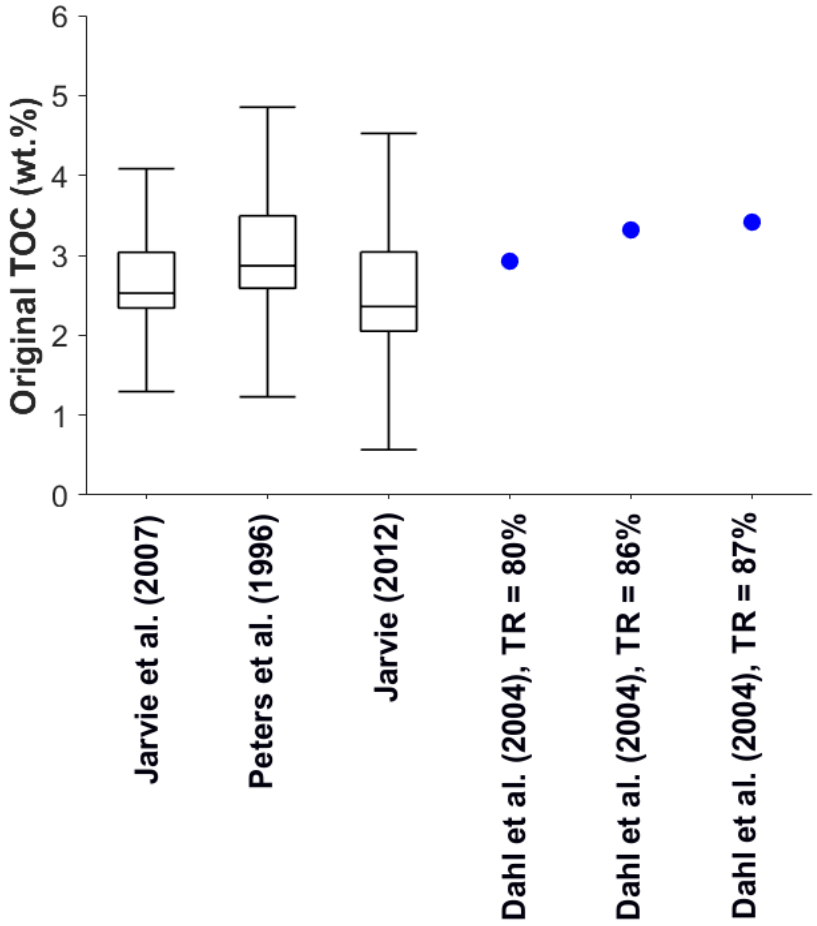

Figure 42. Initial organic carbon content (TOC_o) of the Passhatten Member as estimated by the different methods.

4.2.1.5 Initial hydrocarbon generative potential ($S2_o$)

The Jarvie et al. (2007) method, the Dahl et al. (2004) method with a transformation ratio input of 80% and the Jarvie (2012) methods yielded very similar mean initial hydrocarbon generative potential values for the Passhatten Member (Fig. 43). When used with the transformation ratio inputs of 86% and 87%, the Dahl et al. (2004) method yielded higher results than the other

methods. The maximum difference between the lowest and highest obtained mean values is 4.66 mg HC/g Rock.

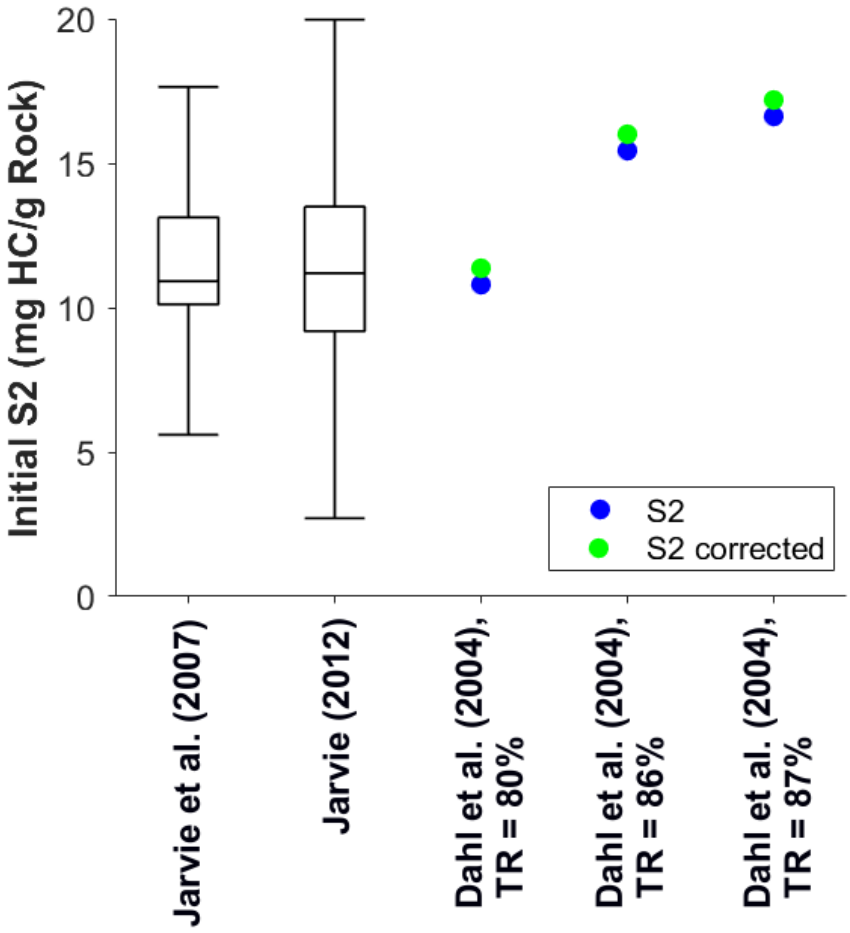

Figure 43. Initial petroleum potential (S2) of the Passhatten Member, calculated by the different methods. The results of the Dahl et al. (2004) are shown according to the transformation ratio input.

4.2.1.6 Interpretation of the results

The original hydrogen index value calculated by the Jarvie et al. (2007) method indicates Organic Facies B for the organic matter of the Passhatten member (Jones, 1987). The HI_o values estimated by the Dahl et al. (2004) method on the basis of the transformation ratios of 80%, 86% and 87% classifiy the organic matter as Organic Facies B (Jones, 1987) in the Passhatten Member which is in agreement with the organic facies based on the results of the Jarvie et al. (2007) method. Organic facies B is indicative of sediment deposition in a marine or lacustrine environment under an anoxic water column (Jones, 1987). The mean TOC_o values calculated by all of the methods are also typical for Organic Facies B, which has a general TOC range of 2–10 wt.% (Jones, 1987). The results of all methods suggest the same depositional environment interpretation, which is in agreement with the study of Karcz (2014).

The TOC_o values calculated by the Dahl et al. (2004) and Jarvie et al. (2007) methods for the samples from the Passhatten Member suggest poor to fair organic-richness (Peters & Cassa, 1994). In contrast, the Peters et al. (1996) and Jarvie (2012) methods indicate poor to very good organic-richness (Peters & Cassa, 1994). The mean TOC_o values calculated by all methods suggest very good organic-richness (Peters & Cassa, 1994).

The $S2_o$ values of the different methods show great variation within the sample set. Fair to very good original hydrocarbon generative potential is suggested based on the $S2_o$ values obtained by the Jarvie et al. (2007) and Dahl et al. (2004) methods, while the Jarvie (2012) method indicates poor to very good potential (Peters & Cassa, 1994). The mean $S2_o$ values computed by all methods indicate very good hydrocarbon generative potential (Peters & Cassa, 1994).

Furthermore, all transformation ratio values calculated by the tested methods indicate the presence of overmature organic matter (Peters & Cassa, 1994), which is in agreement with the T_{max} values observed in the Passhatten Member (Karcz, 2014).

The results for the Passhatten Member indicate that the interpretation about the original depositional environment, organic-richness and hydrocarbon generative potential would be the same for all the tested methods.

4.2.2 Results obtained without prior knowledge about the origin of the organic matter

Without having prior knowledge about the depositional environment and the origin of the organic matter in the Passhatten Member, the different maceral groups would be assigned to different kerogen types than in chapter 4.2.1 in equation 3. This results in a different depositional environment intepretation which has significant impact on the estimation of the initial organic carbon content of the section, on the predicted hydrocarbon generative potential and on the estimated maturity of the section. To observe how these parameters change, the results of Karcz (2014) were neglected.

The volume percentage of the liptinite group was regarded as type II kerogen in equation 3. The vitrinite content was assigned to type III kerogen and the inertinite volume percentage was used as type IV kerogen to obtain the original hydrogen index based on the Jarvie et al. (2007) method.

4.2.2.1 Original hydrogen index (HI_o)

The initial hydrogen index values calculated by the Jarvie et al. (2007) and Dahl et al. (2004) methods with respect to the different transformation ratio inputs (discussed in the next paragraph) are shown in Fig. 44. There is a large difference between the uncorrected and corrected original hydrogen index values calculated by the Dahl et al. (2004) method compared to the values obtained in chapter 4.2.1.2, when the origin of the organic matter was known before the methods were applied. Furthermore, both the lowest and highest mean corrected initial hydrogen index values are given by the Dahl et al. (2004) method. The average original hydrogen index value yielded by the Jarvie et al. (2007) method is comparable to the uncorrected HI_o values calculated by the Dahl et al. (2004) method with the transformation ratios of 45–49% (see below).

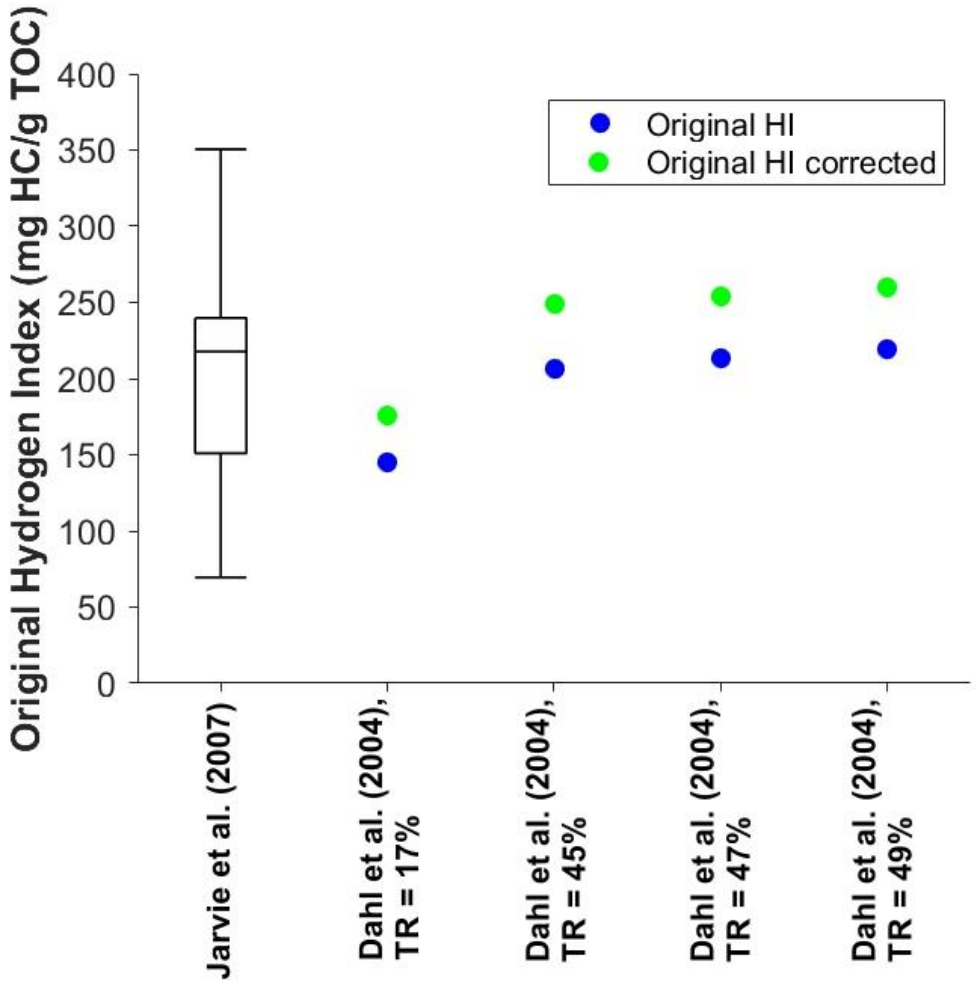

Figure 44. The original hydrogen index values of the Passhatten member, calculated by the different methods.

4.2.2.2 Transformation ratio

The original hydrogen index values given by the Jarvie et al. (2007) method were used as inputs to the Peters et al. (1996) and Jarvie (2012) methods. The transformation ratio values calculated by these methods are similar but show a very wide spread (Fig. 45). Furthermore, the Peters et al. (1996) method gave an average transformation ratio value of 47%, the Jarvie et al. (2007) method yielded 49% and the Jarvie (2012) method estimated 45%. These values are 35–42% lower in general compared to the case when the depositional environment is known before applying the methods (Chapter 4.2.1.1). The methods yielded negative values for two samples, that together with the large spread of the values indicate that the original hydrogen index input is too low.

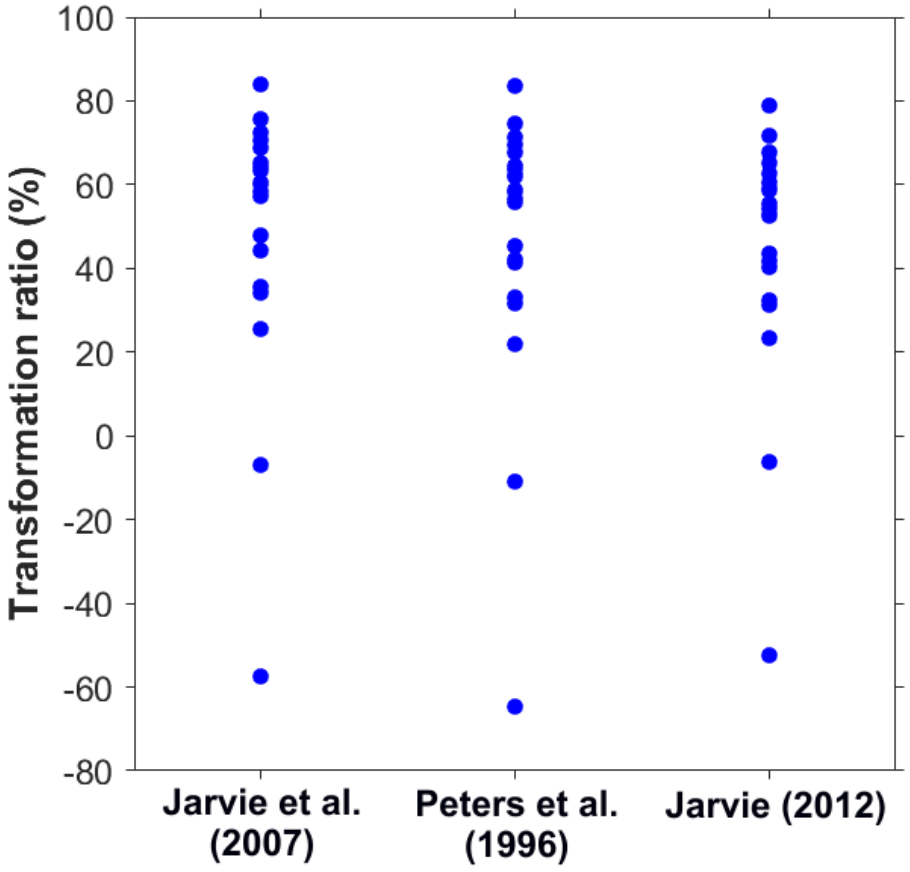

Figure 45. Estimated transformation ratio values of the different methods for the Passhatten Member data. The negative calculated values for two samples indicate the underestimation of the original hydrogen index input value.

4.2.2.3 Gas to oil ratio potential (GORP)

Equation 62 indicates that the minimum transformation ratio for the Dahl et al. (2004) method to work is 51%. Furthermore, the majority of the data points falls out of the GORP range when the mean production index value (17%) or the transformation ratio values calculated by the other methods are used as inputs (Figs. 46 and 47 respectively) indicating that in theory, the method is not applicable with such low input values. The method however, yields results on the basis of the overlay which can be used for interpretation, especially in this case, when the outcomes of the methods are tested in case there is no information available about the origin and maturity of the organic matter. The GORP value is calculated to be larger than 1 by equation 59 for all of the possible input values, which gives negative oil-prone organic carbon values in all cases. For this reason, the GORP was set to 0.9 manually based on Figs. 46 and 47, following the methodology of Dahl et al. (2004) for estimating the GORP visually to be able to use the method.

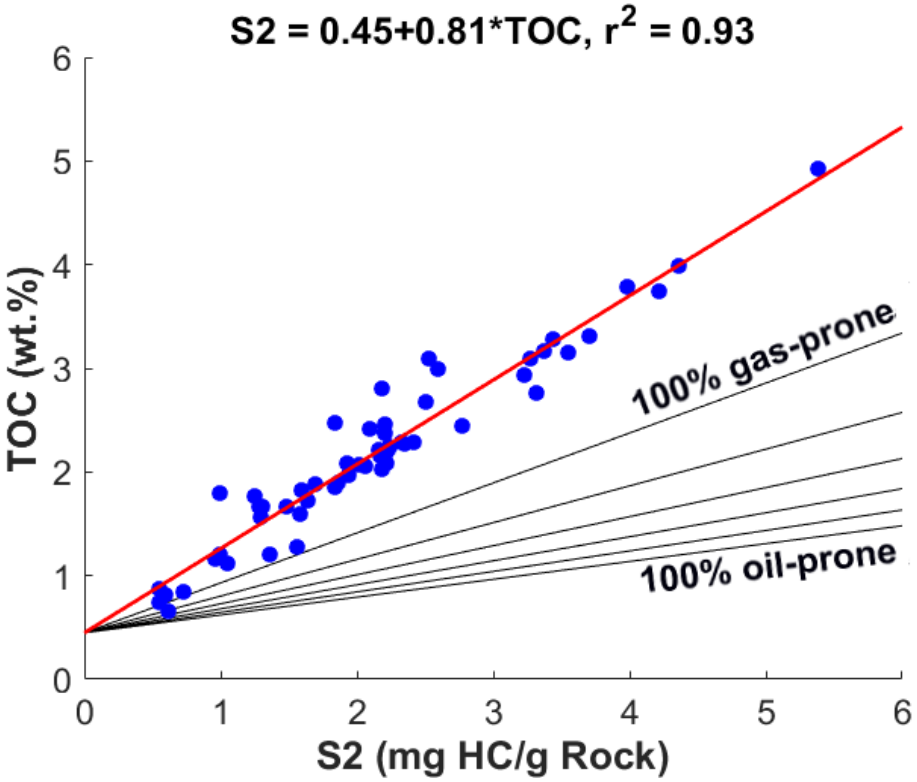

Figure 46. S2–TOC cross plot of the Passhatten Member when the average production index value of the section (17%) was used as input. The regression line (red), the generated overlay (black lines), the equation of the regression line and the linear correlation coefficient (r^2) are also shown.

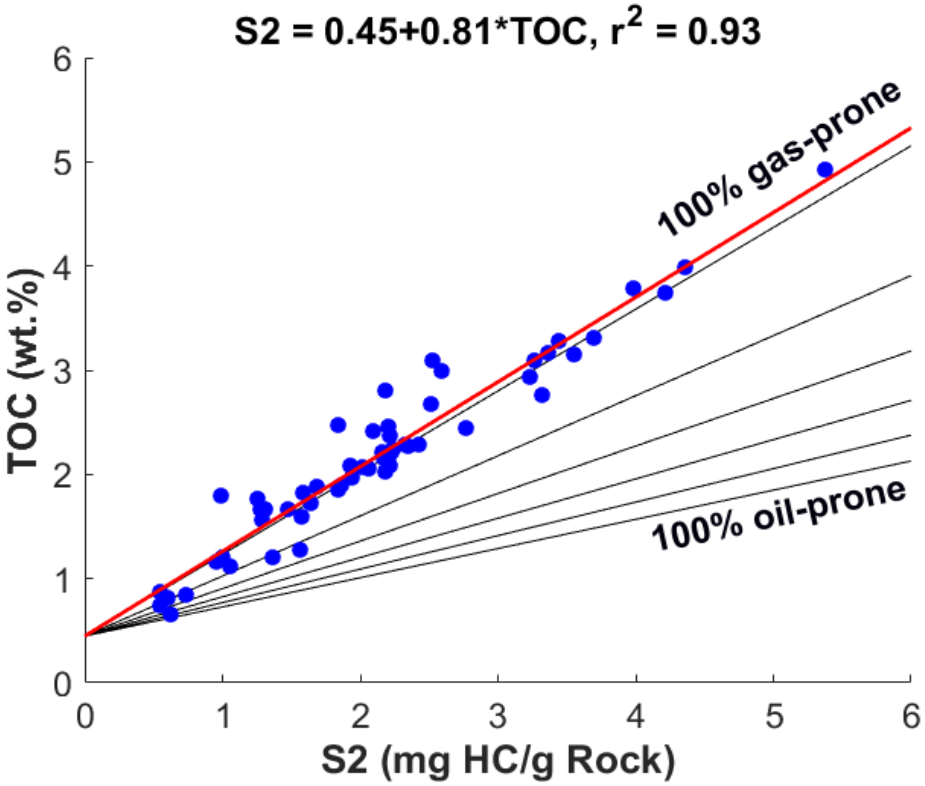

Figure 47. S2–TOC cross plot of the samples from the Passhatten Member, using a transformation ratio of 49% as input. The trend line (red), the generated overlay (black lines), the regression equation and the linear correlation coefficient (r^2) are also shown. Note the similarity of the trend line equation and r^2 compared to the previous figure. Due to the different transformation ratio used here, the section is shown to be slightly more oil-prone.

In all cases, the section is shown to be mainly gas-prone. The S2–TOC cross plots are only shown for the cases when the transformation ratios of 17% and 49% were used as inputs. The reason for this is the similarity of the S2–TOC cross plots to Fig 47. when the values of 45% and 47% are used.

4.2.2.4 Original organic carbon content (TOC_0)

The total organic carbon content calculated by all methods yielded similar values (Fig. 48) which are approximately 0.4–0.8 wt.% lower on average than when the origin of the organic matter was used (chapter 4.2.1.4). The lowest mean value comes from the Jarvie et al. (2007) method, while the highest was calculated by the Dahl et al. (2004) method using a transformation input of 49%.

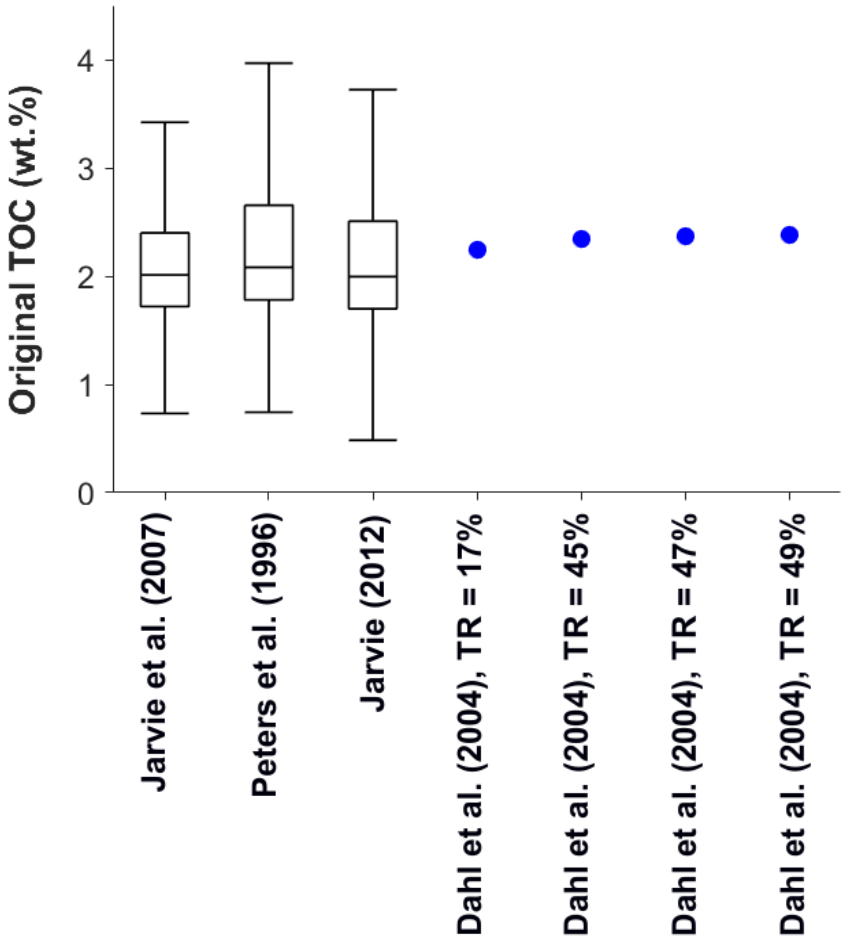

Figure 48. Estimated original organic carbon content (TOC_o) of the Passhatten Member samples by the different methods, not using depositional environment information.

4.2.2.5 Initial hydrocarbon generative potential ($S2_o$)

The original hydrocarbon generative potential values calculated by the methods are lower than the ones presented in chapter 4.2.1.5. The greatest differences between the values esitmated by knowing the origin of the organic matter and when this information is not available, are observed for the Dahl et al. (2004) method (Fig. 49). The lowest mean $S2_o$ values were given by the Dahl et al. (2004) method using 17% as input value, while the highest mean $S2_o$ values come from the Jarvie et al. (2007) method. The reason for the high calculated values given by the Jarvie et al. (2007) method is probably that equation 6 is only valid for type II kerogen, while the calculations of the other methods do not depend on the kerogen type.

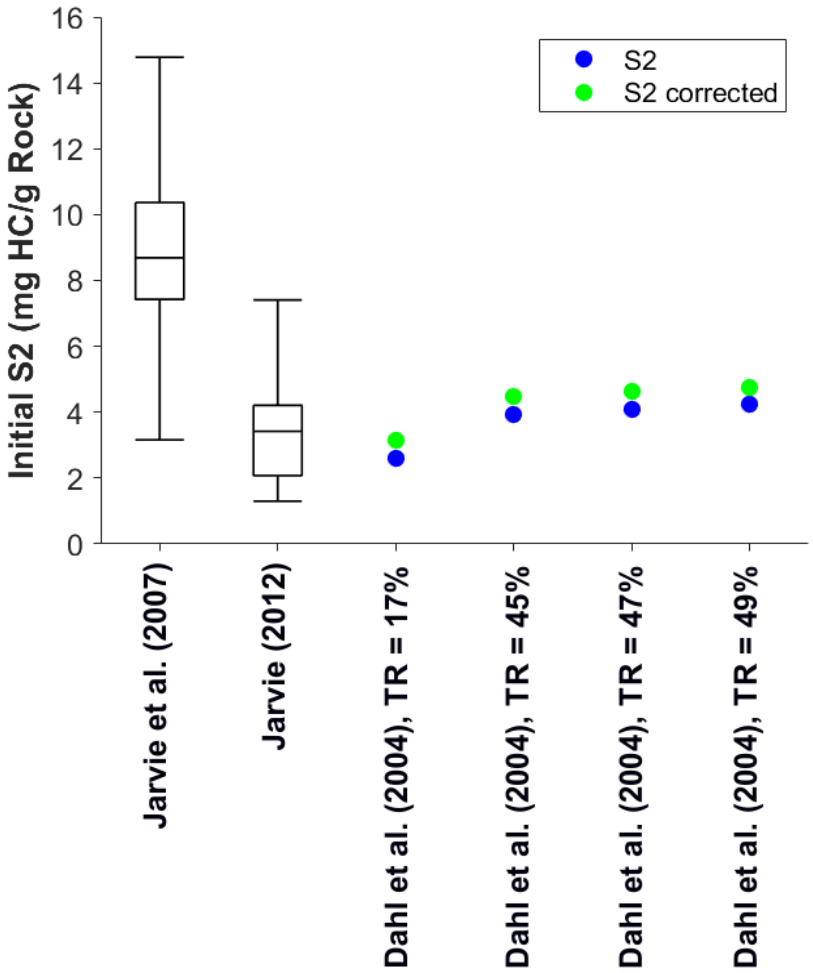

Figure 49. Initial hydrocarbon potential of the Passhatten Member estimated by the different methods.

4.2.2.6 Interpretation of the results

The average original hydrogen index estimated by the Jarvie et al. (2007) method (202 mg HC/g TOC) indicates Organic Facies C for the organic matter in the Passhatten Member (Jones, 1987). The Dahl et al. (2004) method yielded a range of uncorrected original hydrogen index values between 145 mg HC/g TOC when the average production index value (17%) was used as input and 219 mg HC/g TOC when calculating by the transformation ratio of 49%. These values are also indicative of Organic Facies C (Jones, 1987). Organic Facies C is typically deposited in oxic water on the shelf and continental slope where high depositional rates are present (Jones, 1987). The presence of Organic Facies C would imply mainly terrestrially derived organic matter (Jones, 1987). The matrix corrected initial hydrogen index values calculated by the Dahl et al. (2004) method yielded a range of 176–260 mg HC/g TOC with respect to the transformation ratio input. Among these values, the ones calculated by the

transformation ratio inputs of 17% and 45%, 176 mg HC/g TOC and 249 mg HC/g TOC respectively, also indicate Organic Facies C in the member (Jones, 1987). However, the corrected HI_o values obtained by the transformation ratio values of 45% and 49%, 254 mg HC/g TOC and 260 mg HC/g TOC respectively, are indicative of Organic Facies BC (Jones, 1987). Organic facies BC is formed in marine and lacustrine settings, usually in proximity of major river systems and is composed of mainly terrestrial organic matter (Jones, 1987). The TOC_o values calculated all of the methods can be characteristic for both organic facies as the total organic carbon content of Organic Facies BC and C are highly variable (Jones, 1987). In contrast to the interpretation suggested by the back calculated HI_o values of the methods, the organic matter in the Passhatten Member is mainly marine and was deposited under anoxic conditions, occasionally interrupted by dysoxic bottom currents (Karcz, 2014).

The average transformation ratio values provided by the methods indicate late mature stage for the organic matter, while the mean production index value suggests early maturity (Peters & Cassa, 1994). None of the calculated average transformation ratio values are in agreement with the T_{max} values of the section, which suggest that the organic matter is overmature (Peters & Cassa, 1994). The mean TOC_o values show very good organic-richness (Peters & Cassa, 1994).

The average $S2_o$ values of the methods suggest fair initial hydrocarbon generative potential with the exception of the Jarvie et al. (2007) method, which indicates good hydrocarbon generative potential (Peters & Cassa, 1994).

Conclusively, the application of the methods without confident knowledge about the origin of the organic matter leads to the underestimation of the original organic carbon content, the maturation stage, the hydrocarbon generative potential and the quality of organic matter in the Passhatten Member.

4.3 Volg–2 sequence, Jeppe-1 well, Danish Central Graben

Only a few data values have been published for the Volg–2 sequence. The Rock-Eval data of the sequence are given in Dahl et al. (2004), however they lack intepretation. Geochemical reports, logs and sedimentological data from the well have not been given which makes the interpretation of the depositional environment complicated. As a result of the absence of any depositional environment indicators from the well, the maceral composition and degree of degradation of the organic matter in the Volg–2 sequence are not known. For this reason, the proper application of the methods is hard. Here, two scenarios were tested for all methods. First,

a composition of type III and IV kerogen was tested based on the degraded organic matter in the sequence. This kerogen composition was determined from Figs. 15 and 16. Second, a mixture of type II and III kerogen was tested, assuming that the organic matter was degraded and had better quality before maturation. The basis of the assumption about the kerogen composition of the non-degraded organic matter is the depositional environment of the Volg–2 sequence and the maturity stage of the degraded organic matter. According to Andsbjerg & Dybkjær (2003), the organic matter in the sequence was deposited under an anoxic water column on the basin floor. This suggests that the organic matter had better quality before maturation (better quality than what is suggested by Figs. 15 and 16 on the basis of the degraded organic matter). Moreover, the production index values of the section indicate peak to late maturity for the samples, which suggests that the organic matter quality was degraded upon maturation (the original hydrogen index values of the samples were reduced).

4.3.1 Results based on degraded organic matter

Based on the data of Dahl et al. (2004), the organic matter of the Volg–2 sequence in the Jeppe-1 well consists of 63% type III and 37% type IV kerogen (chapter 2.2.4). The kerogen composition of the section and the corresponding correction factor (k = 0; Jarvie et al. 2007) was put into equation 3 to obtain the original hydrogen index of the section by the Jarvie et al. (2007) method. For the Volg–2 sequence, visual kerogen assessment has not been carried out due to the lack of data. For this reason, the volume percentages of the different maceral groups are not known and therefore it was not possible to use the Jarvie et al. (2007) method to obtain a separate original hydrogen index value for each sample. Instead, based on the kerogen composition, a mean initial hydrogen index value was obtained for the section. This is the reason for presenting only single values on the figures as results of the Peters et al. (1996), Jarvie et al. (2007) and Jarvie (2012) methods in chapter 4.3.

4.3.1.1 Original hydrogen index (HI_o)

According to the Jarvie et al. (2007) method, the original hydrogen index of the sequence is 92 mg HC/g TOC. The original hydrogen index given by the Dahl et al. (2004) method is a function of the transformation ratio (Fig. 50). Based on the Dahl et al. (2004) method, the calculated transformation ratio values of 17%, 21.74% and 27.62% yielded original hydrogen index values of 230 mg HC/g TOC, 241 mg HC/g TOC and 256 mg HC/g TOC respectively. The initial hydrogen index calculated by the same method, using the average production index value of

the sequence (40%) is 296 mg HC/g TOC. The correction of the obtained original hydrogen index values of the Dahl et al. (2004) method for matrix effect results in much higher hydrogen index values. For the transformation ratio values of 17%, 21.74%, 27.62% and 40% the calculated matrix corrected hydrogen index values are 442 mg HC/g TOC, 451 mg HC/g TOC, 465 mg HC/g TOC and 493 mg HC/g TOC respectively. The large variation between the hydrogen index values corrected and not corrected for matrix effect is the result of the large amount of retained pyrolysable organic matter in the section (5.88 mg HC/g Rock). Among the calculated initial hydrogen index values, the Jarvie et al. (2007) method yielded the lowest average value.

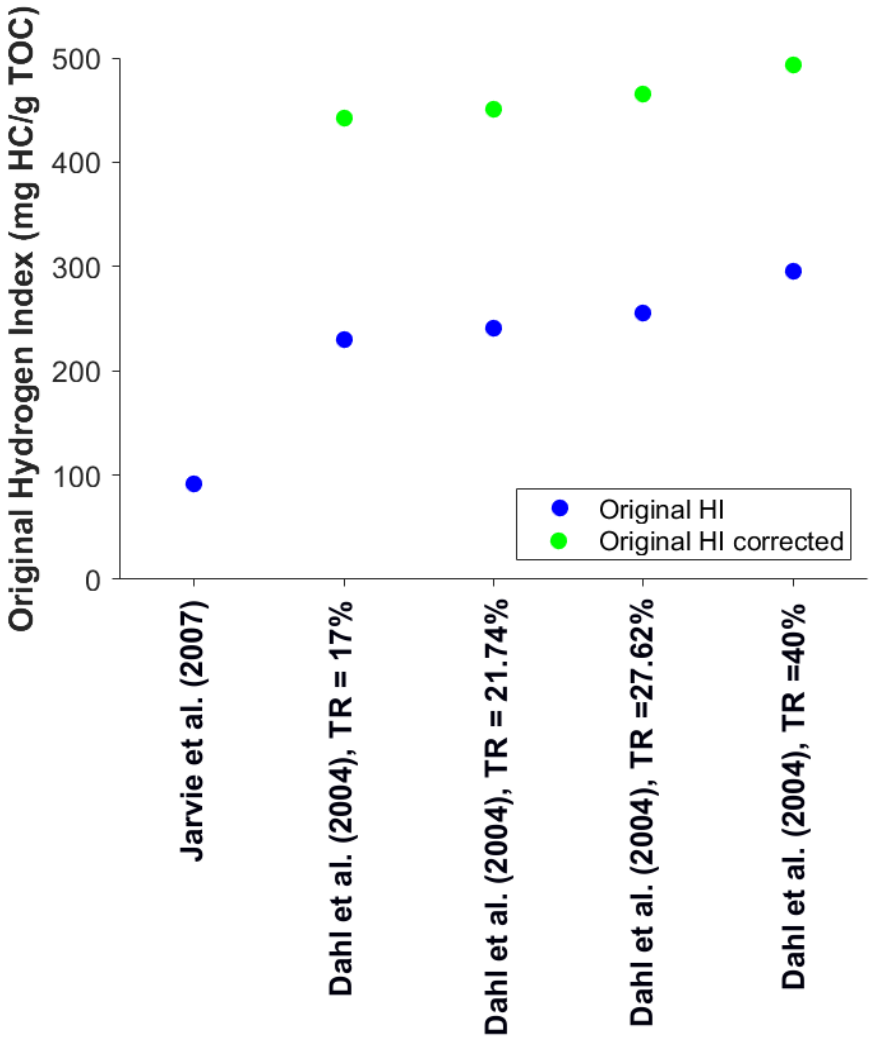

Figure 50. Original hydrogen index values of the Volg–2 sequence calculated by the different methods.

4.3.1.2 Transformation ratio

The transformation ratio values calculated using the original hydrogen index value of 92 mg HC/g TOC are different for the Peters et al. (1996), Jarvie et al. (2007) and for the Jarvie (2012) methods. The Peters et al. (1996) method yielded a similar transformation ratio value (17%) to the result of the Jarvie (2012) method (21.74%). The transformation ratio calculated by the Jarvie et al. (2007) method is higher than the results of the other methods, 27.62%.

The calculations of the Dahl et al. (2004) method were repeated three times to see how the results change by using the different transformation ratio estimates of the Peters et al. (1996), Jarvie et al. (2007) and Jarvie (2012) methods as inputs. When the transformation ratio of 17% was used as input, the code gave a warning message that the transformation ratio for the method to work should be higher than 21.18% on the basis of equation 62. In spite of this, the method calculates results on the basis of the generated overlay.

4.3.1.3 Gas to oil ratio potential (GORP)

The GORP for the Volg–2 sequence obtained by equation 59 for the transformation ratios of 17%, 21.74%, 27.62% and 40% are shown in Table 15. The GORP calculated by equation 59 for the Volg–2 sequence by using the transformation ratio output of the Peters et al. (1996) was greater than one. The reason for this are the scattered data points on the overlay given by a transformation ratio input of 17% and that the regression line is out of the overlay range (Fig. 51). For this reason, the GORP was manually set to 0.9 on the basis of Fig. 51, following the methodology for the estimation of the GORP of Dahl et al. (2004).

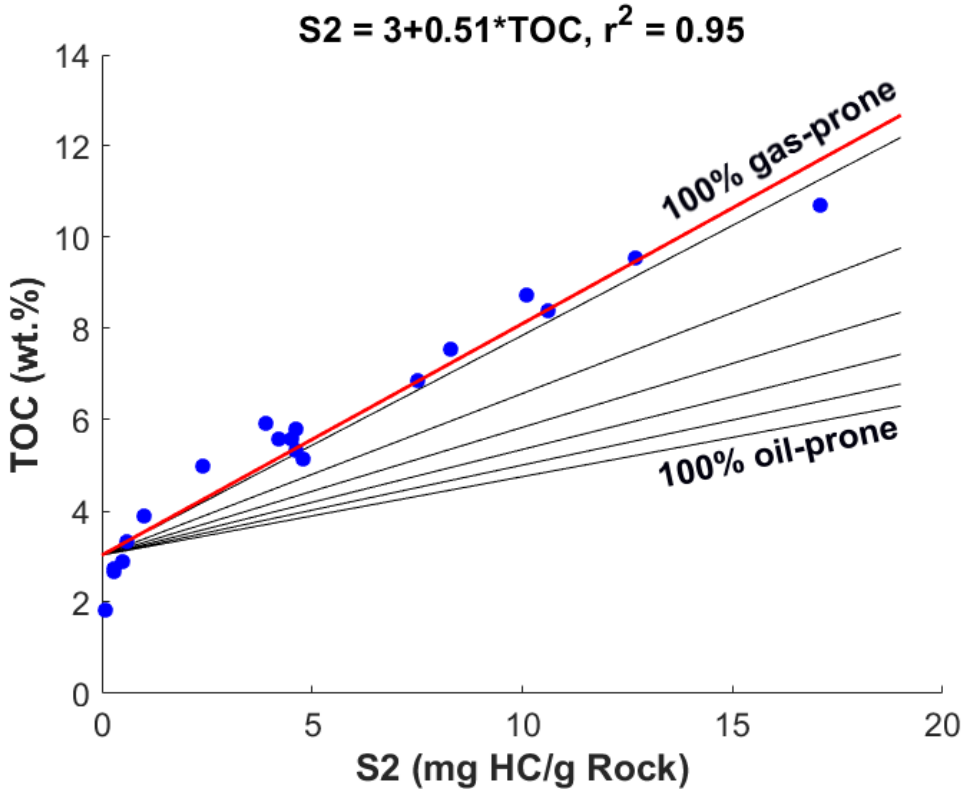

Figure 51. S2–TOC cross plot of the Volg–2 sequence given by the Dahl et al. (2004) method using a transformation ratio input of 17%. The regression line (marked by red), the generated overlay (black lines), the equation of the trend line and the linear correlation coefficient (r^2) are also shown.

Following Dahl et al. (2004) who used 40% as a transformation ratio input to their method, the GORP given by equation 59 is 0.83. The results estimated by using a GORP of 0.83 and by 0.9 (used in Dahl et al., 2004 for this section) are similar to each other. The similarity of the results given by using the GORP calculated from equation 59 and by the GORP value read off from the overlay (as carried out by Dahl et al., 2004) suggests the applicability and correctness of equation 59. Moreover, all GORP values suggest the dominance of gas-prone organic matter in the sequence.

Table 15. Gas to oil ratio potential values obtained for the different transformation ratio inputs by equation 59 or by visual inspection on the basis of the overlay.

Transformation ratio	Gas to oil ratio potential (GORP)	
	Obtained by equation 59	Estimated on the basis of the overlay
17%	1.03	0.9
21.74%	0.996	–
27.62%	0.95	–
40%	0.83	0.9

4.3.1.4 Original organic carbon content (TOC_o)

The original carbon contents calculated by the methods only show minor variations (Fig. 52).

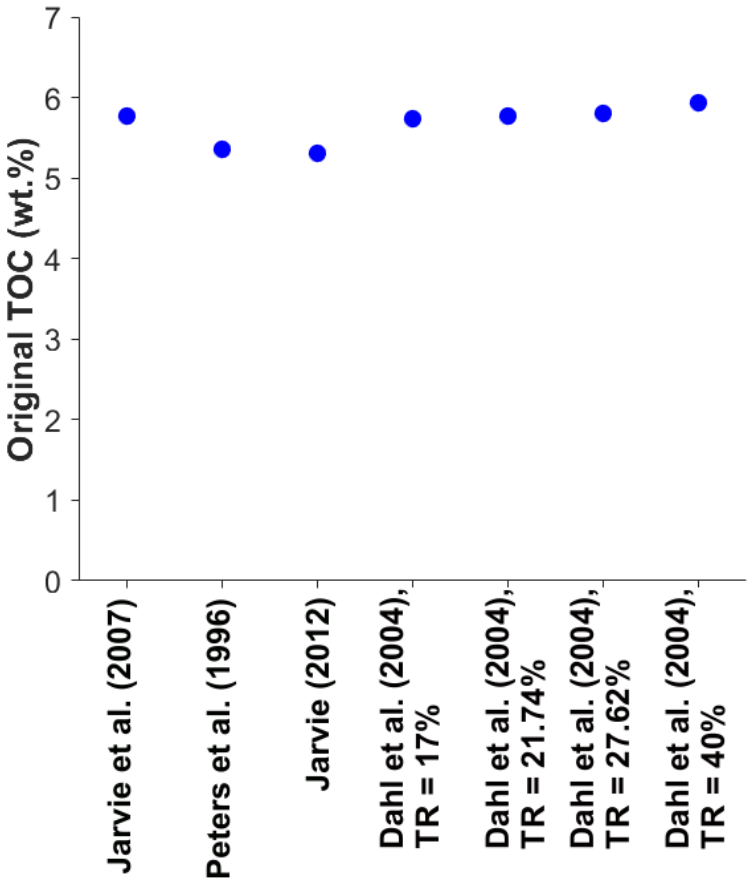

Figure 52. Original organic carbon values for the Volg–2 sequence, estimated by the different methods.

The difference between the lowest and highest TOC_o is 0.63 wt.%. The different TOC_o values given by the Dahl et al. (2004) method change with the transformation ratio. The higher the transformation ratio is, the larger the estimated TOC_o is (Fig. 52).

4.3.1.5 Initial hydrocarbon generative potential ($S2_o$)

The lowest original hydrocarbon generative potential was calculated by the Jarvie (2012) method, while the Jarvie et al. (2007) method yielded the highest value (Fig. 53). The $S2_o$ calculated by the Dahl et al. (2004) method is greater when the transformation ratio of the organic matter is larger (Fig. 53). Furthermore, the results of the Jarvie (2012) and Dahl et al. (2004) methods are comparable. The high $S2_o$ calculated by the Jarvie et al. (2007) method is probably the result of the correction factor in the $S2_o$ equation which is only valid for tpye II kerogen (the author did provide correction factors for the other kerogen types).

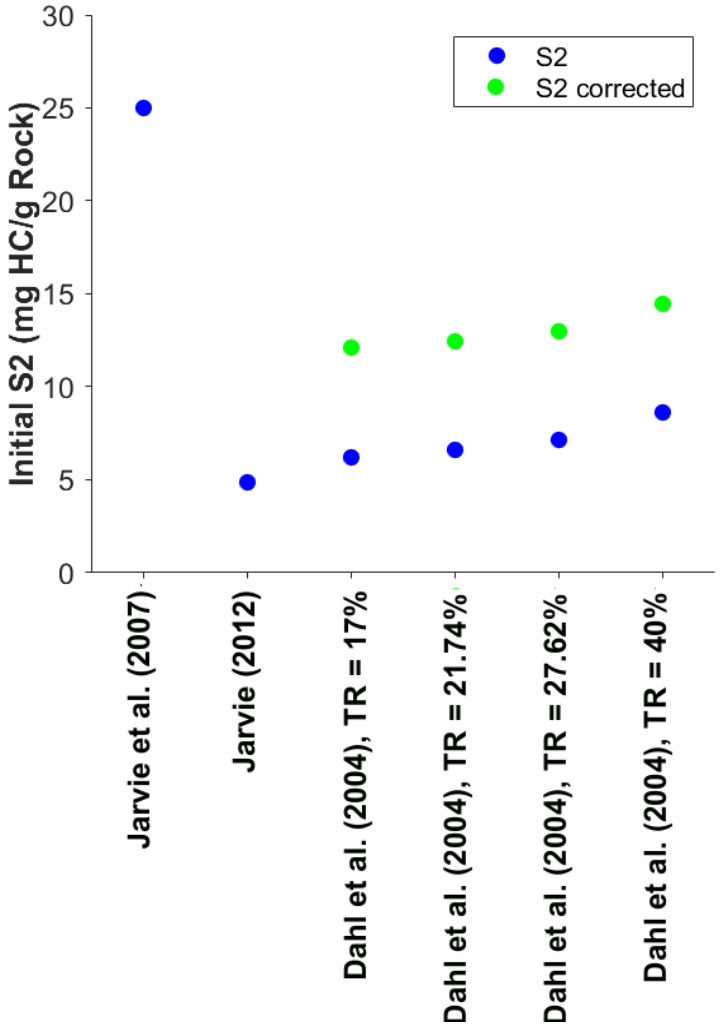

Figure 53. Initial hydrocarbon generative potential of the Volg–2 sequence according to the different methods.

4.3.1.6 Interpretation of the results

The uncorrected original hydrogen index values calculated by the Dahl et al. (2004) method indicate Organic Facies C when the transformation ratio values of 17% and 21.74% are used, whereas for 27.62% and for 40%, the suggested organic facies type for the sequence is BC (Jones, 1987). The initial hydrogen index values given by the Dahl et al. (2004), corrected for matrix retention, indicate organic facies B in the sequence (Jones, 1987). According to the original hydrogen index calculated by the Jarvie et al. (2007) method, the organic matter of the Volg–2 sequence was deposited as organic facies CD (Jones, 1987). The back calculated TOC_o values of all methods are indicative of organic facies B as this type of organic facies is characterised by a general TOC range of 2–10 wt.% (Jones, 1987). Organic Facies B is deposited under anoxic water column in a marine or lacustrine environment (Jones, 1987). Organic facies BC can be deposited under marine, anoxic conditions by receiving substantial amounts of terrestrially derived organic matter (Jones, 1987). Organic facies C represents mainly terrestrial organic matter with some degree of oxidisation (Jones, 1987). This facies is deposited under an oxic water column in marine or swamp environments characterised by high sedimentation rates (Jones, 1987). Organic facies CD represents highly oxidised and reworked organic matter deposited in an inner-shelf marine or lacustrine environment (Jones, 1987). According to Andsbjerg & Dybkjær (2003), the organic material in the Volg–2 sequence was deposited on the basin floor under an anoxic water column. Beyond the scope of the project, further research is needed to determine which depositional environment intepretation is correct as this information is not sufficient to make a conclusion.

According to the calculated TOC_o values, all methods indicate excellent organic-richness for the sequence (Peters & Cassa, 1994). The $S2_o$ values of the Jarvie et al. (2007) method suggests excellent organic-richness for the Volg–2 sequence (Peters & Cassa, 1994). The Jarvie (2012) method and the uncorrected results of the Dahl et al. (2004) method suggest good, while the corrected $S2_o$ values of the Dahl et al. (2004) method indicate very good initial hydrocarbon generative potential (Peters & Cassa, 1994).

The transformation ratio calculated by the Peters et al. (1996) method indicates early mature stage for the organic matter in the section, which is agreement with the maturity stage suggested by the T_{max} values (Peters & Cassa, 1994). The transformation ratio results of the Jarvie et al. (2007) and Jarvie (2012) methods indicate peak maturity, which is higher than the maturity stage based on the T_{max} values (Peters & Cassa, 1994; Dahl et al., 2004).

In conclusion, the interpretation of the organic facies, the organic-richness and hydrocarbon generative potential of the organic matter in the Volg–2 sequence varies with the method used for back calculation.

4.3.2 Results based on the assumed kerogen composition of the non-degraded organic matter

Based on the assumption that during preservation and maturation, the organic matter of the Volg–2 sequence was degraded, the kerogen composition of the degraded material was changed from type III and IV to type II and III. The assumption about the original kerogen composition of the organic matter is based on the study of Andsbjerg & Dybkjær (2003), who concluded that the organic matter of the sequence was deposited under an anoxic water column on the basin floor. This depositional environment interpretation suggests better organic matter quality than what is indicated by the degraded organic material on figs. 15 and 16. Moreover, the hydrogen index of the organic matter reduces due to maturation (Tissot & Welte, 1984). The organic material in the Volg–2 sequence is in a peak to late mature stage, which indicates that the original hydrogen index of the organic matter in the sequence was higher before maturation (this also indicates better original quality).

The volume percentage of type III kerogen (63%) and type IV kerogen (37%) in the organic matter was used in the Jarvie et al. (2007) method (equation 3) as type II and type III kerogen respectively to obtain an original hydrogen index value for the sequence. Furthermore, a correction factor of 0.15 was applied in equation 3 due to the assumed dominance of type II kerogen (Jarvie et al., 2007). Similarly to chapter 4.3.1, the Jarvie et al. (2007) method yielded only an average HI_o, TOC_o and $S2_o$ value for the sequence as the kerogen composition of the samples is not known.

4.3.2.1 Original hydrogen index (HI_o)

The average original hydrogen index of the sequence was calculated to be 330 mg HC/g TOC by the Jarvie et al. (2007) method. The original hydrogen index results show large variations (Fig. 54). The HI_o value calculated by the Jarvie et al. (2007) method is significantly lower than the values computed by the Dahl et al. (2004) method. The matrix and non-matrix corrected HI_o values calculated by the Dahl et al. (2004) method also show large differences compared to each other.

The difference between the corrected and uncorrected values is the result of the retained organic matter. The unusually high original hydrogen index values computed by the Dahl et al. (2004) method are the results of the high transformation ratio inputs (described below) compared to the ones in chapter 4.3.1.2.

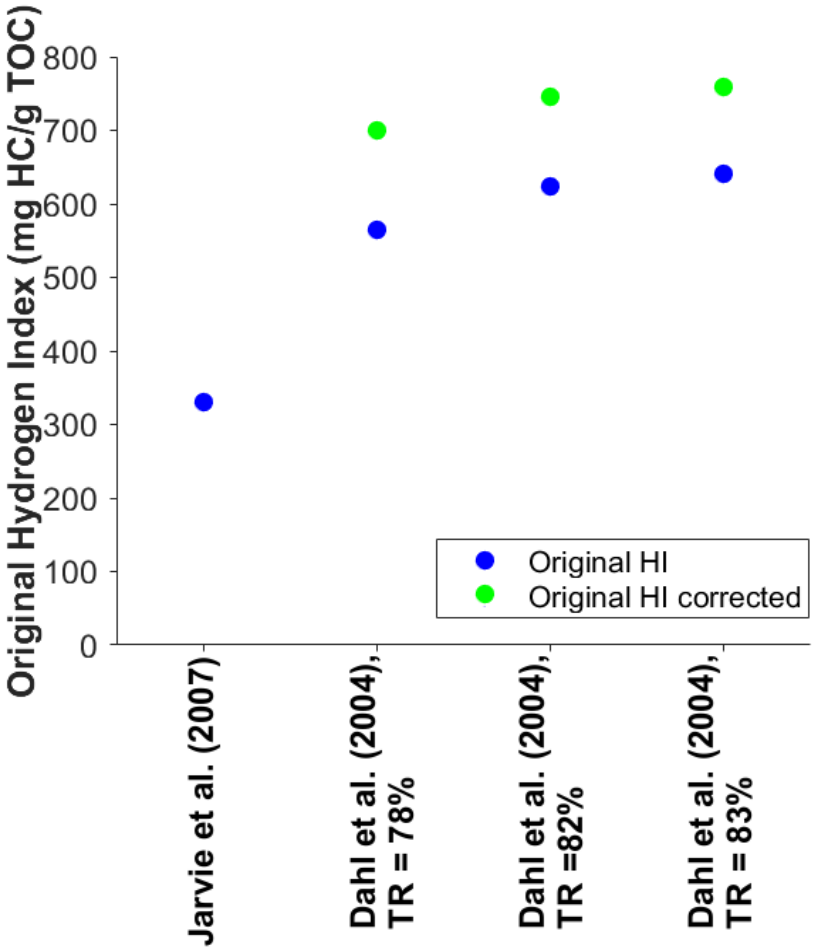

Figure 54. Original hydrogen index values of the Volg–2 sequence, calculated by the different methods.

4.3.2.2 Transformation ratio

Applying the original hydrogen index value calculated by the Jarvie et al. (2007) method as input into the Peters et al. (1996), Jarvie et al. (2007) and Jarvie (2012) methods yielded transformation ratios of 82%, 83% and 78% respectively.

The transformation ratios were used as inputs to the Dahl et al. (2004) method, however, the code of the method showed a warning message that all of these values are too high for the method to work. According to equation 65, the transformation ratio input value should be lower

than 72% for the method to work. However, the method calculated results on the basis of the overlay.

4.3.2.3 Gas to oil ratio potential (GORP)

The GORP values yielded by equation 59 for the transformation ratios of 78%, 82% and 83% were negative, resulting in negative TOC and S2 values for the oil-prone end-member. For this reason, the GORP was set manually to 0.1 on the basis of Figs. 55 and 56, following the GORP estimation workflow of Dahl et al. (2004). The GORP value of 0.1 indicates a mostly oil-prone section. The S2–TOC cross plot of the data set given by the Dahl et al. (2004) method when using a transformation ratio input of 82% is not shown as it is similar to Fig. 56.

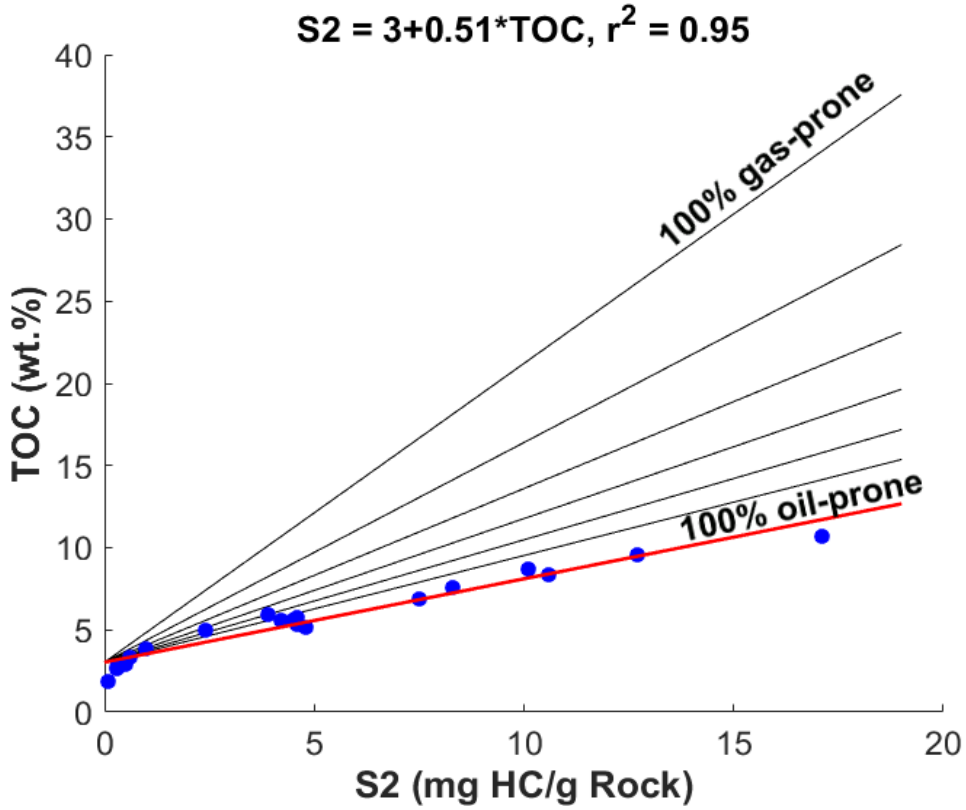

Figure 55. S2–TOC cross plot of the Volg–2 sequence on the basis of the Dahl et al. (2004) method when a transformation ratio value of 78% is used as input. The trend line (red), the overlay (black lines), the equation of the regression line and the linear regression coefficient (r^2) are also shown.

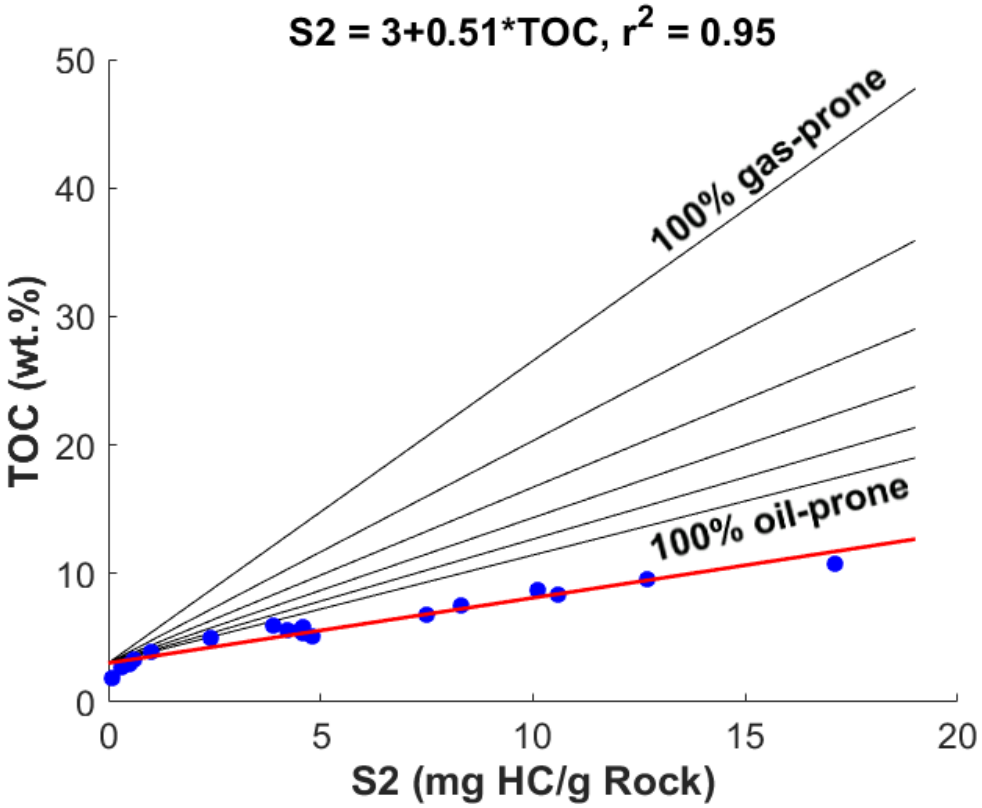

Figure 56. S2–TOC cross plot of the Volg–2 sequence samples given by the Dahl et al. (2004) method when a transformation ratio value of 83% is used as input. The regression line (red), the overlay (black lines), the equation of the trend line and the linear correlation coefficient (r^2) are also shown. The trend line equation and r^2 are the same as for the previous figure, but due to the higher transformation ratio used here, the section is shown to be more oil-prone.

4.3.2.4 Original organic carbon content (TOC_0)

The original organic carbon content values calculated by the methods yielded comparable values with a maximum difference of 1.51 wt.% (Fig. 57). The lowest value was calculated by the Jarvie et al. (2007) method, while the highest value was given by the Dahl et al. (2004) method based on the highest transformation ratio input (83%).

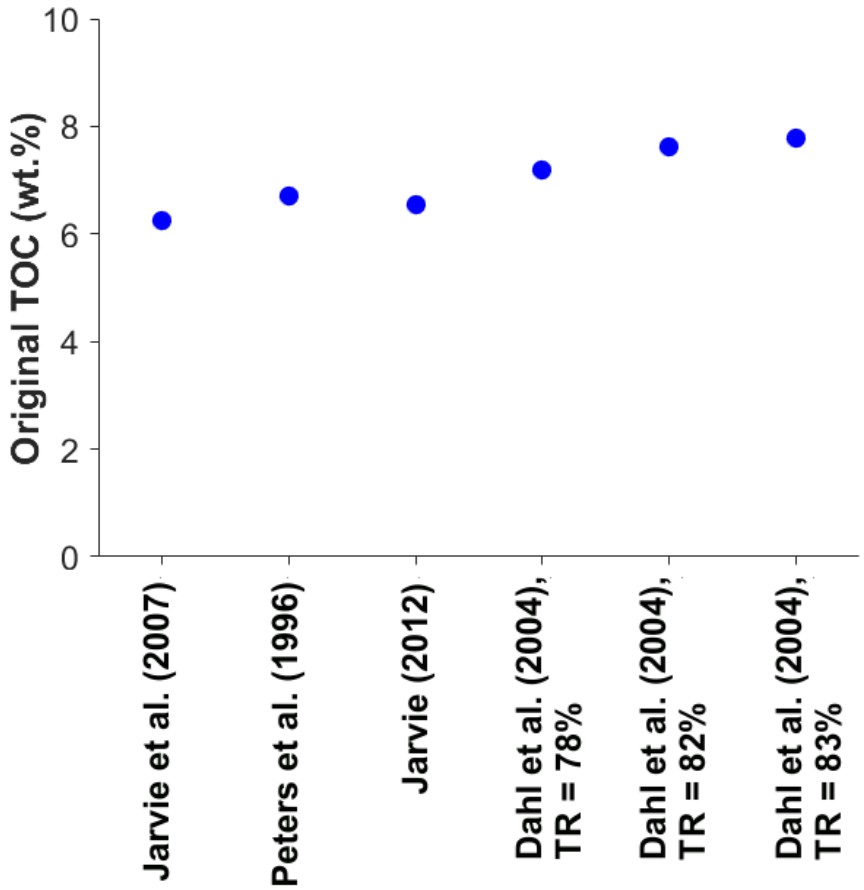

Figure 57. Original total organic carbon values of the Volg–2 sequence as calculated by the different methods.

4.3.2.5 Initial hydrocarbon generative potential ($S2_o$)

The $S2_o$ values calculated by the different methods show large variations (Fig. 58). The lowest initial hydrocarbon generative potential was obtained by the Jarvie (2012) method, while the highest value was estimated by the Dahl et al. (2004) method (Fig. 58). The initial S2 calculated by the Jarvie (2012) method is comparable to the non-matrix corrected value computed by the Dahl et al. (2004) method using a transformation ratio of 78%. The non-matrix corrected results of the Dahl et al. (2004) method obtained using the transformation ratio inputs of 82% and 83% are similar to the outcome of the Jarvie et al. (2007) method. The matrix corrected $S2_o$ values obtained by the Dahl et al. (2004) method are higher than the other results due to the retained amount of pyrolysable material in the section.

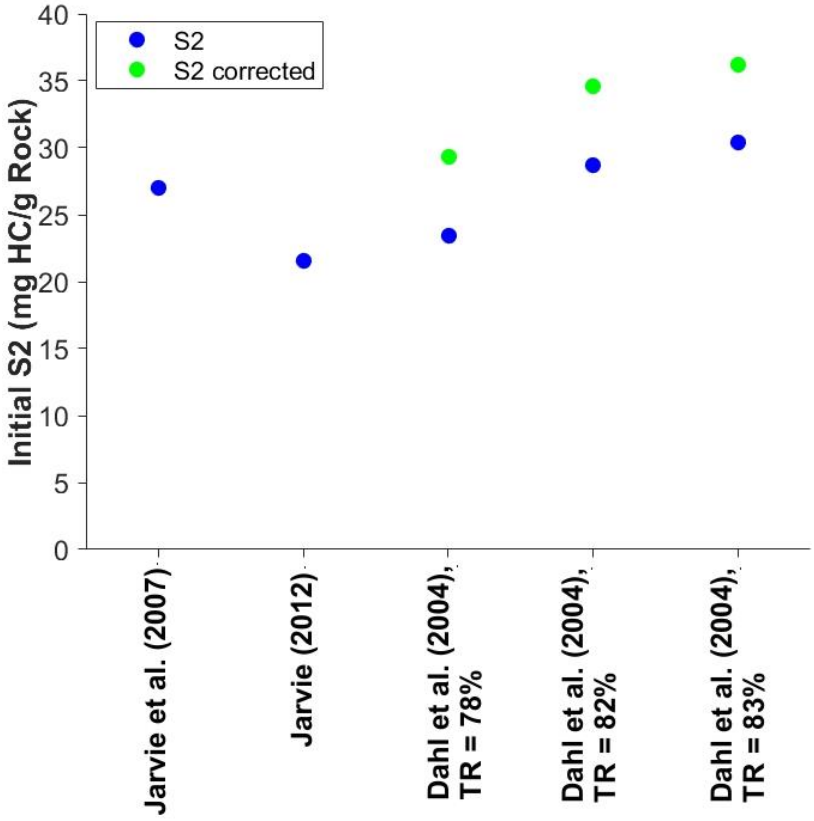

Figure 58. Initial hydrocarbon potential of the Volg–2 sequence according to the different methods.

4.3.2.6 Interpretation of the results

The transformation ratios calculated by the methods indicate the presence of overmature organic matter in the Volg–2 sequence, which contradicts with the early mature stage suggested by the T_{max} values (Peters & Cassa, 1994; Dahl et al., 2004). The estimated original carbon content and hydrocarbon generative potential values suggest excellent organic-richness for the sequence (Peters & Cassa, 1994).

The original hydrogen index calculated by the Jarvie et al. (2007) method is 330 mg HC/g TOC, indicating the presence of Organic Facies BC (Jones, 1987). The non-matrix corrected original hydrogen index values estimated by the Dahl et al. (2004) method are indicative of Organic Facies B, while the matrix corrected values suggest Organic Facies AB (Jones, 1987). The back calculated TOC_o values suggest organic facies AB or B as both of these organic facies can have TOC values between 3–10 wt.% (Jones, 1987). Organic Facies AB and B are deposited under an anoxic water column in marine or lacustrine environments, while Organic Facies BC is

typical in the proximity of major river systems also in lacustrine or marine settings (Jones, 1987). Organic Facies AB is mainly composed of marine organic matter, Organic Facies B contains more terrestrial organic material (Jones, 1987). Organic Facies BC is a mixture of marine and terrestrial organic material (Jones, 1987). The shales of the Volg–2 sequence were deposited under marine and probably anoxic conditions on the basin floor (Andsbjerg & Dybkjær, 2003) but this information is not sufficient to decide which of the depositional environment interpretations discussed above is correct.

In conclusion, the depositional environment interpretation, the inferred organic-richness and the maturity of the organic matter is different with respect to the assumed kerogen composition depending on the method used for back calculation.

4.4 Southern North China Basin, Central China

According to Dang et al. (2016), the organic matter in the Taiyuan and Shanxi shales is characterised by extremely high thermal maturity. Due to the high thermal maturity of the samples, the organic matter in the formations is greatly degraded and therefore the majority of the measured data and the results of organic petrography can lead to misinterpretation bout the origin of the organic matter (Tissot & Welte, 1984; Dang et al., 2016). As a result of the uncertainty of the data at such high maturity, no assumption was made about the kerogen composition of the immature organic matter; the methods were tested based on the composition of the degraded material.

To obtain the original hydrogen index for the samples using the Jarvie et al. (2007) method, the volume percentage of the liptinite maceral group in the organic matter of the Shanxi and Taiyuan formations were assigned to type II kerogen in equation 3. The vitrinite content of the samples was used as type III kerogen and the inertinite volume percentage was applied as type IV kerogen in equation 3 (Dang et al., 2016).

4.4.1 Original hydrogen index (HI_0) and transformation ratio

Based on the original hydrogen index values for the samples calculated by equation 3 (Fig. 59), the Peters et al. (1996), the Jarvie et al. (2007) and the Jarvie (2012) methods yielded an average transformation ratio value of 91% (Fig. 60). The calculated transformation ratio ranges yielded by the methods show only minor variations.

The transformation ratio value of 91% was used as input to the Dahl et al. (2004) method, however, the code gave a warning message that this value is too large for the method to work on the basis of equation 65. According to equation 65, the maximum transformation ratio value for the method to work in this data set is 63%. Another limitation of the Dahl et al. (2004) method in this data set is that the data points are too scattered (Fig. 61), fall out of the overlay range and the linear correlation coefficient is too low ($r^2 = 0.0026$). In case the data of the two formations are used separately in the method, the linear correlation coefficients are also too low to obtain results for interpretation: $r^2 = 0.2752$ for the Shanxi Formation and $r^2 = 0.1032$ for the Taiyuan Formation respectively.

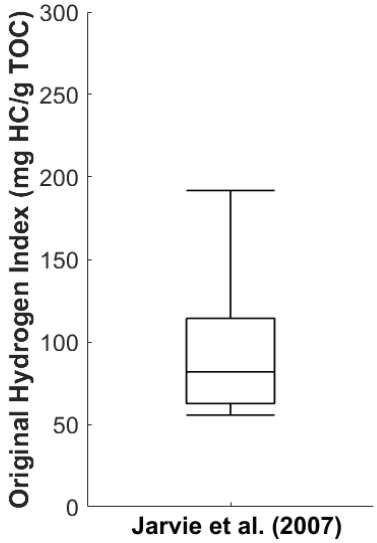

Figure 59. Original hydrogen index of the samples in the Shanxi and Taiyuan formations estimated by the Jarvie et al. (2007) method.

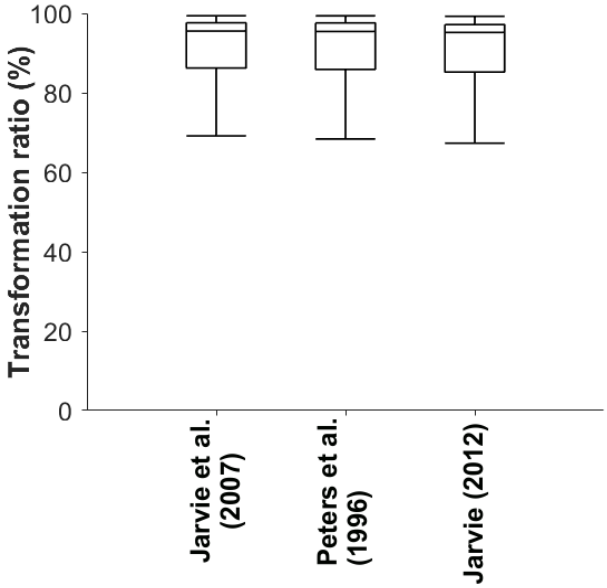

Figure 60. Transformation ratio estimation of the Shanxi and Taiyuan shales by the different methods.

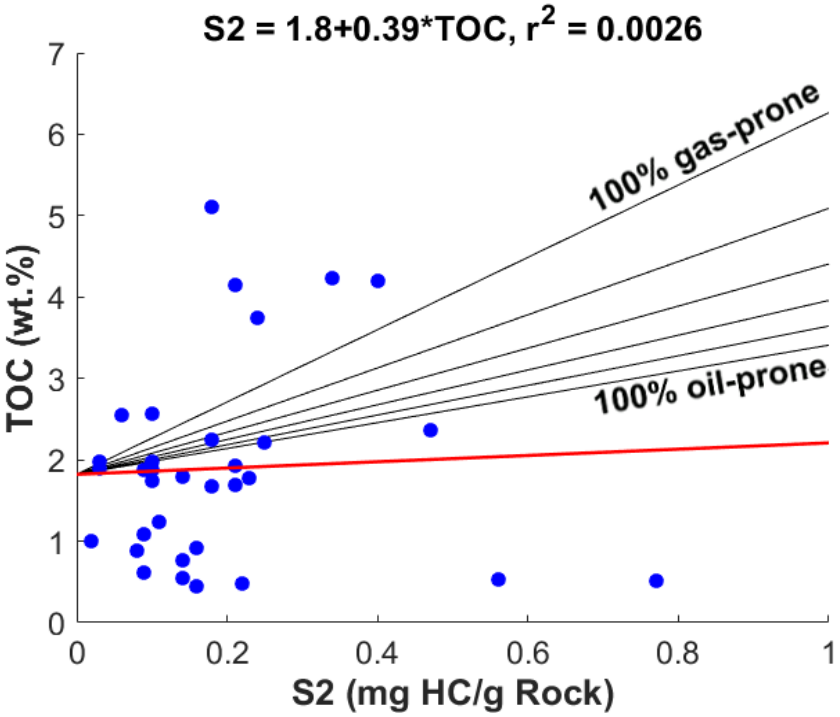

Figure 61. S2–TOC cross plot of the samples of the Shanxi and Taiyuan samples based on the Dahl et al. (2004) method. The trend line (red), the overlay (black lines), the equation of the regression line and the linear correlation coefficient (r^2) are also shown.

4.4.2 Original organic carbon content (TOC_o)

The original organic carbon contents given by the Peters et al. (1996), the Jarvie et al. (2007) and the Jarvie (2012) methods are similar and show only minor variations (Fig. 62).

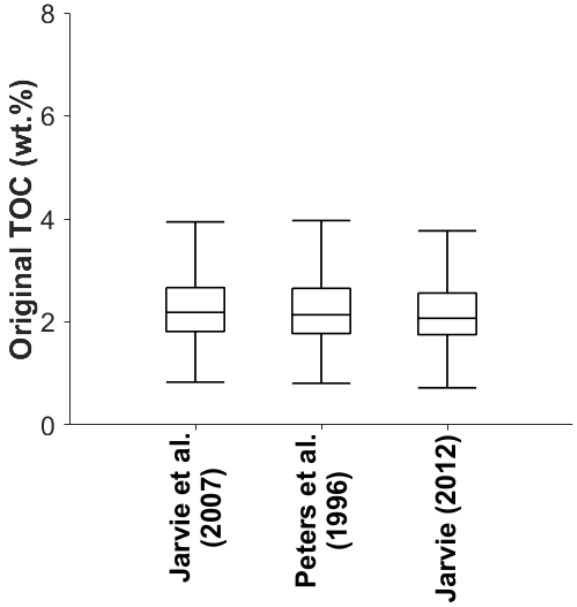

Figure 62. Original organic carbon content estimated by the different methods for the Taiyuan and Shanxi formations.

The lowest values were calculated by the Jarvie (2012) method, the highest values came from the Jarvie et al. (2007) method.

4.4.3 Initial hydrocarbon generative potential ($S2_o$)

The initial hydrocarbon generative potential values calculated by the Jarvie et al. (2007) and the Jarvie (2012) methods show large differences (Fig. 63). The former yielded much higher values than the Jarvie (2012) method. The equations for calculating $S2_o$ in both methods rely on the original generative organic carbon content but the Jarvie et al. (2007) method uses a correction factor in the equation which is only valid for type II kerogen. This can result in large computed $S2_o$ values as shown in Fig. 63.

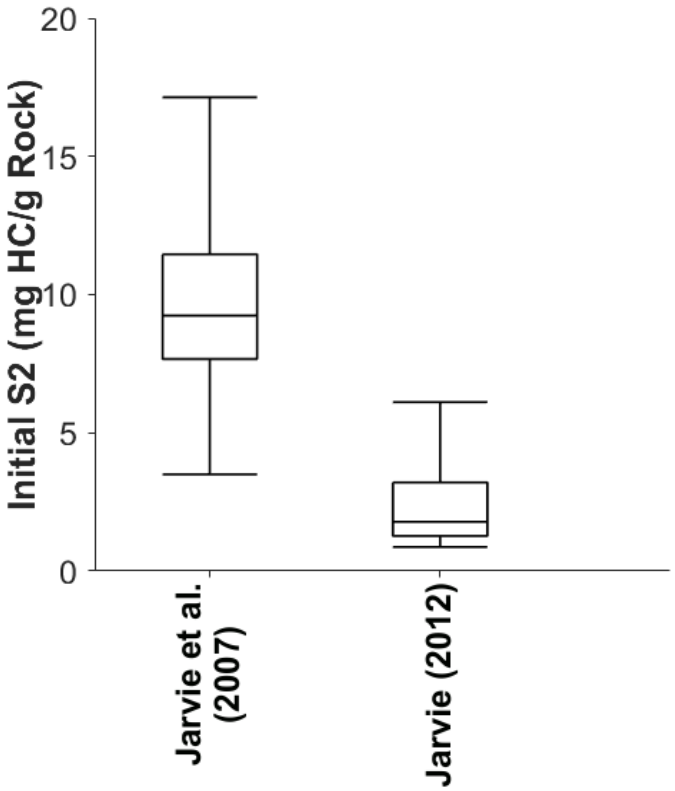

Figure 63. Initial hydrocarbon potential of the Taiyuan and Shanxi shales estimated by the Jarvie et al. (2007) and Jarvie (2012) methods.

4.4.4 Interpretation of the results

The TOC_o values calculated by the methods indicate very good organic-richness for the immature organic matter of the Shanxi and Taiyuan formations (Peters & Cassa, 1994). The $S2_o$ results suggest good organic-richness based on the Jarvie et al. (2007) method (Peters & Cassa, 1994). The Jarvie (2012) method indicates fair organic-richness on the basis of the $S2_o$ estimations (Peters & Cassa, 1994). The calculated transformation ratio values of all methods

indicate postmature stage for the organic matter in the Shanxi and Taiyuan formations, which is in agreement with the measured T_{max} values in the section (Peters & Cassa, 1994).

The Jarvie et al. (2007) method indicates Organic Facies CD for the Taiyuan Formation (HI_o = 87 mg HC/g TOC) and Organic Facies C for the Shanxi Formation (HI_o = 144 mg HC/g TOC) (Jones, 1987). These values indicate an inner-shelf environment and the dominance of terrestrial organic matter in the formations (Jones, 1987). The depositional environment characteristics outlined based on the scheme of Jones (1987) are congruent with the sedimentary conditions during the Early Permian in the Southern North China Basin (Yu et al., 2005; Zhou et al., 2010). The TOC_o values of the methods do not help to distinguish between organic facies C and CD because the TOC content of these facies are variable (Jones, 1987).

The results of the successfully tested methods in this data set indicate that the interpretation of the original geochemical parameters of the Shanxi and Taiyuan formations are the same with respect to the back calculated TOC_o and transformaiton ratio values, regardless of which method is used for computation. The $S2_o$ results of the Jarvie et al. (2007) and Jarvie (2012) methods show large variation and the interpretation of the organic-richness would be different based on this parameter.

4.5 Wenchang Formation, Huizhou Depression, South China Sea

The organic matter in 94.3% of the studied samples taken from the Wenchang Formation consists of type II kerogen, 4.3% of the samples is classified as type I kerogen and 1.4% is composed of type III kerogen (Jiang et al., 2015). The kerogen composition of the sample set was incorporated into equation 3 to obtain the original hydrogen index of the section by the Jarvie et al. (2007) method. A correction factor of 0.15 was used in the method as most of the organic matter in the formation consists of type II kerogen. Another kerogen composition was not tested for the samples due to the varying maturity level of the samples (immature–post mature) and due to the absence of visual kerogen assessment data. Organic petrographic information could be used to assume better organic matter quality for certain samples in equation 3 but since only the average kerogen composition of the sample set is known, testing all samples with better assumed organic matter quality would be incorrect because some of the organic matter in the formation is immature and early mature (not degraded). The results of the Jarvie et al. (2007) method are presented as single values in this subchapter because only the

average kerogen composition of the data set was available for testing, detailed organic petrographic information was not published by Jiang et al. (2015).

4.5.1 Original hydrogen index (HI_o) and transformation ratio

The average initial hydrogen index of the Wenchang Formation was calculated to be 458 mg HC/g TOC by the Jarvie et al. (2007) method. Applying this value in the Peters et al. (1996), Jarvie et al. (2007) and Jarvie (2012) methods, the transformation ratio value for the organic matter in the Wenchang Formation was estimated to be 72%, 74% and 63% respectively. The original hydrogen index values computed by the Dahl et al. (2004) method yielded a range of 321–647 mg HC/g TOC, while the matrix corrected initial hydrogen index values are between 467–733 mg HC/g TOC. Fig. 64 shows that there is a large difference between the matrix corrected and non-matrix corrected HI_o values calculated by the Dahl et al. (2004) method due to the amount of pyrolysable organic matter (1.39 mg HC/g Rock) retained by the mineral matrix. The result of the Jarvie et al. (2007) method is comparable to the matrix corrected HI_o computed by the Dahl et al. (2004) method using a transformation input of 16%.

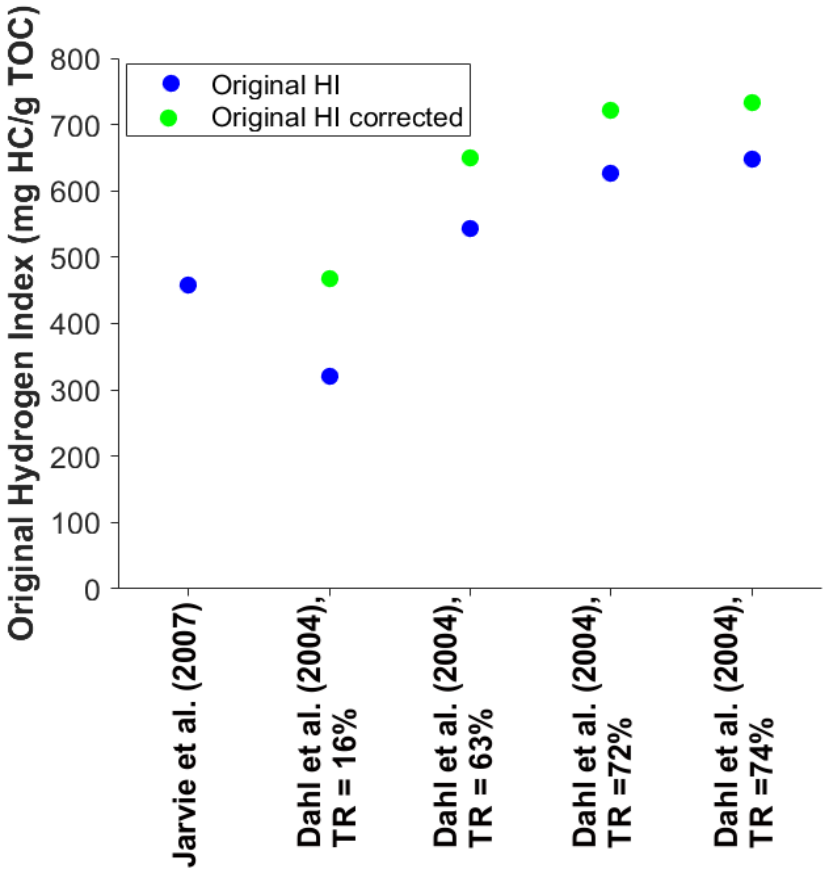

Figure 64. Original hydrogen index of the Wenchang Formation calculated by the different methods.

The transformation ratio values of 16%, 63%, 72% and 74% were used as inputs into the Dahl et al. (2004) method but according to equation 65, the maximum transformation ratio for the method to work in this data set is 59.75%. The results of the method however can be used for interpretation due to the high linear correlation coefficient (r^2 = 0.82).

4.5.2 Gas to oil ratio potential (GORP)

When using the mean production index value (16%) of the sample set as input, the GORP obtained by the Dahl et al. (2004) method is 0.81 on the basis of equation 59, suggesting the presence of mostly gas-prone organic matter (Fig. 65).

The transformation ratio values of 63%, 72% and 74% yielded negative GORP and gas-prone end-member values. For this reason, the GORP was manually set to 0.2 based on the workflow for GORP estimation of Dahl et al. (2004). The GORP value of 0.2 indicates the presence of mostly oil-prone organic matter in the section (Figs. 66 and 67). The S2–TOC cross plots of the samples are shown with overlays given by the transformation ratio values of 16%, 63% and 74% in Figs. 65−67. The figures indicate that with increasing transformation ratio, the quality of the organic matter of the Wenchang Formation changes from gas- to oil-prone, the equation of the trend line and the linear correlation coefficient are the same for all of the transformation ratio values.

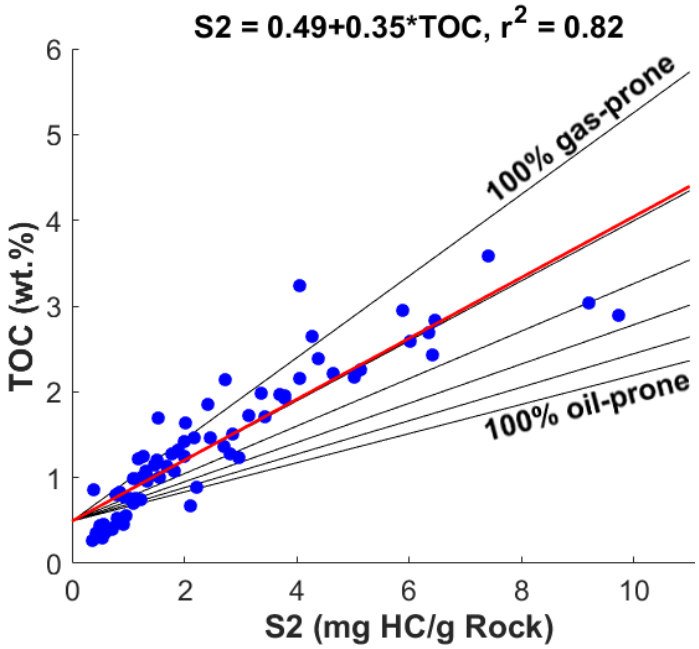

Figure 65. S2–TOC cross plot of the organic matter in the Wenchang Formation given by the Dahl et al. (2004) method considering the transformation ratio to be 16%. The regression line (red), the overlay (black lines), the equation of the trend line and the linear regression coefficient are also shown.

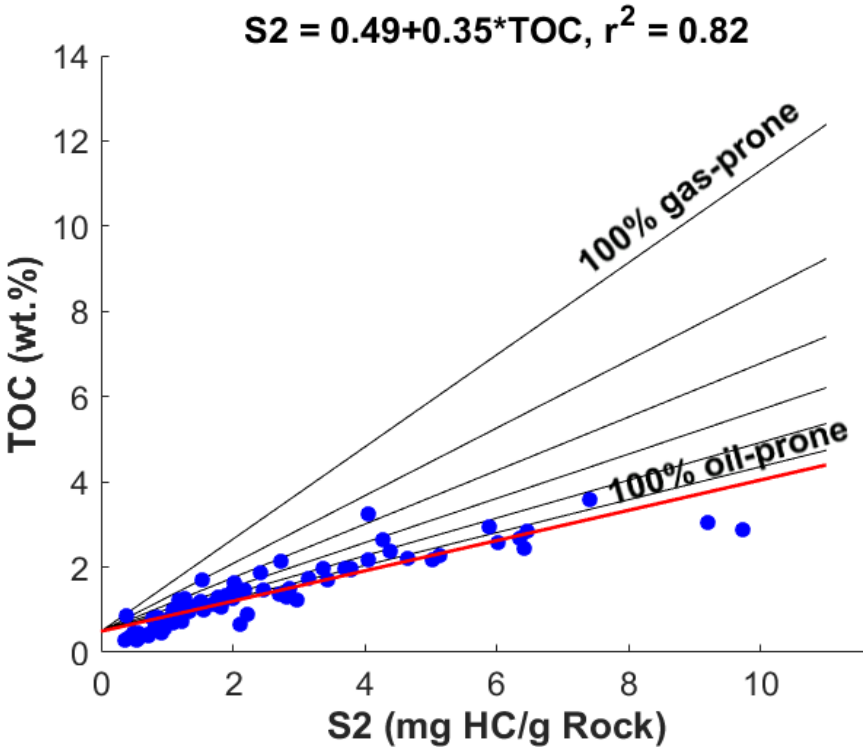

Figure 66. S2–TOC cross plot of the samples on the basis of the Dahl et al. (2004) method considering the transformation ratio to be 63%. The regression line (red), the overlay (black lines), the equation of the trend line and the linear regression coefficient are also shown.

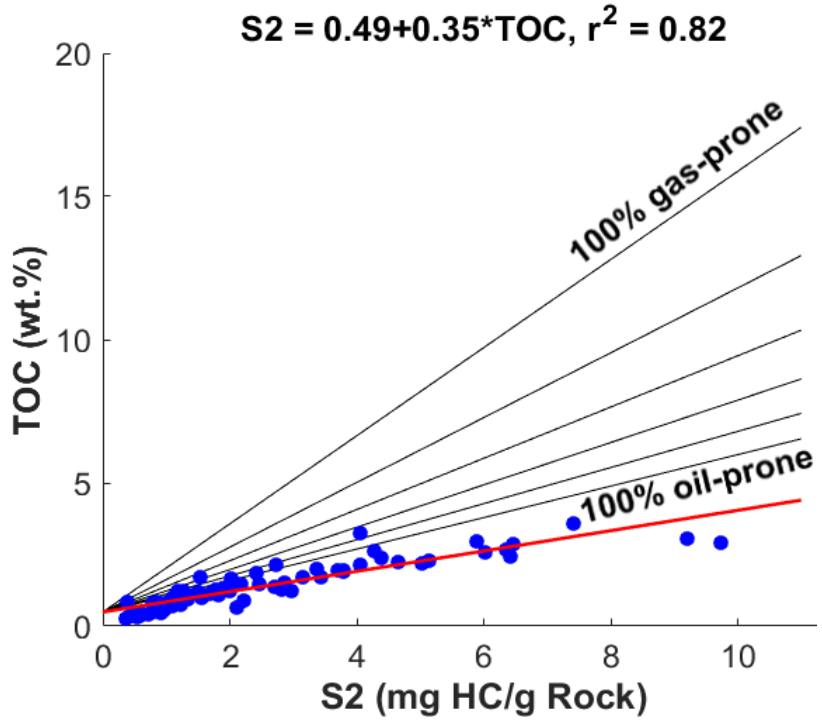

Figure 67. S2–TOC cross plot of the sample set based on the Dahl et al. (2004) method considering the transformation ratio to be 74%. The regression line (red), the overlay (black lines), the equation of the trend line and the linear regression coefficient are also shown.

4.5.3 Original organic carbon content (TOC_o)

The original organic carbon content of the samples estimated by the Peters et al. (1996), the Dahl et al. (2004) with transformation ratio inputs of 63–74% and the Jarvie et al. (2007) methods show minor variations (Fig. 68). The lowest TOC_o value was calculated by the Jarvie (2012) method and is comparable to values computed by the Dahl et al. (2004) method using a low transformation ratio (16%). The difference between the lowest and higest value is 0.72 wt.%.

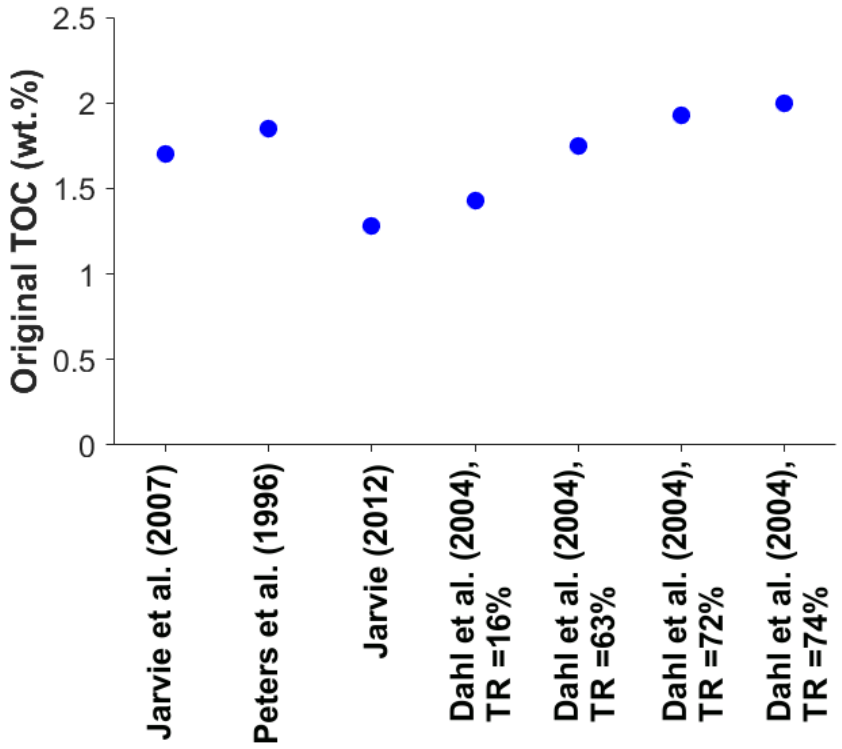

Figure 68. Original carbon content estimated for the Wenchang samples by the different methods.

4.5.4 Initial hydrocarbon generative potential ($S2_o$)

The calculated initial hydrocarbon generative potential values show large variation (Fig. 69). The lowest and highest $S2_o$ values were both calculated by the Dahl et al. (2004) method using the lowest (16%) and highest (74%) transformation ratio values as inputs. The results of the Jarvie et al. (2007) and Jarvie (2012) methods are comparable to the values calculated by the Dahl et al. (2004) using a transformation ratio of 63%.

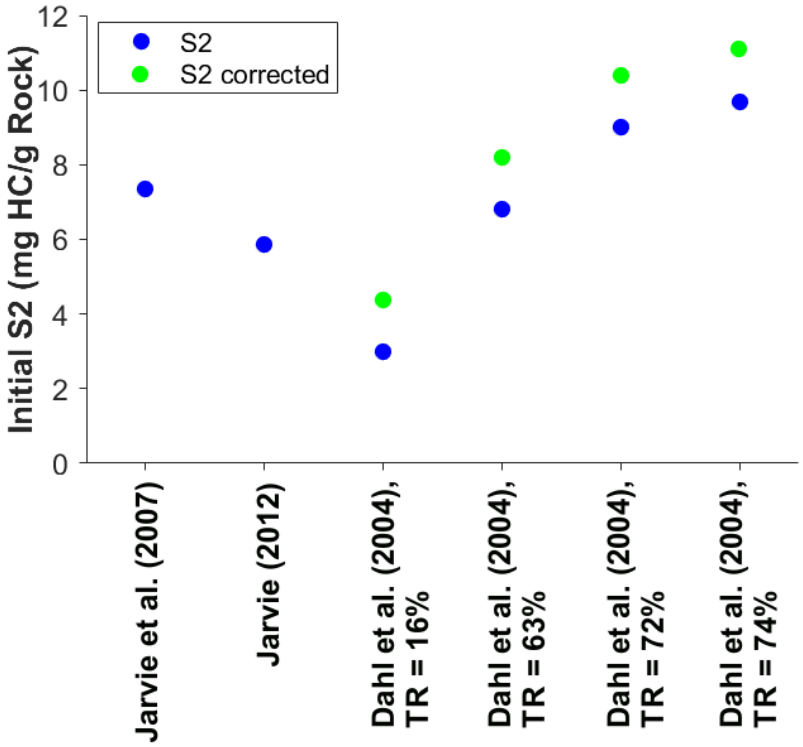

Figure 69. Initial hydrocarbon potential estimated by the different methods for the organic matter of the Wenchang Formation.

4.5.5 Interpretation of the results

The TOC_o values of the samples estimated by all methods indicate good organic-richness for the immature organic matter (Peters & Cassa, 1994). The $S2_o$ values estimated by the Jarvie et al. (2007) and Jarvie (2012) methods suggest good initial hydrocarbon generative potential, while the uncorrected $S2_o$ values given by the Dahl et al. (2004) indicate fair to good generative potential for the Wenchang Formation depending on the transformation ratio input (Peters & Cassa, 1994). The corrected $S2_o$ results of the Dahl et al. (2004) method suggest fair to very good generative potential with respect to the transformation ratio input (Peters & Cassa, 1994).

The non-matrix corrected original hydrogen index given by the Dahl et al. (2004) method (321 mg HC/g TOC) using a transformation ratio of 16%, indicates that the organic matter in the Wenchang Formation was deposited as Organic Facies BC (Jones, 1987). The matrix corrected value obtained by the same transformation ratio is 467 mg HC/g TOC, suggesting Organic Facies B (Jones, 1987). The HI_o yielded by the Jarvie et al. (2007) method (458 mg HC/g TOC) suggests the presence of Organic Facies B in the original organic matter (Jones, 1987). When the Dahl et al. (2004) method was used with transformation ratio inputs of 63%, 72% and 74%, the obtained uncorrected original hydrogen index values (543–647 mg HC/g TOC) are

indicative of Organic Facies B in the immature organic matter, while the matrix corrected values (650–733 mg HC/g TOC) suggest Organic Facies AB (Jones, 1987). The TOC_o values suggest Organic Facies BC, which usually has a TOC content of 1–3 wt.% (Jones, 1987). Organic Facies AB is of mostly marine origin and is deposited under anoxic conditions in lacustrine or marine environments (Jones, 1987). Organic Facies B is indicative of a similar depositional environment as Organic Facies AB but it is composed of less marine and more terrestrial organic matter and the oxygenation of the bottom water during deposition and preservation can fluctuate (Jones, 1987). Organic Facies BC can also be deposited in a marine or lacustrine environment but the presence of this facies indicates oxidation of the organic matter (Jones, 1987). Based on the biomarker study of Jiang et al. (2015), the organic material in the Wenchang Formation was deposited in a lacustrine basin isolated from marine conditions. Moreover, the sedimentary environment was characterised by weak oxidation–weak reduction. Based on the information given by Jiang et al. (2015), the methods suggesting that the immature organic matter can be classified as Organic Facies B or BC are probably the most realistic. Howvere, further research is needed to determine which organic facies describes best the type of the organic matter in the Wenchang Formation.

Overall, on the basis of the TOC_o values the methods suggests the same organic-richness for the Wenchang Formation with the exception of the Dahl et al. (2004) method when using a low transformation ratio input (16%) (Peters & Cassa, 1994). The $S2_o$ values of the Dahl et al. (2004) method using a transformation ratio of 16%, suggest fair initial hydrocarbon generative potential (Peters & Cassa, 1994). The results of the Jarvie et al. (2007), Jarvie (2012) methods and the uncorrected $S2_o$ values computed by the Dahl et al. (2004) method using transformation ratios of 63%, 72% and 74% indicate good original generative potential (Peters & Cassa, 1994). The corrected $S2_o$ obtained by the Dahl et al. (2004) using a transformation ratio of 63% suggests good generative potential, while the corrected $S2_o$ results of the same method using transformation ratios of 72% and 74% indicatevery generatvie potential (Peters & Cassa, 1994).

The transformation ratio estimates of the methods are in agreement with the study of Jiang et al. (2015), suggesting that most of the samples are in the main stage of hydrocarbon generation. This suggests that using the production index (16%) as transformation input into the Dahl et al. (2004) in this case does not reflect reality and underestimates the hydrocarbon generative potential of the Wenchang Formation. Furthermore, the depositional environment interpretation based on the Dahl et al. (2004) method using this value appears to be incorrect.

5. Discussion

5.1 Equation type

Estimates of the original hydrogen index (HI_o), initial organic carbon content (TOC_o) and organic-richness ($S2_o$) are useful indicators of the quality and quantity of the deposited organic matter (Jones, 1987). The original hydrogen index can be applied to obtain information about the type of the initially deposited organic carbon and therefore the original depositional environment (Jones, 1987; Karcz, 2014). Furthermore, the original carbon content also provides information about the amount of the buried organic carbon in the geological past, indicating a certain depositional environment and/or palaeoclimate (Jones, 1987; Killops & Killops, 2013).

The most commonly used equations in the literature to obtain the back calculated values of these parameters are derived by mass balance equations or line-fitting (Jarvie et al., 2007; Dahl et al., 2004). Both type of equations use values that are functions of the environment (Peters et al., 2005). The mass-balance-based methods either require an original hydrogen index input value (Peters et al., 1996; Jarvie, 2012) or knowledge about the degree of degradation and the origin of the organic material (Jarvie et al., 2007). When this information is not available, the calculated amount of deposited organic carbon, the computed organic-richness and the inferred type of organic matter as well as the interpreted depositional environment might not reflect reality (see chapter 4.2.2).

The best-fit methods (Banerjee et al., 1998; Dahl et al., 2004) calculate from a regression line based on a certain form of equation to obtain the back calculated geochemical parameters. The application of these methods is easier than the mass-balance-based methods because all the geochemical values are automatically derived by an algorithm. Dahl et al. (2004) highlighted that their the curve-fitting approach is not able to account for depositional environments with frequent changes between oxic and anoxic conditions as this results in very scattered data points and low linear correlation coefficient, which show no trends (see Fig. 61). According to Dahl et al. (2004), the method cannot represent geological settings where large shifts in the oxygenation of bottom water and in the sedimentation rate occurred as these result in a varying chemical composition of the same kerogen type. Furthermore, line-fitting is also problematic where different types of kerogen compositions change quickly, for example organic facies C or CD (containing mainly terrestrial organic matter) is interbedded with organic facies A, AB, consisting of marine organic material (Dahl et al., 2004). For this reason, the line-fitting

methods should be adjusted to be able to represent frequent changes between oxic and anoxic conditions and varying chemical compositions of the same organic matter type.

5.2 Comparison of the results

The results showed that the mean original organic carbon values calculated by the methods indicate the same organic-richness for the immature organic matter in each data. When testing the methods on data from the Wenchang Formation (chapter 4.5), the Dahl et al. (2004) method was used with the average production index value of the section (16%). Using the mean production index value as input to the Dahl et al. (2004) method yielded lower results than the other methods or the Dahl et al. (2004) method when it was used with higher transformation ratio inputs calculated by the Peters et al. (1996), Jarvie et al. (2007) and Jarvie (2012) methods. As a result, the Dahl et al. (2004) method used with the mean production index value of the Wenchang Formation suggested less hydrocarbon generative potential. Furthermore, the uncorrected original hydrogen index value computed by this approach indicated worse organic matter quality, while the corrected initial hydrogen index calculated by the same input value (16%), suggested similar organic matter quality to the results of the Jarvie et al. (2007) method and the Dahl et al. (2004) method, when higher transformation ratio input values were used (63%−74%). Moreover, the mean production index value of the organic matter in the Wenchang Formation is lower than the ones ones calculated by the Peters et al. (1996), Jarvie et al. (2007) and Jarvie (2012) methods and contradicts with the maturity stage suggested by the T_{max} values in the section, shown in Tables 7 and 8. In contrast, the interpretation of the maturity based on the transformation ratio results of the Peters et al. (1996); Jarvie et al. (2007) and Jarvie (2012) methods are in agreement with the interpretation based on the T_{max} values in the section. Conclusively, using the mean production index value of a section following the methodology of Dahl et al. (2004) might yield unrealistic results.

During most of the tests, the Jarvie et al. (2007) method provided the largest initial hydrocarbon generative potential values. The results of the Jarvie (2012) and the Dahl et al. (2004) methods calculated lower values in general. The reason for this is that the equation for obtaining $S2_o$ of Jarvie et al. (2007) (equation 6 in chapter 3.2.4) contains a correction factor, which is only valid for type II kerogen. Due to the correction factor in the equation, the application of the Jarvie et al. (2007) method resulted in larger back calculated values than the ones computed by the Jarvie (2012) method.

In most of the tests, the mass-balance-based methods calculated similar transformation ratio values with the exception of chapter 4.3.1.2, where the the methods were tested on the kerogen composition of the degraded organic matter in the Volg−2 sequence. In this case, the Peters et al. (1996) method calculated a lower mean transformation ratio value than the other methods. Furthermore, the transformation ratio value computed by the Peters et al. (1996) method suggests the same maturity as the measured T_{max} values in the section. The results of the other methods contradict with the maturity interpretation inferred from the T_{max} values.

The original hydrogen index values calculated by the methods show large variation and in general, result in different depositional environment intepretation. In some cases however, the back calculated TOC_o values helped to determine the most realistic interpretation (e.g. chapter 4.3.2.6). Furthermore, the corrected initial hydrogen index values computed by the Dahl et al. (2004) method are higher than the uncorrected values. The difference between the uncorrected and corrected values depends on the amount of retained pyrolysable organic matter in the samples. In case the retained amount of pyrolysable material is high, the corrected values suggest a different depositional environment interpretation than the uncorrected values (e.g. chapter 4.3.1.6).

5.3 Initial assumptions

It is crucial for the mass-balance-based methods to apply a realistic original hydrogen index value as all of the other calculations depend on it. In case the origin of the organic matter is not known, it is problematic to assign the maceral groups to the right kerogen type in the Jarvie et al. (2007) method. When using a too low initial hydrogen index value as input to the mass-balance-based methods, the results might underestimate the quantity and quality of organic matter. Beyond the scope of the project, further research is needed to test this assumption with calibration data. In case the origin and kerogen composition of the organic matter is known, the mass-balance-based methods can be used with any types of organic matter and in any depositional environment.

It can be concluded from the results, that the output values of the Dahl et al. (2004) method increase in general with increasing transformation ratio so defining a correct transformation ratio input value is crucial for the method to obtain realistic results.

The results of the Dahl et al. (2004) method also depend on the obtained gas to oil ratio potential. For example, when estimating the organic-richness, the original hydrogen index of

the section and the hydrocarbon potential of the kerogen end-members in the Volg–2 sequence in the Danish Central Graben, Dahl et al. (2004) needed an assumption about the transformation ratio of the organic matter in the section as required by the method. They used the average production index of the section (46%) as a basis and then estimated the GORP based on the overlay constructed for the transformation ratio of 40%. This approach yielded a GORP of 0.9. In theory, using a transformation ratio of 40% instead of 46% and estimating the GORP manually (i.e. not by an equation) yields imprecise results. However, in practice, using the GORP estimated on the basis of visual inspection from the overlay or calculated by equation 59 gives similar results. For a transformation ratio value of 40%, the GORP is 0.83 and when using the mean transformation ratio value of the section (46%), the GORP is 0.74. All of these transformation ratio input values result in the same TOC_o (6 wt.%) and similar $S2_o$ and HI_o values (Figs. 70 and 71).

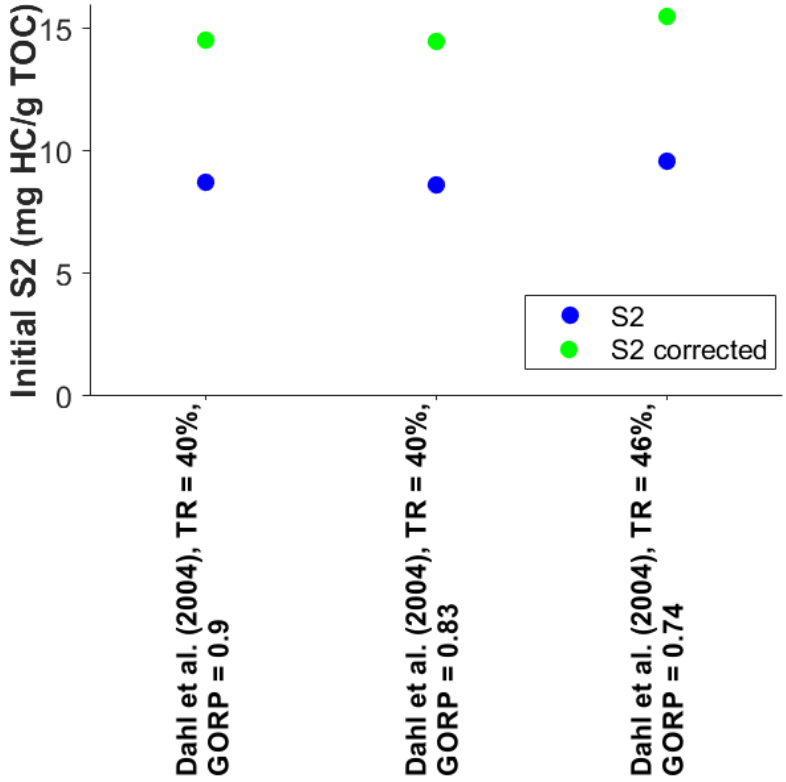

Figure 70. Initial S2 values calculated by the Dahl et al. (2004) method for the Volg–2 sequence with slightly different transformation ratio and GORP values.

Using a transformation ratio input of 40% with GORP values of 0.9 and 0.83 gives an HI_o value of 296 mg HC/g TOC, while calculating with the transformation ratio of 46% results in an HI_o of 320 mg HC/g TOC. The matrix corrected values of these results are 493 mg HC/g TOC and

515 mg HC/g TOC respectively. These results show that minor differences between the transformation ratio input values and obtained GORP values do not change the results.

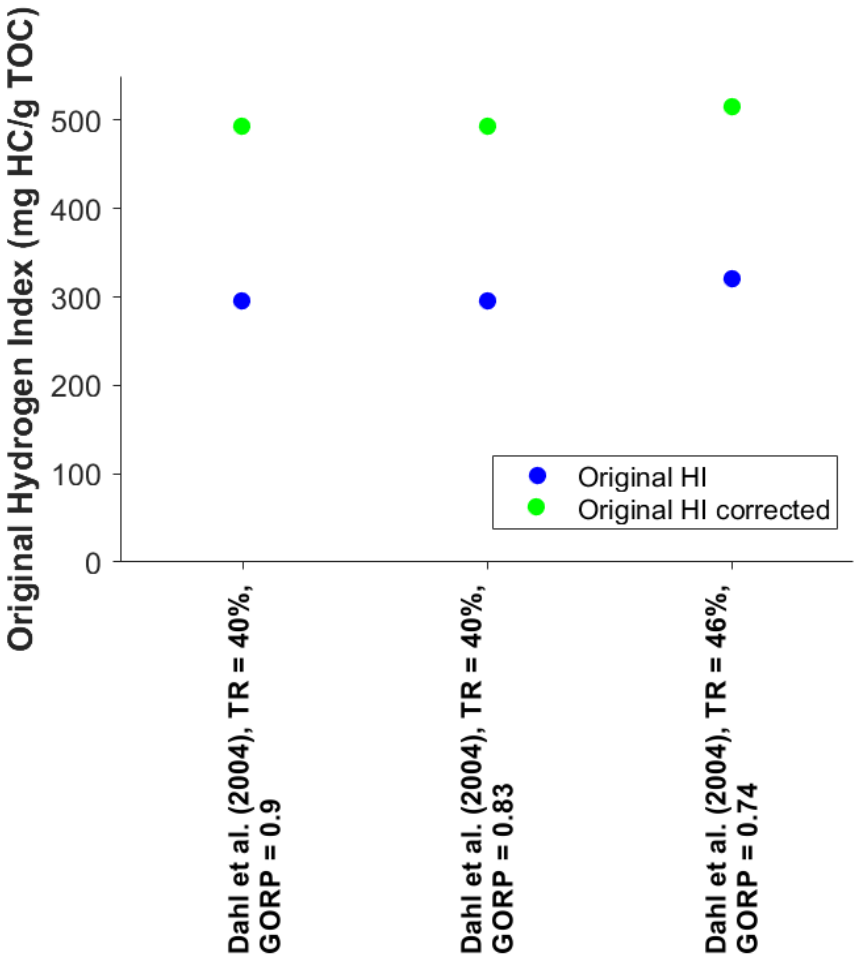

Figure 71. Original hydrogen index values calculated by the Dahl et al. (2004) method for the Volg–2 sequence when there are only minor differences between the input values.

Moreover, when the Dahl et al. 82004) was tested with transformation ratio values given by other methods (Peters et al., 1996; Jarvie et al., 2007; Jarvie, 2012), the results suggested similar organic-richness and depositional environment interpretations. This shows that any of the tested mass-balance-based methods can be used to obtain a transformation ratio value for the Dahl et al. (2004) method.

The results of the Dahl et al. (2004) method also depend on the kerogen end member values. The method was tested with the end-member values of 250 mg HC/g TOC for HI(gas) and 700 mg HC/g TOC for HI(oil). However, these values cannot be used in case the organic matter consists of type I kerogen. As the overlays of the method depend on the transformation ratio and the end-member values, it is crucial to define the correct values in the equation because the increment between the overlay lines and angle of the slope will change with respect to different

end-member values. Using incorrect end-member values might influence the obtained GORP value and therefore the final results. However, further tests are needed to clarify this.

5.4 Data availability and uncertainty of the results

In case there is no information on the origin of the organic matter or immature organic matter is not available to determine the kerogen composition of the studied sample set, there is no tool to know whether the results reflect reality. In such cases, the kerogen composition used in the mass balance equations needs to be defined on the basis of degraded organic material which might result in an unrealistic depositional environment interpretation depending on the data set. For example, the back calculated geochemical parameters and the depositional environment intepretation made on the basis of these values is different if the origin of the organic matter is not known (see chapter 4.2). To avoid misinterpretation and calculating unrealistic results it might be beneficial to study the immature facies equivalent of the organic matter. However, such facies equivalents might not be available either but the studied methods are able to indicate if the initial input is too low. For example, during the testing of the Passhatten Member, all the mass-balance-based equations yielded negative transformation ratio values for some samples when the tests were carried out without applying any information about the origin of the organic matter (Fig. 45). The negative values obtained for some samples were the results of the too low estimated initial hydrogen index. Moreover, the underestimation of the original hydrogen index can be suspected if the average back calculated initial hydrogen index value is lower than the present day hydrogen index value of some samples, which was seen during testing the Jarvie et al. (2007) method in the Volg–2 sequence (Fig. 72). During the testing of the Dahl et al. (2004) method on the Passhatten Member data, the GORP calculated by equation 59 was larger than one, which resulted in a negative oil fraction and oil potential. These negative values might be an indication that the transformation ratio input was too low for the method to work.

Jarvie (2012) discussed that representative hydrogen index values should be obtained for each kerogen type to obtain more reliable results. Based on the study of the a global collection of immature marine organic matter, Jarvie (2012) emphasized that the hydrogen index values for kerogen types I and II are overestimated in equation 1 of Jarvie et al. (2007). For this reason, new representative hydrogen index values should be used in the Jarvie et al. (2007) method based on the study of Jarvie (2012), although suggestions for these values were not published by the author. Although beyond the scope of this project, lower hydrogen index values should be tested in the Jarvie et al. (2007) method and the results should be compared to the ones

obtained by the values in the original publication (Jarvie et al., 2007) to see how the interpretation based on the new results would change.

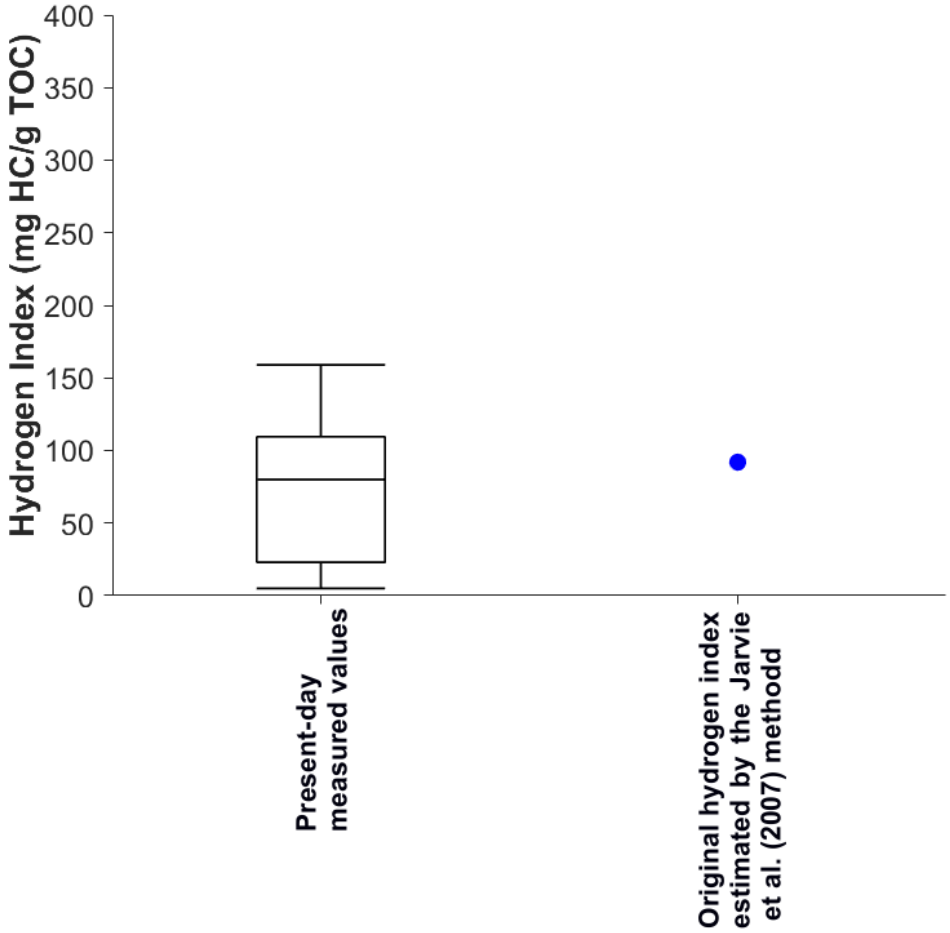

Figure 72. Original hydrogen index of the Volg–2 estimated on the basis of average kerogen composition by the Jarvie et al. (2007) method compared to the present-day hydrogen index values.

Moreover, to test which of the available methods calculate the most and least realistic results, artificial maturation studies should be carried out on numerous samples and all methods should be tested on such data sets.

6. Conclusions

A comparison of different equations to calculate the organic-richness and quality of the immature organic matter was carried out on four data sets. The original organic carbon content calculated by both the line-fitting and mass-balance-based methods yielded similar results suggesting the same organic-richness for each data set.

The transformation ratio of the organic matter estimated by the mass balance equations yielded close results to each other, however, none of the methods calculated consistently lower or higher values than the others. The computed transformation ratio values indicated the same maturity stage for the organic matter with the exception of one test, when the result of the Peters et al. (1996) method was lower than the values computed by the other methods. Furthermore, the methods yielded a large transformation ratio spread when they were tested on data from the Passhatten Member, using the kerogen composition of the degraded organic matter. In this case, the methods yielded negative values for some samples, suggesting that the initial hydrogen index input is too low.

The variation in the computed initial S2 values are larger than observed for the TOC_o values and no consistent trend can be observed in the results. During most tests, the Jarvie et al. (2007) method yielded the highest initial hydrocarbon generative potential values. This is the result of using a correction factor in the equation of Jarvie et al. (2007), which is only valid for type II kerogen.

Regarding the original hydrogen index calculations, the corrected values of the Dahl et al. (2004) suggested a different depositional environment than the uncorrected values of the same method and the mass-balance-based equations when the amount of retained pyrolysable organic matter was high in the studied sample set. The results of the mass-balance-based methods are in general, comparable to the uncorrected results of the Dahl et al. (2004) method. When the different back calculated original hydrogen index values suggest several depositional environment interpretations, the computed TOC_o values can help to determine the most realistic interpretation.

The mass balance equations are dependent on the kerogen composition and origin of the non-degraded organic matter. The best-fit methods give different results with respect to the transformation ratio input and/or to the depositional environment of the non-degraded organic

material. This means if the kerogen composition and the origin of the organic matter are known, the mass balance equations can be used for any kind of organic material originating from any geological settings. In contrast, the line-fitting methods cannot account for large shifts in the oxygen content of bottom waters or for kerogen types consisting of different blends of organic facies.

In case of a lack of sufficient data about the origin of the organic matter, the application of the methods is hard as the input values to the methods have to be decided on the basis of degraded organic material. In such cases, the methods might provide unrealistic results.

7. Further work

In future studies, upgrading the existing line-fitting methods would be beneficial to expand the application of the best-fit approaches to more depositional environments.

New methods could also be constructed from a mixture of mass balance equations and line-fittting methods. This might reduce the sensitivity of the methods to the initial input values. Furthermore, mixing the two types of equations might enable the construction of a method which is able to calculate all geochemical parameters needed for it to work and therefore would be independent from other methods.

8. References

Andsbjerg, J. & Dybkjær, K. (2003). Sequence stratigraphy of the Jurassic of the Danish Central Graben. *Geological Survey of Denmark and Greenland Bulletin, 1,* pp. 265–300.

Banerjee, A., Sinha, A.K., Jain, A.K., Thomas, N.J., Misra, K.N. & Chandra, K. (1998). A mathematical representation of Rock-Eval hydrogen index vs T_{max} profiles. *Organic Geochemistry, 28 (1/2),* pp. 43–55.

Baskin, D.K. (1997). Atomic H/C ratio of kerogen as an estimate of thermal maturity and organic matter conversion. *American Association of Petroleum Geologists (AAPG) Bulletin, 81,* pp. 1437–1450.

Birkenmajer, K. (1977). Triassic sedimentary formations of the Horsund area, Spitsbergen. *Studia Geologica Polonica, 51,* pp. 7–74.

Bordenave, M. L. (1993). Applied Petroleum Geochemistry. *Technip, Paris,* 524 pp.

Bou Daher, S., Nader, F.H., Müller, C. & Littke, R. (2015). Geochemical and petrographic characterization of Campanian – Lower Maastrichtian calcareous petroleum source rocks of Hasbayya, South Lebanon. *Marine and Petroleum Geology, 64,* pp. 304-323.

Bradley, R.S. (2015). *Paleoclimatology: Reconstructing Climates of the Quaternary* (third edition). Oxford: Elsevier, 696 pp.

Burnham, A. K. (1989). On the validity of the pristane formation index: *Geochimica Cosmochimica Acta, 53,* pp. 1693–1697.

Cao, Q.Y. (1985). Identification of microcomponents and types of kerogen under transmitted light. *Petroleum Exploration and Development, 5,* pp. 14-23.

Chen, Z. & Jiang, C. (2015). A data driven model for studying kerogen kinetics with application examples from Canadian sedimentary basins. *Marine and Petroleum Geology, 67,* pp. 795–803.

Chen, Z. & Jiang, C. (2016). A revised method for organic porosity estimation in shale reservoirs using Rock-Eval data: Example from Duvernay Formation in the Western Canada Sedimentary Basin. *American Associaton of Petroleum Geologists Bulletin, 100 (3),* pp. 405–422.

Chen, J.P., Zhao, C.Y. & He, Z.H., (1997). Criteria for evaluating the hydrocarbon generating potential of organic matter in coal measures. *Petroleum Exploration and Development, 1*, pp. 1-5.

Clayton, J.L. & Ryder, R.T. (1984). Organic geochemistry of black shales and oils in the Minnelusa Formation (Permian and Pennsylvanian), Powder River basin, Wyoming. In Woodward, J., Meissner, F.F., Clayton, J.L. (Eds.), *Hydrocarbon Source Rocks of the Greater Rocky Mountain Region.* Rocky Mt. Assoc. Geol., Denver, CO, pp. 231–253.

Connan, J. (1974). Time-temperature relation in oil genesis: geologic notes. *AAPG Bulletin, 58 (12),* pp. 2516-2521.

Cornford, C., (1994). The Mandal-Ekofisk(!) Petroleum System in the Central Graben of the North Sea. In Magoon, L.B., Dow, W.G. (Eds.), *The Petroleum System − from Source to Trap.* American Association of Petroleum Geologists Memoir, 60, pp. 537–571.

Cornford, C., Gardner, P. & Burgess, C. (1998). Geochemical truths in large data sets I: Geochemical screening data. *Organic Geochemistry, 29,* pp. 519–530.

Dahl, B., Bojesen–Koefoed, J., Holm, A., Justwan, H., Rasmussen, E. & Thomsen, E. (2004). A new approach to intepreting Rock-Eval S_2 and TOC data for kerogen quality assessment. *Oragnic Geochemistry, 35,* pp. 1461–1477.

Dahl, B. & Yukler, M.A. (1991). The role of petroleum geochemistry in basin modelling of the Oseberg Area, North Sea. In Merrill, R.K. (Ed.), *Treatise of Petroleum Geology Handbook, Source and Migration Processes and Evaluation Techniques.* American Association of Petroleum Geologists, Oklahoma, OK: Tulsa, pp. 65–85.

Dang, W., Zhang, J., Tang, X., Chen, Q., Han, S., Li, Z., Du, X., Wei, X., Zhang, M., Liu, J., Peng, J. & Huang, Z. (2016). Shale gas potential of Lower Permian marine-continental transitional black shales in the Southern North China Basin, central China: Characterization of organic geochemistry. *Journal of Natural Gas Science and Engineering, 28,* pp. 639-650.

Espitalié, J. & Bordenave, M.L. (1993). Rock-Eval pyrolysis. In Bordenave, M.L. (Ed.), *Applied Petroleum Geochemistry*. Editions Technip, Paris, pp. 237–261.

Espitalié J., Daroo, G. & Marquis, F. (1985). La pyrolyse Rock-Eval et ses applications. *Revue de l'Institute Francais du Pétrole, 40,* pp. 563–579 and pp. 755–784.

Espitalié J., Daroo, G. & Marquis, F. (1986). Rock-Eval pyrolysis and its applications. Part III. Revue de *l'Institut Français du Pétrole, 41,* pp. 73-89.

Espitalié, J., La Porte, J.L., Madec, M., Marquis, F., Le Plat, P., Paulet, J. & Boutefeu, A. (1977). Méthode rapide de caractérization des roches méres de leur potential pétrolier et de leur degreé d'évolution. *Revue de l'Institute Francais du Pétrole, 32,* pp. 23–42.

Espitalié, J., Madec, M. & Tissot, B., (1980). Role of mineral matrix in kerogen pyrolysis: influence on petroleum generation and migration. *American Association of Petroleum Geologists Bulletin 4 (1),* pp. 59–66.

Espitalié, J., Madec, M. & Tissot, B. (1984). Geochemical logging. In K. J. Voorhees, (Ed.), *Analytical pyrolysis—Techniques and applications.* Boston, Butterworth, pp. 276– 304.

Espitalié, J., Marquis, F., Sage, L. & Barsony, I. (1987). Géochimie organique du bassin de Paris. *Revue de l'Institut Français du Pétrole, 42*, pp. 271–302.

Galimov, E.M., Lopatin, N.V. & Espitalié, J. (1988). Oil-source properties of the Bazhenovskaya suite at Salym area, Western Siberia. *Geokhimiya, 4,* pp. 467-478.

Hao, S.S. (1993). Study on the dynamic balance theory and accumulation of natural gas. *Nat. Gas. Geosci., (Z1),* pp. 95-108.

Hunt J.M. (1996). Petroleum Geochemistry and Geology. New York, N.Y.: W.H. Freeman and Company, 743 pp.

Ineson, J.R., Bojesen-Koefoed, J.A., Dybkjær, K. & Nielsen, L.H. (2003). Volgian–Ryazanian 'hot shales' of the Bo Member (Farsund Formation) in the Danish Central Graben, North Sea: stratigraphy, facies and geochemistry. In Ineson, J.R. & Surlyk, F. (Eds.), The Jurassic of Denmark and Greenland. *Geological Survey of Denmark and Greenland Bulletin, 1,* pp. 403–436.

Isaksen, G.H. & Ledje, K.H.I. (2001). Source rock quality and hydrocarbon migration pathways within the greater Utsira High area, Viking Graben, Norwegian North Sea. *AAPG Bulletin, 85 (5),* pp. 861−883.

Jarvie, D.M., Burgess, J.D., Morelos, A., Mariotti, P.A. & Lindsey, R. (2001). Permian Basin petroleum systems investigations; inferences from oil geochemistry and source rocks. *AAPG Bulletin, 85 (9),* pp. 1693-1694.

Jarvie, D.M., Hill, R.J., Ruble, T.E. & Pollastro, R.M. (2007). Unconventional shale gas systems: The Mississippian Barnett Shale of north-central Texas as one model for thermogenic shale gas assessment. In Hill, R.J. & Jarvie, D.M. (Eds.), *AAPG Bulletin Special Issue: Barnett Shale, 90 (4),* pp. 475–499.

Jarvie, D.M. (2012). Shale Resource Systems for Oil and Gas: Part 1 – Shale-gas Resource Systems. In Breyer, J.A. (Ed.), *Shale reservoirs—Giant resources for the 21st century*. AAPG Memoir, 97, pp. 69–87.

Jensen, T.F., Holm, L., Frandsen, N. & Michelsen, O. (1986). Jurassic – Lower Cretaceous lithostratigraphic nomenclature for the Danish Central Trough. *Danmarks Geologiske Undersøgelse Serie, A 12,* 65 pp.

Jiang, H., Pang, X., Shi, H., Yu, Q., Cao, Z., Yu, R., Chen, D., Long, Z. & Jiang, F. (2015). Source rock characteristics and hydrocarbon expulsion potential of the Middle Eocene Wenchang formation in the Huizhou depression, Pearl River Mouth basin, south China sea. *Marine and Petroleum Geology, 67,* pp. 635-652.

Jones, R.W. (1987). Organic facies. In Brooks, J. & Welte, D.H. (Eds.), *Advances in Petroleum Geochemistry*. New York, N.Y.: Academic Press, pp. 1–90.

Karcz, P. (2010). Relationships between development of organic−rich shallow shelf facies and variation in isotopic composition of pyrite (Middle Triassic, Spitsbergen). *Polish Polar Research, 31,* pp. 239–254.

Karcz, P. (2014). Depositional conditions and petroleum potential of the Middle Triassic Passhatten Member (Bravaisberget Formation), Spitsbergen. *Polish Polar Research, 35 (1),* pp. 41-71.

Katz, B. J. (1983). Limitations of Rock-Eval pyrolysis for typing of organic matter. *Organic Geochemistry, 4,* pp. 195–199.

Killops, S.D. & Killops, V.J. (2013). *Introduction to Organic Geochemistry* (second edition). Oxford: Blackwell Publishing, 393 pp.

Krajewski, K.P., Karcz, P., Woźny E. & Mørk, A. (2007). Type section of the Bravaisberget Formation (Middle Triassic) at Bravaisberget, western Nathorst Land, Spitsbergen, Svalbard. *Polish Polar Research, 28,* pp. 79–122.

Krajewski, P.K. & Weitschat, W. (2015). Depositional history of the youngest strata of the Sassendalen Group (Bravaisberget Formation, Middle Triassic-Carnian) in Southern Spitzbergen, Svalbard. *Annales Societatis Geologorum Poloniae, 85*, pp. 151-175.

Langford, F.F. & Blanc-Valleron, M.-M. (1990). Interpreting Rock-Eval pyrolysis data using graphs of pyrolizable hydrocarbons vs. total organic carbon. *American Association of Petroleum Geologists Bulletin, 74 (6),* pp. 799–804.

Liu, B., Qian, X.L. & Wang, Y.H., (1999). Tectonic-sedimentary evolution of North China plate in Early Paleozoic. *Sci. Geol. Sin., 34 (3),* 347−356.

Lopatin, N. V., Zubairaev, S. L., Kos, I. M., Emets, T. P., Romanov E. A. & Malchikhina, O. V. (2003). Unconventional oil accumulation in the Upper Jurassic Bazhenov black shale Formation, West Siberian Basin: a self sourced reservoir system. *Journal of Petroleum Geology, 26 (2),* pp. 225-244.

McCarthy, K., Rojas, K., Niemann, M., Palmowski, D., Peters, K. & Stankiewicz, A. (2011). Basic Petroleum Geochemistry for Source Rock Evaluation. *Oilfield Review, 23 (2),* pp. 32–43.

Meyers, P. A. (1977). Organic geochemical proxies of paleoceanographic, paleolimnologic and paleoclimatologic processes. *Organic Geochemistry, 27 (5/6),* pp. 213–250.

Modica, C.J. & Lapierre, S.G. (2012). Estimation of kerogen porosity in source rocks as a function of thermal transformation: Example from theMowry shale in the Powder River Basin of Wyoming. *AAPG Bulletin, 96 (1),* pp. 87–108.

Mørk A., Knarud, R. & Worsley, D. (1982). Depositional and diagenetic environments of the Triassic and Lower Jurassic succession of Svalbard. In Embry, A.F. & Balkwill, H.R. (Eds.), Arctic Geology and Geophysics. *Canadian Society of Petroleum Geologist Memoir, 8,* pp. 371–398.

Nicholas, B.H., Katherine, H.F., Richard, D.P., Timothy, S.W. & Gareth, D.M. (2004). The character and origin of lacustrine source rocks in the Lower Cretaceous synrift section, Congo Basin, West Africa. *AAPG Bulletin, 88,* pp. 1163-1184.

Peters, K.E. (1986). Guidelines for Evaluating Petroleum Source Rock Using Programmed Pyrolysis. *American Associaton of Petroleum Geologists Bulletin, 70 (3),* pp. 318–329.

Peters, K.E., & Cassa, M.R. (1994). Applied source rock geochemistry. In Magoon, L.B. & Dow, W. G. (Eds.), *The petroleum system – from source to trap.* American Association of Petroleum Geologists Memoir, 60, pp. 93–117.

Peters, K.E., Cunningham, A.E., Walters, C.C., Jigang, J. & Zhaoan, F. (1996). Petroleum systems in the Jiangling–Dangyang area, Jianghan Basin, China. *Organic Geochemistry, 24 (10/11),* pp. 1035–1060.

Peters, K.E., Walters, C.C. & Moldovan, J.M. (2005). *The Biomarker Guide: V. 1 – Biomarkers and Isotopes in the Environment and Human History*. Cambridge: Cambridge University Press, 492 pp.

Robert, P. (1988). *Organic Metamorphism and Geothermal History*. Dordrecht: Elf – Aguitaine and D. Reidel Publishing Company, 311 pp.

Romero-Sarmiento, M.-F., Ducros, M., Carpentier, B., Lorant, L., Cacas, M. C., Pegaz-Fiornet, S., Wolf, S., Rohais, S. & Moretti, E. (2013). Quantitative evaluation of TOC, organic porosity and gas retention distribution in a gas shale play using petroleum system modeling: Application to the Mississippian Barnett Shale. *Marine and Petroleum Geology, 45,* pp. 315–330.

Snowdon, L. R. (1995). Rock-Eval T_{max} suppression: documentation and amelioration. *AAPG Bulletin, 79,* pp. 1337-1348.

Tissot, B.P. & Welte, D.H. (1978). *Petroleum Formation and Occurrence* (first edition). Springer−Verlag Berlin Heidelberg, 538 pp.

Tissot, B.P. & Welte, D.H. (1984). *Petroleum Formation and Occurrence* (second edition). Springer−Verlag Berlin Heidelberg, 702 pp.

Vollset, J. & Doré, A.G. (1984). A revised Triassic and Jurassic lithostratigraphic nomenclature for the Norwegian North Sea. *Norwegian Petroleum Directorate Bulletin, 3,* 53 pp.

Wu, W., Wang, Y.H., Cao, G.S., Huang, X.F. & Liu, W.Q. (2015). The geochemical characteristics of the carboniferous and Permian Source Rocks in the Western Henan, the southern North China Basin. *Nat. Gas. Geosci., 26 (1),* pp. 128-136.

Xu, S.H., Li, S.F. & Yuan, C.P. (2012). Resource potential of water-soluble gas in the Palaeogene Huizhou Sag, Pearl River Mouth Basin. *Petroleum Exploration and Development, 39,* pp. 194-201.

Yu, H.Z., Lv, F.L., Guo, Q.X., Lu, W.Z., Wu, J.Y. & Han, S.H. (2005). Proto-sediment basin types and tectonic evolution in the southern edge of North China Plate. *Pet. Geol. Exp., 27 (2),* pp. 111-117.

Zhao, J.F., Liu, C.Y., Liu, Y.T., He, Z.G., Mao, W. & Zhu, B. (2011). Reconstruction of thermal evolutionary history of the Upper Paleozoic in the southern North China. *Oil Gas Geol., 32 (1),* pp. 64-74.

Zhou, X.J., Ni, C.H. & Yang, F. (2010). The Paleozoic prototype basins and their tectonic deformation in North China and their controlling effects upon hydrocarbon accumulation. *Oil Gas Geol., 31 (6),* pp. 779-794.

Ziegler, P.A. (1990). Tectonic and palaeogeographic development of the North Sea rift system. In Blundell, D.J. & Gibbs, A.D. (Eds.), Tectonic evolution of the North Sea rifts. Oxford: Clarendon Press, pp. 1–36.

Appendix A

MATLAB code of the Peters et al. (1996) method

```
% load data
data = load('.txt'); %load the file with the input data
TOC_pd = data(:,); % measured TOC
HI_pd = data(:,); %measured hydrogen index
PI_pd = data(:,); %measured production index
HI_o = data(:,); %original hydrogen index values of the
samples

%Calculate the transformation ratio. PI_o is assumed to be
0.02 for immature source rocks.

PI_o = 0.02;

TR= 1-((HI_pd .*((1200-HI_o)./(1-PI_o))./ (HI_o.*(1200-
(HI_pd./(1-PI_pd)))));

% Calculate the original organic carbon content.

TOC_o = HI_pd.* TOC_pd.* 83.33./ (HI_o.*(1-TR).*(83.33-
TOC_pd)+HI_pd.*TOC_pd);
```

Appendix B

MATLAB code of the Jarvie et al. (2007) method

```
% load data
data = load('.txt'); %load the file with the input data
TOC_pd = data(:,); % measured TOC
HI_pd = data(:,);%measured hydrogen index
PC = data(:,);%measured pyrolysable carbon content
percent_type_I = data(:,); %volume contents of maceral group
assessed as type I kerogen
percent_type_II = data(:,); %volume contents of maceral group
assessed as type II kerogen
percent_type_III = data(:,); %volume contents of maceral group
assessed as type III kerogen
percent_type_IV = data(:,); %volume contents of maceral group
assessed as type IV kerogen

%Calculate the original hydrogen index

HI_o
=(percent_type_I/100*750)+(percent_type_II/100*450)+(percent_t
ype_III/100*125)+(percent_type_IV/100*50);

%Calculate the transformation ratio

TR = 1-((HI_pd.*(1200-HI_o))./(HI_o.*(1200-HI_pd)));

%Calculate the correction factor

k=(TR.*PC)/100;
k(k<0) = -k(k<0);%based on pers.comm. with P. Karcz (2016)

%Calculate the oriignal carbon content

TOC_o=HI_pd.*(TOC_pd./(1+k))*83.33 ./ (HI_o.*(1-TR).*(83.33-
(TOC_pd./(1+k))) + HI_pd.*(TOC_pd./(1+k)));

%Calculate the initial hydrocarbon generative potential

S2_o=TOC_o*0.36/0.08333;
```

Appendix C

MATLAB code of the Jarvie (2012) method

```
%load data
data = load('.txt'); %load the file with the input data
HI_pd = data(:,); %measured hydrogen index
TOC_pd = data(:,); %measured TOC
S1_pd = data (:,); %measured S1
S2_pd = data (:,); %measured S2
HI_o = data (:,); %original hydrogen index of the samples

%Calculate transformation ratio
TR = (HI_o-HI_pd)/HI_o;

%Calculate the fraction of organic carbon (OC)in S1+S2
OC = 0.085*(S1_pd+S2_pd);

%Correction in TOC_pd for bitumen and kerogen (wt.%)
TOC_pdbkfree = TOC_pd-OC;

%Minor correction to TOC_pd for added carbonaceous char from
bitumen and/or
%oil cracking (NGOC = Non-Generative Organic Carbon; wt.%)
NGOC_correction = HI_o*0.0008;

%Calculate TOC_pd adjusted, corrected for carbon in kerogen
and bitumen (wt.%)
TOC_pdngocadjusted = TOC_pdbkfree-NGOC_correction;

%Calculate the fraction of reactive carbon in TOC_o (GOC in
TOC_o)
GOC = HI_o/1177;

%Calculate the original organic carbon content (TOC_o)
TOC_o = TOC_pdngocadjusted/(1-GOC);

%Calculate GOC_o
GOC_o = TOC_o*GOC;

%Calculate NGOC_o
NGOC_o = TOC_o-GOC_o;

%Calculate the initial hydrocarbon generative potential (S2_o
in mg HC/g rock)
S2_o_mghc = GOC_o/0.085;
```

Appendix D

Code of the Banerjee et al. (1998) method using the curve-fitting procedure of MATLAB

```
% load data
data = load('.txt'); %load the file with the input data
Tmax = data(:,); % measured T_max values
HI = data(:,);   % measured hydrogen index

HI_o = 100:1:300; %initial guess for the range of the original
hydrogen index
srs = zeros(1,length(HI_o));

% transform input values
x = Tmax-435;
for i=1:length(HI_o)
    y = (HI_o(i)./HI-1)/HI_o(i);
    % fit an exponential function
    f = fit(x,y,'exp1');
    srs(i)=sum((f(x)-y).^2);
end

[minval,index]=min(srs);
HI_o_best=HI_o(index);
y = (HI_o_best./HI-1)/HI_o_best;
% fit an exponential function
[f, g] = fit(x,y,'exp1');

disp(['HI_o_best = ', num2str(HI_o_best)])
disp(f)
disp(g)

plot(f,x,y)
```

Appendix E

Implementation of the code of Banerjee et al. (1998) into the MATLAB programming language

```
% load data
data=load('.txt'); %load the file with the input data
Tmax = data(:,); %measured T_max values
HI_in = data(:,);   %measured hydrogen index

HI_low = 80; %initial guess for lower limit of the original
hydrogen index
HI_high = 900; %initial guess for upper limit of the original
hydrogen index

% initial definitions
slope=0.25;
cnst=1;
tol=1e-7;
iter=100;

HI = HI_in;

x=zeros(1,length(Tmax));
y=zeros(1,length(Tmax));
ex=zeros(1,length(Tmax));
a=0;

srsl=0; srsr=1; hio1=HI_low; hio2=HI_high;
hiol=hio1; hior=hio2;

while (srsr ~=srsl && hio2-hio1 > 2* cnst)
    func_reduce(Tmax,cnst,slope);
end
hio_min=0.5*(hiol+hior);
func_data1(Tmax,hio_min);
srs_min = func_curve(x,y,slope);
rsq = func_ccor(x,y);
a=a/(100*hio_min);
disp(['a = ', num2str(a)]);
disp(['b = ', num2str(b)])
disp(['SRSmin = ', num2str(srs_min)]);
disp(['r2 = ', num2str(rsq)]);
disp(['hio_min = ', num2str(hio_min)]);

% plot results (not part of the original code)
figure(1), clf
tmax_plot=430:460;
```

```
vals=1./(a*exp(b*(tmax_plot-435))+1/(hio_min));
plot(tmax_plot,vals,Tmax,HI_in,'ko','markerfacecolor','k','Lin
ewidth',1.5)
ylim([100 600])
xlabel('T_{max} (°C)', 'Fontweight', 'bold','Fontsize',12),
ylabel('Hydrogen Index (HI; mg HC/g TOC)','Fontweight',
'bold','Fontsize',12)



    function func_reduce(Tmax,cnst,slope)
        % search interval reduction
        hiol = hio1+0.5*(hio2-hio1-cnst);
        hior=hiol+cnst;
        func_data1(Tmax,hiol);
        srsl = func_curve(x,y,slope);
        func_data1(Tmax,hior);
        srsr = func_curve(x,y,slope);
        if (srsl>srsr)
            hio1=hior;
            return
        elseif (srsl<srsr)
            hio2=hiol;
            return
        end
    end

    function srs = func_curve(x,y,slope)
        % calculate fitting parameters and sum of residuals
squared
        b=slope;
        func_newt(x,y);
        resid = (a*ex - y)/100;
        srs = sum(resid.*resid);
    end

    function func_newt(x,y)
        for i=1:iter
            b1=b;
            [fb, dfb] = func_func(x,y);
            db=fb/dfb;
            b=b1-db;
            tb=tol*b;
            if (abs(db) <= abs(tb))
                return
            end
        end
    end

    function [fb, dfb] = func_func(x,y)
        ex = exp(b*x);
```

```
        x2=x.*x;
        ex2=ex.^2;
        y2=y.^2;
        s1=sum(x.*ex2./y2);
        s2=sum(ex./y);
        s3=sum(x.*ex./y);
        s4=sum(ex2./y2);
        s5=sum(2*x2.*ex2./y2);
        s6=sum(x2.*ex./y);
        fb=s1*s2-s3*s4;
        dfb=s2*s5-s1*s3-s4*s6;
        a=s2/s4;
    end

    function rsq = func_ccor(x,y)
        % r-squared value for function fit (correlation
coefficient)
        sx2=sum(x.^2);
        sy2=sum(log(y).^2);
        sxy=sum(x.*log(y));
        rsq=(sxy^2)/(sx2*sy2);
    end

    function func_data1(Tmax, cx)
        % transform data for curve fitting
        x=Tmax-435;
        HI(HI==cx)=cx-5;
        y=100*(cx./HI-1);
    end

end
```

Appendix F

MATLAB code of the Dahl et al. (2004) method

```
HI_gas=250; %hydrogen index of the gas-prone end-member
HI_oil=700; %hydrogen index of the oil-prone end-member
TR= ; %transformation ratio of the samples (in fraction)
alpha=0.084; %stoichiometric factor

% load data
data = load('dahl_volg.txt'); %load the file with the input
data
TOC = data(:,); %measured TOC
S2 = data(:,); %measured S2
[f,g] = fit(S2,TOC,'poly1');

 disp(f)
% disp(' ')
 disp(g)

%curve-fitting of the sample population
coeffvals=coeffvalues(f);
slope = coeffvals(1);
TOC_inert = coeffvals(2); %determination of the amount of
inert TOC

% minimum transformation needed for the method to work
% in that case m=0
min_TR=1-100/(slope*HI_gas);
if (TR < min_TR)
    disp(' ')
    disp(['      Note: TR should be > ', num2str(min_TR),...
        ' for this method to work in this case.'])
    disp(' ')
end
% maximum transformation ratio for which the method works
% in that case m=1
max_TR=1-100/(slope*HI_oil);
if (TR>max_TR)
    disp(' ')
    disp(['      Note: TR should be < ', num2str(max_TR),...
        ' for this method to work in this case.'])
    disp(' ')
end

% GORP
GORP=1-(100/(slope*(1-TR)) - HI_gas)/(HI_oil-HI_gas);

% Calculate TOC(live), TOC(oil) and TOC(gas)
```

```
TOC_live = mean(TOC) - TOC_inert;
TOC_gas = mean(TOC_live)*GORP;
TOC_oil = mean(TOC_live)*(1-GORP);

%Calculate original values
S2_o = mean (S2)/(1-TR);
TOC_o = mean (TOC) + alpha*(mean(S2)*TR/(1-TR));
HI_o = 100*S2_o./(TOC_o - TOC_inert);

%Restore TOC(live), TOC(oil) and TOC(gas)
TOC_live_restored=TOC_o-TOC_inert;
TOC_oil_restored=TOC_live_restored*(1-GORP);
TOC_gas_restored=TOC_live_restored*GORP;

%Restore S2(oil) and S2(gas)
S2_oil = TOC_oil*HI_o/100;
S2_gas = S2_o-S2_oil;

% S2-TOC cross plot with overlay
figure(3), clf
hold on
for m_overlay=0:0.2:1;
    S2_plot=0:ceil(1.1*max(S2));
    HI_overlay=(HI_oil*m_overlay + HI_gas*(1-m_overlay))*(1-
TR);
    TOC_overlay=TOC_inert + 100*S2_plot/HI_overlay;
    plot(S2_plot,TOC_overlay)
end
plot(S2,TOC,'kx')  % measured data
plot(S2_plot,TOC_inert + slope*S2_plot,'r') % regression line
hold off
xlabel('S_2 (mg HC/g rock)'), ylabel('TOC (wt.%)')
title('overlay method')
```